EPRI
Electric Power
Research Institute

Keywords:
Spent fuel storage
Radioactive waste management
Temperature limits

EPRI TR-103949
Project 3290-03
Final Report
May 1994

Temperature Limit Determination for the Inert Dry Storage of Spent Nuclear Fuel

Prepared by
Brookhaven National Laboratory
Upton, New York

Legacy - 2J

BROOKHAVEN NATIONAL LABORATORY
ASSOCIATED UNIVERSITIES, INC.

P.O. Box 5000
Upton, New York 11973-5000
TEL (516) 344- 2820
FAX (516) 344- 4486
E-MAIL

Department of Advanced Technology

August 26, 1996

Dr. Tae Ahn
MS T7 C6
U.S. Nuclear Regulatory Commission
Washington, DC 20555-0001

Dear Dr. Ahn:

As you requested; enclosed please find a copy of the report, "Temperature Limit Determination for the Inert Dry Storage of Spent Nuclear Fuel," EPRI TR-103949. If you have any questions, please do not hesitate to contact me.

Sincerely,

Terry Sullivan

Terry Sullivan
Environmental and Waste Technology Center

TS:la

enclosure

NRC report ?

TELEX: 6852516 BNL DOE

CABLE: BROOKLAB UPTONNY

Temperature Limit Determination for the Inert Dry Storage of Spent Nuclear Fuel

Current U.S. temperature limits for the dry cask storage of spent nuclear fuel are very conservative. The two methods now used to determine these limits suffer from a lack of experimental support and consistency. An empirical correlation of temperature and cladding failure developed in Germany appears to offer a more technically credible approach.

INTEREST CATEGORIES

Radioactive waste management
Light water reactor fuel

KEYWORDS

Spent fuel storage
Radioactive waste management
Temperature limits

BACKGROUND Delays in the implementation of U.S. high-level waste disposal policies have forced nuclear utilities to consider expanding spent-fuel storage space. One viable option is to store spent-fuel assemblies in dry casks filled with helium. The licensing of facilities containing such casks is based on a number of safety and waste handling considerations, one of which is the need to protect the fuel cladding against degradation leading to gross rupture. Cavitation creep rupture has been identified as the foremost failure mechanism for Zircaloy cladding, and temperature is a key factor in determining when this kind of failure might occur. Current U.S. methods for evaluating critical temperatures are different than those used in European countries and yield lower maximum temperature limits. Increasing these temperature limits would allow U.S. utilities to increase payloads and reduce the number of casks.

OBJECTIVES To evaluate the failure mechanisms for Zircaloy cladding under inert dry storage conditions; to evaluate the methods used to predict the failure of Zircaloy cladding; to recommend a better approach for determining the maximum temperature limit during dry storage.

APPROACH The project team reviewed previous studies of cladding degradation and failure mechanisms. The team appraised the creep modeling approaches used to describe the deformation behavior of cladding during dry storage.

RESULTS Cladding creep is the rate-determining degradation and failure mechanism for setting the maximum allowable temperature limit during inerted dry storage of spent fuel. However, the possibility of gross rupture leading to potential release of spent-fuel particles can be excluded under dry storage conditions. If creep were allowed to proceed to rupture, the most likely fracture mode would be of the pinhole type. Nevertheless, restricting the possibility of all failures is desirable and can be accomplished by confining creep degradation to its primary and early secondary stages. Such an approach would be in keeping with standard creep engineering practice as now implemented in Germany and under consideration in Japan.

Methods used in the United States to determine maximum allowable temperature limits during inerted dry storage suffer from a lack of basis in experimental data and an overreliance on theoretical considerations. While both models in use in the United States are extremely conservative and provide wide margins of safety, they

appear to be inconsistent with one another. In contrast, the empirical correlation of temperature and cladding failure developed in Germany is sound, well-validated, and conservative in its predictions. When this approach was used to predict independent data generated in the United States, excellent agreement was obtained. Application of the German correlation would allow significantly higher maximum allowable temperatures.

EPRI PERSPECTIVE The cost to store and dispose of spent fuel is extremely high. Because temperature limits for spent fuel play a major role in determining the capacity, design, and efficiency of a storage package, it is important that these limits neither incur unnecessary costs nor compromise safety.

This report shows that the methods used in the United States to determine temperature limits are inconsistent with one another, lack a strong technical basis, and are not supported by experimental data. Other approaches suggest that higher limits are appropriate and result in no significantly increased risks. While the current incentive to raise temperature limits is the need for additional fuel storage, issues related to final disposal may provide an even stronger motivation to revisit the temperature limit issue.

PROJECT
RP3290-03
Project Manager: Ray W. Lambert
Nuclear Power Group
Contractor: Brookhaven National Laboratory

For further information on EPRI research programs, call
EPRI Technical Information Specialists (415) 855-2411.

Temperature Limit Determination for the Inert Dry Storage of Spent Nuclear Fuel

TR-103949
Research Project 3290-03

Final Report, May 1994

Prepared by
BROOKHAVEN NATIONAL LABORATORY
Upton, New York 11973-5000

Principal Investigators
C. Pescatore
M. Cowgill

Prepared for
Electric Power Research Institute
3412 Hillview Avenue
Palo Alto, California 94304

EPRI Project Manager
R. W. Lambert

Fuel Reliability, Storage and Disposal
Nuclear Power Group

DISCLAIMER OF WARRANTIES AND LIMITATION OF LIABILITIES

ORGANIZATION(S) THAT PREPARED THIS REPORT:

BROOKHAVEN NATIONAL LABORATORY

ORDERING INFORMATION

Requests for copies of this report should be directed to the EPRI Distribution Center, 207 Coggins Drive, P.O. Box 23205, Pleasant Hill, CA 94523, (510) 934-4212. There is no charge for reports requested by EPRI member utilities.

ABSTRACT

The present report briefly reviews the most important cladding degradation and failure mechanisms under inert, dry storage conditions and analyzes the currently available methodologies for the prediction of Zircaloy cladding failure due to creep. Recommendations are provided regarding a preferred methodological approach that would allow higher maximum temperature limits than currently allowed in the United States.

ACKNOWLEDGMENTS

The authors gratefully acknowledge the critical reviews provided by Drs. Romney Duffey, Peter Soo and Terry Sullivan (Brookhaven National Laboratory), Marvin Smith (Virginia Power Co.) and Martin Peehs (Kraftwerk Union AG). Many thanks must also go to Ms. Ali Lopez, Laura Ayres and Melissa Collichio for coordinating and assembling the final report.

TABLE OF CONTENTS

TABLE OF CONTENTS (continued)

TABLE OF CONTENTS (continued)

ILLUSTRATIONS

ILLUSTRATIONS (continued)

TABLES

LIST OF ABBREVIATIONS

A/CR	-	Annealed, Cold-Rolled
BWR	-	Boiling Water Reactor
CSFM	-	Commercial Spent Fuel Management
DCCG	-	Diffusion Controlled Cavity Growth
DHC	-	Delayed Hydride Cracking
DOE	-	Department of Energy
FSSCC	-	Fuel Side SCC
HT	-	Heat Treated
IDS	-	Inerted Dry Storage
ISCC	-	Iodine-induced SCC
ISFSI	-	Independent Spent Fuel Storage Installation
KWU	-	Kraftwerk Union Aktiengesellschaft
MAT	-	Maximum Allowable Temperature
NRC	-	Nuclear Regulatory Commission
PCI	-	Particle Cladding Interactions
PWR	-	Pressurized Water Reactor
SCC	-	Stress Corrosion Cracking
SER	-	Safety Evaluation Report
SRA	-	Stress Relief Anneal
TSAR	-	Topical Safety Analysis Report

TEMPERATURE-LIMITS DETERMINATION FOR THE INERT DRY-STORAGE OF SPENT NUCLEAR FUEL

Phase I: Review of available methodologies

1. INTRODUCTION

1.1 Background and objective of the present study

Because of delays in the implementation of US high-level waste disposal policies, the nuclear utilities are facing a shortage of spent fuel storage space. A viable alternative to building new spent fuel pools has proven to be the storage of the spent fuel assemblies in dry casks filled with helium.

Independent storage casks facilities at reactor sites are licensed based on a number of safety and waste handling considerations. In the United States, one important criterion requires that "*The spent fuel cladding must be protected during dry storage against degradation that leads to gross ruptures ...* ." Several studies have analyzed with different degrees of detail the potential degradation and failure mechanisms applicable to intact spent fuel cladding. The Nuclear Regulatory Commission (NRC) and independent studies sponsored by the Department of Energy (DOE) have identified cavitation creep rupture as the foremost failure mechanism of Zircaloy cladding. Zircaloy creep would be brought about by the relatively high internal pressures that will exist in LWR fuel pins at storage temperature due to the presence of the original fill gas and of fission gases released from the fuel pellets during reactor operation. The storage temperature is controlled by several variables. All other conditions being the same, higher temperatures will be obtained with less-decayed fuel, with greater-burnup fuel, upon increasing the quantity of fuel to be placed in each storage cask, upon utilizing gases other than helium as the storage casks fill gas, and/or upon implementing a cask or storage facility design with lower overall heat transfer coefficient.

The current, maximum allowable temperature limits during dry storage are somewhat lower in the US than in European countries. The reference methodology is also different. Higher temperature limits are desirable as they would allow the US utilities more flexibility in adjusting payloads and, therefore, the number of storage casks. In order that a case be made to that effect, a better methodology needs to be identified and demonstrated.

The present report briefly reviews the most important cladding degradation and failure mechanisms under inert, dry storage conditions and analyzes the currently available methodologies for the prediction of Zircaloy cladding failure due to creep. Recommendations are provided regarding a preferred methodological approach that would allow defensible, maximum temperature limits.

1.2 Organization of the report

The report is is divided into several chapters, of which this Introduction is the first. The second chapter provides a summary of the reference conditions surrounding spent fuel, including the stress-temperature region of relevance and the properties of the irradiated cladding material. Chapter 3 presents an overview of previous studies of cladding degradation and failure mechanisms. This is followed by a chapter devoted to evaluating some aspects of cladding degradation, including the likelihood of gross rupture occurring during dry storage, creep of the Zircaloys and the importance of cavity formation in the deformation processes. The fifth chapter discusses the creep modeling approaches adopted to describe the deformation behavior of the cladding during dry storage. The report concludes with a summary of the preceding discussions and recommendations concerning which methodologies are most appropriate for predicting the integrity of spent fuel cladding during dry storage.

2. REFERENCE CONDITIONS AND MATERIALS PROPERTIES

The US commercial nuclear power derives almost entirely from Boiling Water (BWR) and Pressurized Water (PWR) reactors. There exist several manufacturers of fuel assemblies, but the fuel rod cladding material is almost exclusively Zircaloy-2 for BWRs and Zircaloy-4 for PWRs (Tables 2.1 and 2.2).

BWR fuel rods are longer and have thicker cladding than their PWR counterparts. All fuel rods are filled with helium but, as they leave the fabrication facility, the PWR fuel rods are pressurized at much higher levels than the BWR fuel rods (Table 2.3). Thus, from the point of view of stress analysis and performance under dry storage conditions, the BWR fuel rods and the PWR fuel rods constitute two distinct population groups. It is shown in Section 2.1 that, for the same average fill gas temperature and percent fission gas release, the cladding hoop stress is roughly *ten times* larger in PWR rods than in BWR rods.

2.1 Stress-temperature region

The most critical stress in cylindrical tubes subject to both an internal and an external pressure is the hoop stress at the inner wall of the cylinder. In spent fuel rods, the cladding hoop stress should be computed utilizing the formula for thick-walled cylinders as the ratio between the cladding thickness and the internal radius of the rods (Table 2.3) is greater than 0.1 [Roark, 1975]. The formula for thin-walled cylinders yields slightly lower hoop stresses (5-10% less) when used as originally intended (employing the value of the internal radius). However, if the mid-wall radius is inserted in the formula, the hoop stress thus calculated will be very close (within 1%) to that obtained from the thick-wall formula.

Furthermore, it must be observed that, because the gas present in the spent fuel is free to circulate within the fuel rods, the internal pressure acting on the cladding walls is determined by the *average* gas temperature within the rods. The average gas temperature can be taken to coincide with the temperature of the gas which collects in the plenum, as the latter provides the largest open volume within the fuel rod. The temperature of the gas plenum is expected

Table 2.1 BWR Fuel Assemblies Cladding Materials
(Adapted from [DOE, 1987])

Assembly Manufacturer	Array Size	Version	Clad Material
Allis Chalmers	10 x 10		Stainless Steel 348H
Siemens Power*	6 x 6	GE	Zircaloy-2
Siemens Power	6 x 6	HUM.BAY	
Siemens Power	7 x 7	GE	Zircaloy-2
Siemens Power	8 x 8	JP-3	Zircaloy-2
Siemens Power	8 x 8	JP-4,5	Zircaloy-2
Siemens Power	9 x 9	JP-3	Zircaloy-2
Siemens Power	9 x 9	JP-4,5	Zircaloy-2
Siemens Power	9 x 9	BRP	Zircaloy-2
Siemens Power	10 x 10	AC	Stainless Steel 348H
Siemens Power	11 x 11	GE	Zircaloy-2
Siemens Power	14 x 14	Ft.Cal	
General Electric	6 x 6	DRES-1	Zircaloy-2
General Electric	6 x 6	HUM.BAY	
General Electric	7 x 7	/2,3:V1	Zircaloy-2
General Electric	7 x 7	/2,3:V2	Zircaloy-2
General Electric	7 x 7	/4,5	Zircaloy-2
General Electric	7 x 7	HUM.BAY	
General Electric	8 x 8	/2,3	Zircaloy-2
General Electric	8 x 8	/4,5:V1	Zircaloy-2
General Electric	8 x 8	/4,5:V2	
General Electric	9 x 9	BRP	Zircaloy-2
General Electric	11 x 11	BRP	
Westinghouse	8 x 8	QUAD+	Zircaloy-2

* Formerly Exxon/ANF

Table 2.2 PWR Fuel Assemblies Cladding Materials
(Adapted from [DOE, 1987])

Assembly Manufacturer	Array Size	Version	Clad Material	Clad Final Conditioning
Babcock & Wilcox	14 x 14			
Babcock & Wilcox	15 x 15	Mark B	Zircaloy-4	SRA
Babcock & Wilcox	15 x 15	St.Stl.	Stainless Steel 304	SRA
Babcock & Wilcox	15 x 15	Mark BZ	Zircaloy-4	SRA
Babcock & Wilcox	17 x 17	Mark C	Zircaloy-4	SRA
Combustion Engineering	14 x 14	Std	Zircaloy-4	HT,SRA
Combustion Engineering	14 x 14	Ft.Cal.	Zircaloy-4	HT,SRA
Combustion Engineering	15 x 15	Palis.	Zircaloy-4	HT,SRA
Combustion Engineering	16 x 16	Onofre	Zircaloy-4	HT,SRA
Combustion Engineering	16 x 16	Lucie 2	Zircaloy-4	HT,SRA
Combustion Engineering	16 x 16	ANO2	Zircaloy-4	HT,SRA
Combustion Engineering	16 x 16	SYS80	Zircaloy-4	HT,SRA
Combustion Engineering	15 x 16	Yankee	Zircaloy-4	HT,SRA
Siemens Power	14 x 14	WE	Zircaloy-4	
Siemens Power	14 x 14	CE	Zircaloy-4	
Siemens Power	14 x 14	TOP ROD	Zircaloy-4	
Siemens Power	15 x 15	WE	Zircaloy-4	
Siemens Power	15 x 15	CE	Zircaloy-4	
Siemens Power	15 x 16	WE	Zircaloy-4	
Siemens Power	17 x 17	WE	Zircaloy-4	
Westinghouse	13 x 13			
Westinghouse	14 x 14	Std/ZCA	Zircaloy-4	HT,SRA
Westinghouse	14 x 14	OFA	Zircaloy-4	HT,SRA
Westinghouse	14 x 14	Std/ZCB	Zircaloy-4	HT,SRA
Westinghouse	14 x 14	Std/SC	Stainless Steel 304	A/CR
Westinghouse	14 x 14	Model C	Zircaloy-4	HT,SRA
Westinghouse	15 x 15	Std/ZC	Zircaloy-4	HT,SRA
Westinghouse	15 x 15	OFA	Zircaloy-4	HT,SRA
Westinghouse	15 x 15	Std/SC	Stainless Steel 304	A/CR
Westinghouse	15 x 16			
Westinghouse	17 x 17	Std	Zircaloy-4	HT,SRA
Westinghouse	17 x 17	OFA	Zircaloy-4	HT,SRA
Westinghouse	17 x 17	Vant 5	Zircaloy-4	
Westinghouse	17 x 17	XLR	Zircaloy-4	

Table 2.3 Fuel Rod Characteristics For Typical PWR and BWR* Assemblies
(Data taken from [DOE, 1987])

Vendor	Array Size	Assembly Version	Rod Length (mm)	Plenum Length (mm)	Outer Diameter (mm)	Cladding Thickness (mm)	Fill Gas Pressure (psig)
		PWR					
Babcock & Wilson	15 x 15	MARK B	3903.47	297.69	10.92	0.67	415.00
Babcock & Wilson	15 x 15	MARK BZ	3903.47	297.69	10.92	0.67	415.00
Combustion Engineering	14 x 14	Std	3733.80	212.73	11.18	0.71	300-450
Westinghouse	14 x 14	Std/ZCA	3773-3871	177.55	10.72	0.57	0 - 460
Westinghouse	15 x 15	Std/ZC	3773-3871	208.28	10.72	0.61	0 - 475
Westinghouse	17 x 17	Std	3850.64	160.02	9.50	0.57	275-500
Westinghouse	17 x 17	OFA	3850.64	175.26	9.14	0.57	275-500
		BWR					
Siemens Power	7 x 7	GE	4017.01	165.6-172	14.48	0.91-1.17	0.00
Siemens Power	8 x 8	JP-3	4030.09	254.51	12.29	0.91	45.00
Siemens Power	8 x 8	JP-4,5	4150.97	254.61	12.29	0.91	30.00
Siemens Power	9 x 9	JP-3	4040.38	243.33	10.77	0.76	60.00
Siemens Power	9 x 9	JP-4,5	4161.54	243.33	10.77	0.76	60.00

*General Electric assemblies data are proprietary. However, they should not be significantly different from the Siemens Power (Exxon/ANF) assemblies data.

to be somewhat smaller than the peak temperature of the cladding because the plenum section is not exposed to local heat generation and because the external temperature tends to be smaller at both ends of a dry storage cask. This situation is exemplified by the axial temperature profile reported in Fig. 2.1.

If Θ_{pl} represents the temperature of the plenum gas expressed in Kelvin and if, conservatively, the potential volumetric expansion of the fuel pin is ignored, the internal pressure is given by the expression:

$$P_i(\Theta_{pl}) = (P_{fill} + P_{fg}) \cdot (\Theta_{pl}/298) \qquad (2.1)$$

with:

P_{fill} - the rod fill gas pressure at room temperature before irradiation; and

P_{fg} - the fission gas pressure contribution at room temperature after irradiation.

The fission gas pressure contribution depends on several parameters, including the fuel rod design, the extent of fuel burnup and the temperatures to which the fuel has been exposed. Computer programs exist which enable calculation of the fission gas release but for present purposes we will consider a maximum bounding condition and an average condition. At the same time, for calculating the stresses on the cladding walls, we will assume that the external pressure acting on the walls remains constant at one atmosphere. Thus, the assumption being made is conservative in nature.

The maximum bounding condition is considered to be defined by the reactor operating system parameters (Table 2.4). For PWRs, this means that fuel rod internal pressures will be limited ultimately by the system pressure, 140-160 atmospheres (14-16 MPa, 2050-2350 psi). If this is taken to occur at a peak temperature of 370°C, then the 16 MPa would be equivalent to an internal pressure at room temperature of about 7.3 MPa (1060 psi). As can be seen from the data given in Table 2.3, this represents a more-than-doubling of the He fill gas pressure.

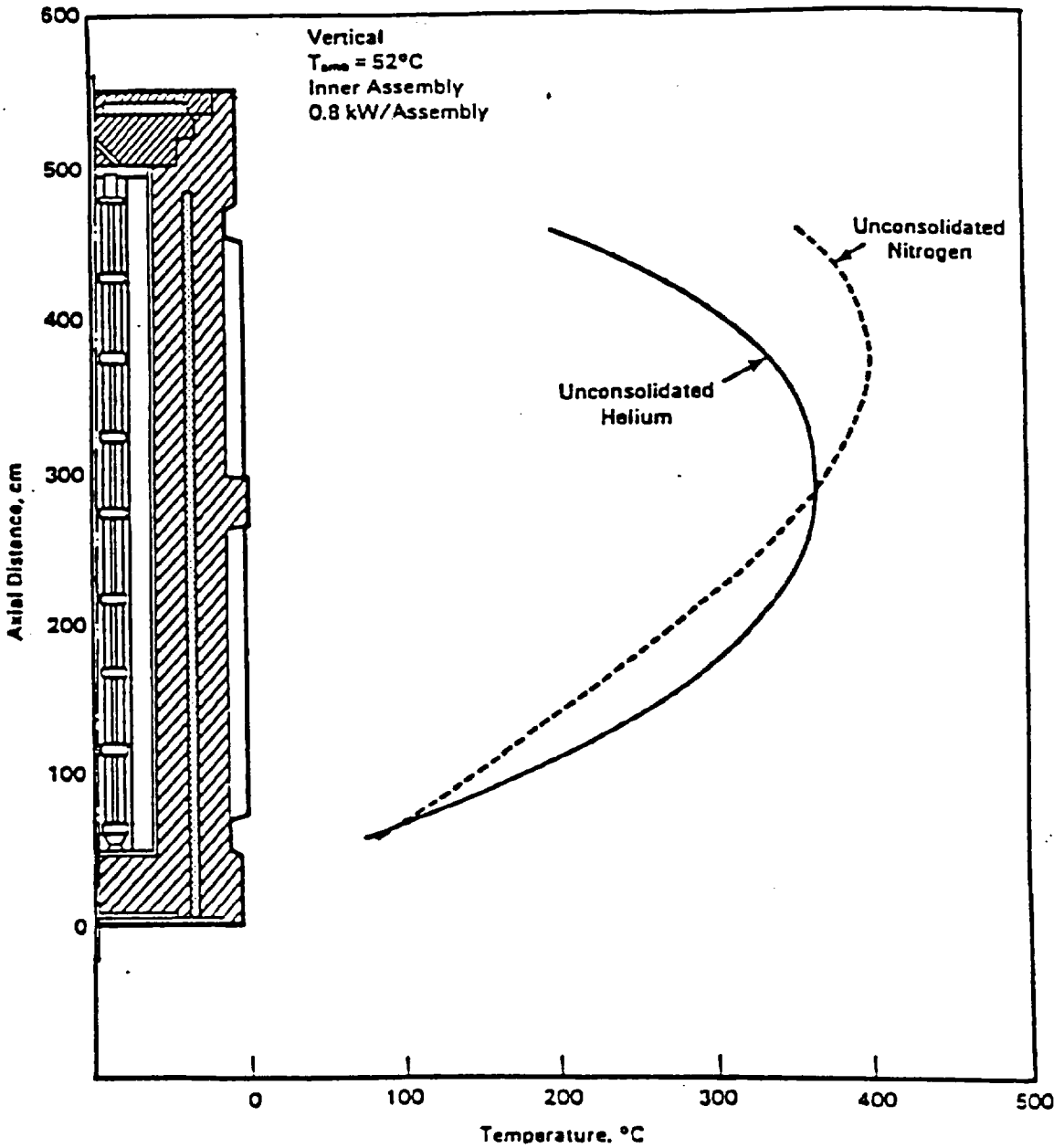

Figure 2.1 Axial temperature profile predictions for unconsolidated fuel in nitrogen and helium in a CASTOR-1C dry storage cask. [Rector, 1986]

Table 2.4 Peak Values of Important Variables During Reactor Operation
(Adapted from [IAEA, 1982])

Variable	PWR	BWR
Fuel center temperature (°C)	1200 - 1700	1400 - 1800
ID clad temperature (°C)	340 - 370	320 - 360
Water temperature (°C)	300 - 330	260 - 330
Pressure outside fuel rod (atm)	140 - 160	70
Fission gases released to rod filler gas (%)	1 - 13	1 - 11
Assembly burn-up (GW-d/t U)	35	27
OD heat fluxes (W/cm^2)	100	70
Neutron flux, >1 MeV (n/cm^2-s)	(5-6) x 10^{13}	(4-6) x 10^{13}
Gamma field (R/h)	~ 10^9	~ 10^9

While a justification can be made that the maximum internal pressure at full power reactor operation would be somewhat less than 16 MPa, the higher value will be adopted for the current exercise.

To obtain an idea of what an average fuel rod condition might be, consideration was given to what are currently goal burnups and what measurements of rod internal pressures have indicated in such cases. Many of the earlier fuel rods were designed for burnups up to 35 GW-d/t U for PWRs (Table 2.4). However, improvements in fuel technology have focussed on goal burnups of the order of 50-55 GW-d/t U [Strasser, 1987]. [Garde, 1986], reporting on the hot

cell examination of extended burnup fuel from Fort Calhoun, provides data showing one rod with an internal pressure of 4.04 MPa (586 psi) at room temperature at a burnup of 49.7 GW-d/t U. This would be equivalent to an internal pressure of 8.87 MPa (1290 psi) at 370°C. The other eleven rods examined had higher burnups (up to 55.7 GW-d/t U) but lower rod internal pressures, down to 3.51 MPa (508 psi). Again, for the current exercise, we will use the highest internal pressure generated to describe the "average" rod.

A similar approach could be used for BWR rods but it has not been attempted because such rods operate with a limiting system pressure of 7 MPa (1020 psi). This is one half the maximum assumed for the PWR rods and it is also less than the value adopted to describe the "average" PWR rod. Thus by considering the case of the PWR rods, we are enveloping the maximum internal pressure (and, by implication, the maximum hoop stress) situation for the BWR rods.

Following on from the above, the maximum hoop stresses have been calculated for a "maximum" condition rod and an "average" (50 GW-d/t U burnup) rod in the Westinghouse 17x17 standard assembly. These values have been plotted as a function of temperature and are shown in Figure 2.2. The plots themselves define the temperature-stress combinations which are relevant to spent fuel storage.

2.2 Macroscopic properties of irradiated cladding

Reactor operation exposes the fuel rods to relatively high temperatures, external pressures, and neutron fluxes (Table 2.4). Each of these variables influences in turn the final properties and condition of the cladding. Higher temperatures accelerate cladding oxidation but promote the annealing of microscopic damage; higher external pressures promote cladding creep-down and ovalization; high fast neutron fluxes cause irradiation hardening and, in some cases, fuel rod elongation (irradiation growth). Because the above quantities are not constant along the whole length of the fuel rods, cladding oxidation, cladding ovalization and creep, and irradiation hardening take place differentially along the cladding. These macroscopic effects combine with

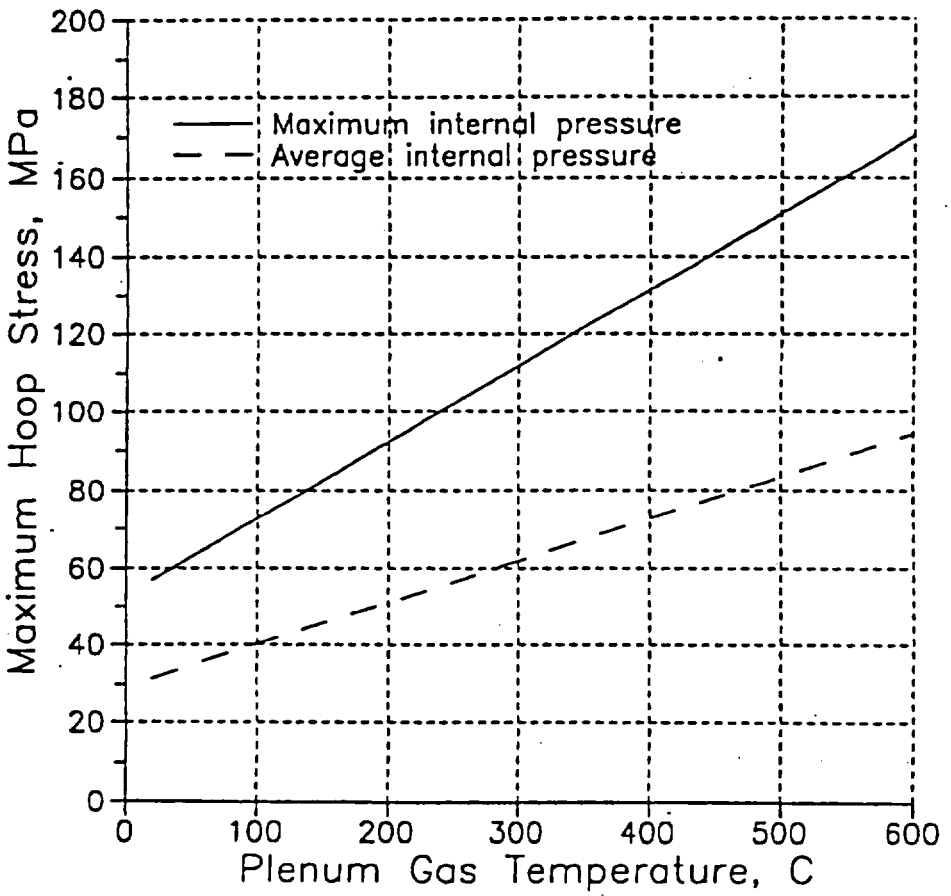

Figure 2.2 Reference stress-temperature regions for PWR and BWR spent fuel under inert dry storage conditions.

microscopic damage (see next section) to yield a final cladding material with non-uniform physical properties. The basic result, however, is that irradiated Zircaloy cladding tends to have higher strength and lower ductility than unirradiated cladding. On the other hand, as has been observed by Chung et al. [Chung, 1987], the presence of irradiation damage, per se, does not necessarily lead to brittle-type fracture behavior.

The material properties of the plenum section of the fuel rod are the ones least affected by reactor operation. The plenum is exposed to the least neutron flux and, possibly, to the highest damage-annealing temperature.

2.3 Microstructural properties of irradiated cladding

The Zircaloys are zirconium-based alloys containing small amounts (total concentration less than two weight percent) of Sn, Fe, Cr and (Zircaloy-2 only) Ni, these elements being added to provide the cladding with in-reactor corrosion resistance. All four elements have a low solubility in α-Zr [Charquet, 1988] so a variety of intermetallic precipitates, both stable and metastable, can be found in the microstructures. Principal among the stable ones are $Zr(Fe,Cr)_2$ and $Zr_2(Fe,Ni)$, the latter only in Zircaloy-2 [Yang, 1986]. However, the actual phases to be found, and their sizes and distribution, are heavily dependent on the thermomechanical treatments imposed on the materials during the cladding fabrication processing. The precipitates themselves contribute little to the mechanical properties of the material, which are mostly dependent on the thermomechanical treatments. In this context, the fabrication of clad tubing typically involves a series of cold-working steps, at the conclusion of which a heat treatment or stress-relief anneal is performed (see, for example, Table 2.2 and [Cheadle, 1977]). Because of the hexagonal close packed structure of α-phase Zircaloys, the final product is usually heavily textured, with the c-axis parallel to the direction of deformation.

Under reactor operating conditions, the microstructure will be affected by both the thermal environment and by neutron radiation. The former will tend to promote the dissolution of some of the metastable intermetallic phases and the growth of the stable ones [Yang, 1986 and 1988a,b]. The exposure to high temperatures will also favor the annealing out of the

mechanically-induced defects (dislocation networks, vacancies, etc.). These effects, which generally result in reduced mechanical strength and increased ductility, will be offset by radiation-induced changes. Neutron radiation can lead to several forms of damage in materials but not all of these have been observed in the Zircaloys [Northwood, 1977]. Radiation can cause dissolution of metastable phases and lead to previously crystalline precipitates becoming amorphous [Yang, 1986 and 1988a,b; Griffiths, 1987]. It has also been observed that c-component dislocation networks introduced during the fabrication processing are retained during neutron radiation [Griffiths, 1988a,b]. It is possible that they may even be enhanced but a more likely scenario is that some thermal recovery might take place and enable the formation of c-component vacancy loops. However, the primary products of neutron irradiation appear to be <a>-type prismatic dislocation loops [Holt, 1982; Griffiths, 1988a,b]. Voids and cavities have been observed only *rarely* in irradiated Zircaloys and essentially only in Zircaloy-2 [Gilbert, 1978; Holt, 1982; Griffiths, 1988a,b]. In fact, zirconium and zirconium-based alloys, as a whole, appear to be generally resistant to radiation-induced void and cavity formation [Wolfenden, 1972], [Yoo, 1974]. One of the factors contributing to this may be the lack of availability of the insoluble gases necessary to stabilize vacancy clusters and prevent their collapse into vacancy loops [Griffiths, 1988]. Zirconium has a very low neutron capture cross-section and there is consequently a very reduced possibility of damage resulting from gaseous transmutation products such as helium [Franklin, 1983].

2.4 Conclusions

The fuel rod cladding material is almost exclusively Zircaloy-2 for BWRs and Zircaloy-4 for PWRs. The variables that contribute most to the mechanical properties of the materials are the thermomechanical treatment at fabrication, and the fast neutron flux and the thermal environment during reactor operation.

Irradiated cladding tends to have higher strength and lower ductility than unirradiated cladding. Irradiated cladding, however, should not be regarded as a brittle material material. In particular, voids and cavities are rarely observed in irradiated cladding, and temperatures above about 350°C result in relatively rapid recovery of any irradiation-induced ductility loss.

The most important environmental variable during dry storage is the average fill gas temperature within the fuel rod. The latter can be taken to coincide with the gas temperature of the plenum. The plenum is also the cladding section which is least affected by radiation hardening and, therefore, it constitutes the cladding section which is most prone to creep.

Cladding hoop stresses in the BWR fuel rods are roughly ten times smaller than those in the PWR rods. Thus creep effects are expected to be much smaller in BWR fuel rods.

3. OVERVIEW OF PREVIOUS STUDIES OF CLADDING DEGRADATION AND FAILURE

The identification of one or more rate-limiting cladding degradation and failure mechanisms requires a methodological approach whereby all credible mechanisms are first identified and then evaluated against a cladding performance criterion.

3.1 Degradation and failure mechanisms

Blackburn et al. provided the first review of potential degradation and failure modes of the irradiated cladding while in dry storage [Blackburn, 1978]. The degradation modes they identified served as the basis for further analyses by several investigators including the NRC and the DOE.

The degradation and failure mechanisms identified by Blackburn et al. are as follows:

1. Creep (stress) rupture
2. Mechanical overload
3. Fuel side stress corrosion cracking (FSSCC)
4. Fracture of flawed cladding
5. Delayed hydrogen cracking (DHC) and fatigue
6. Internal hydriding
7. Oxidation (internal of the UO_2 and external of the cladding proper)

Additional potential mechanisms identified by others are Particle-Cladding Interaction (PCI) [Rothman, 1984; NRC, 1985], cavitation creep rupture [NRC, 1985; Cunningham, 1987], and brittle fracture [Cunningham, 1987].

3.2 Cladding performance criteria

Not all investigators utilize the same operational definition for the failure of the cladding. The NRC [FR, 1988] requires that "*The spent fuel cladding must be protected during dry storage*

against degradation that leads to gross ruptures or the fuel must be otherwise confined such that degradation of the fuel during interim storage will not pose operational safety problems with respect to its removal from storage." Damage modes and failure mechanisms can be tolerated as long as they "... *result in a loss of fuel rod internal pressure and termination of the damage mechanism.*" [NRC, 1985] [see also Section 3.3 of the present study]. A small breach in the cladding, such as pin holes or hairline cracks, that would not release irradiated UO_2 particles would not be considered a gross rupture[1]. Other investigators, including the DOE, also require that no gross ruptures should occur but require further that any small breach should be a low probability event. To that effect they propose directly [Peehs, 1986c; Mayuzumi, 1991] or indirectly [Levy, 1987; Cunningham, 1987] to limit the cladding diametral strain to no more than 1% during storage. Other investigators yet do not differentiate between gross ruptures and small breaches, but propose probabilistic criteria for permissible failure rates [Miller, 1989].

Overall, there appear to exist three main efforts that have attempted to develop a *comprehensive* methodology for determining and predicting the rate-limiting cladding degradation and failure mechanisms. These are, respectively, the work of the NRC, the work sponsored by the DOE, and the work performed in the Federal Republic of Germany. The results of those efforts are presented hereafter.

3.3 The NRC position

The NRC position on the most relevant failure modes of Zircaloy cladding during inert dry storage (IDS) has remained substantially the same since 1985 when it issued a favorable safety evaluation report (SER) of the PWR fuel dry storage cask Castor V/21 manufactured by General Nuclear Systems, Inc. [NRC, 1985]. In this SER the NRC addresses the FSSCC, PCI, DHC, and cavitation creep degradation and failure modes. Of these, only cavitation creep was deemed capable of leading to gross rupture of the cladding.

[1] Likewise, with respect to the need for packaging spent fuel before transportation, the NRC has indicated that "*known or suspected failed fuel assemblies (rods) and fuel with cladding defects greater than pinholes and hairline cracks are not authorized.*" [MacDonald, 1984].

3.3.1 FSSCC and PCI

With regard to FSSCC and PCI, the NRC noted that:

"Stress corrosion cracking (SCC) occurs as a result of a synergistic combination of a susceptible material, an aggressive environment and high stress. The corrosive environment associated with SCC of fuel rods has been attributed to fission products generated during reactor irradiation....SCC may also be related to pellet cladding interaction (PCI), this has only been observed during reactor operation due, in part, to the large external pressure on the fuel rods. The only known cause of cladding failure due to SCC occurred in a reactor during a ramp-up. No other failures from this cause are known to have occurred either during pool storage or under dry storage conditions. One explanation may be the pellet temperatures during dry storage are much lower than those in a reactor. Consequently, the accumulation of fresh fission products at the cladding is slowly reduced during dry storage. Furthermore, the activation of SCC requires stress levels substantially above those that can reasonably be expected to prevail under dry storage conditions. The possibility exists, however, that cracks may be present that were initiated during reactor operation. Under these conditions, the stresses generated at the crack tips may be large enough to cause crack extension. However, should such a crack penetrate the cladding, it is likely that the internal pressure will be relieved and, as a consequence, effectively terminate the progress of the SCC damage mechanism. The staff concludes, therefore, the SCC is not a damage mechanism that can lead to gross rupture of the fuel and cladding." [NRC, 1985, pp. 31-32].

3.3.2 DHC

Delayed hydride cracking is addressed by the NRC as follows:

"...the hoop stresses in the cladding are not expected to be high enough to cause a radial orientation of the hydride and consequent crack initiation. It is remotely possible that pre-existing cracks under stress can induce the diffusion of oxygen to the crack tips where substantially higher concentrations could precipitate hydride in a manner that would encourage crack extension. However, as is the case of SCC, crack propagation would result in a loss of fuel rod internal pressure and termination of the damage mechanism. The staff concludes, therefore, the delayed hydriding is not a damage mechanism that can lead to gross rupture of the fuel rod cladding." [NRC, 1985, pp. 32-33].

3.3.3 Cavitation damage

Pursuant to 10 CFR Part 72 Section 72(h), which regulated that *"The fuel cladding shall be protected against degradation and gross ruptures*[2]," the NRC indicated that:

"For protection to be adequate, the design of the cask should be such that degradation after at least a twenty-year storage life should not preclude the ability of the cladding to resist gross rupture during normal operations associated with cask unloading and subsequent fuel rod handling operations.

After reviewing the current research relating to spent fuel cladding damage mechanisms, the reviewers concluded that a diffusion controlled cavity growth (DCCG) mechanism was the only mechanism of damage for dry storage applicable to the storage conditions of the fuel rods that could cause degradation and gross rupture of the cladding. Under the influence of stress and temperature, this damage mechanism progresses by nucleation and growth of cavities along grain boundaries. This damage mechanism is serious since it can progress without external evidence of damage, may not cause pin holes or through cracks to relieve

[2] Text later amended to read: *"The spent fuel cladding must be protected during dry storage against degradation that leads to gross ruptures or the fuel must be otherwise confined such that degradation of the fuel during storage will not pose operational safety problems with respect to its removal from storage."* [FR, 1988].

the internal pressure, and manifests itself by a sudden non-ductile type of fracture. The staff has therefore paid particular attention to evaluating the potential for cladding damage from this mechanism for the conditions of storage specified in this TSAR." [NRC, 1985, p. 12].

The NRC utilized a diffusion-controlled cavity growth model (DCCG) to predict the accumulation of cavitation damage with stress and temperature. As a measure of damage, the NRC considered the fraction of grain boundary area undergoing decohesion according to a cavitation model developed by Raj and Ashby [Raj, 1975] to predict the intergranular fracture of metals at high temperatures. A fractional decohesion of less than 15% over twenty years was considered sufficient for granting a license. Namely:

"The progress of damage based upon the applied methods indicated the area of decohesion after 20 years of storage would be less than 15%. Based upon the degree of conservatism maintained throughout the analysis, it can be concluded that this level of damage is insignificant and would not be exceeded." [NRC, 1985, p. 33].

The NRC has continued using the DCCG model in more recent SERs, e.g., the NUHOMS®-24P SER [NRC, 1989]. In the latter document the NRC also gave explicit approval of the calculational methodology developed at PNL on behalf of the DOE [Levy, 1987]. Namely:

"Temperature limits for dry storage were developed by I.S. Levy, et al, in Reference 36. The NRC staff has reviewed and accepted the temperature limits developed in Reference 36." [NRC, 1989, p. 4-2]

The calculation methodology of [Levy, 1987] is also available in the open literature in [Chin, 1989] and is reviewed in Sections 3.4 and 5.3 of the current report.

3.3.4 Creep versus cavitation damage

The DCCG model was implemented by the NRC as a predictive tool for creep-rupture in preference to the Larson-Miller parameter approach [NRC, 1985, p. 33; Schwartz, 1987 and 1989]. However, the failure mode described by the NRC as potentially leading to *"a sudden non-ductile type of failure"* with no early manifestation of damage can hardly be identified as creep. By definition, the latter is a macroscopic phenomenon which does progress with *"external evidence of damage"* (creep strain) and manifests itself in three usually well-defined stages. After the accumulation of strain on initial loading, the primary or transient stage of creep occurs, during which strain continues to increase but at an ever decreasing rate. The rate eventually stabilizes and the process enters the secondary stage. The strain rate remains more or less constant during this stage but finally begins to accelerate as the creep process enters the tertiary stage. The tertiary stage is characterized by accelerating creep strain and concludes in rupture. Rupture, in theory, at high enough temperature, may be brought about by grain boundary decohesion due to the formation and linking of cavities.

Creep is a slow deformation phenomenon which can be significant during the high-temperature operation of mechanical equipment. Indeed, Zircaloy cladding creepdown is an important consideration in the design of Zircaloy-clad fuel rods for both PWR and BWR operation [Franklin, 1983]. As a rule, safe engineering practices implement operational conditions by which creep never reaches its tertiary stage. Inasmuch as cavity growth models do not address the evolution of the various stages of creep, they cannot be utilized for creep engineering purposes.

3.4 The DOE-sponsored studies

3.4.1 General results

The work produced on behalf of the DOE was carried out at Pacific Northwest Laboratories over a number of years. The results of the PNL analyses are summarized by Cunningham et al [Cunningham, 1987].

The PNL researchers found that:

> *"Possible cladding breach mechanisms for the spent fuel during IDS are creep rupture, SCC, and hydrogen-related failure mechanisms. Creep rupture (Section 3.1) is the most likely mechanism that could cause a cladding breach and is the principal basis for the IDS temperature limits presented in Section 4.1."* [Cunningham, 1987; p. 3.1].

The maximum cladding hoop stress assumed to exist during dry storage was 70 MPa. This stress level was found insufficient to initiate SCC, DHC and hydrogen-related failures, or other degradation modes (Table 3.1). Those authors also observed that in the discussion of all failure modes (including creep-rupture):

> *"An important point to consider ... is that once a crack breaches the cladding the driving force to continue propagating the crack is removed. The driving force for crack propagation in spent fuel is the stress caused by the pressure differential between the fill gas of the spent fuel and the cover gas. Once the cladding is breached, the pressure differential is relieved and the stress on the cladding is removed. Therefore, the identified degradation/cladding breach mechanisms should result in pinhole or hairline crack cladding breaches that release gas but not in gross ruptures that could release spent fuel particles (Cubicciotti, Jones, and Syrett 1980; Matta, Neimark, and Yaggee 1980)."* [Cunningham, 1987; p. 3.2].

3.4.2 Further details on creep-rupture

Unlike the NRC staff, the PNL researchers fail to give a reason why creep-rupture is deemed to be *the most likely* cladding failure mechanism. The only reason why creep-rupture was singled out seems to be that creep is a no-threshold phenomenon and it is known to take place to some extent when stress is applied over long periods of time (Table 3.1).

Table 3.1 Summary of Zircaloy Cladding Degradation and Failure Mechanisms During IDS (from [Cunningham, 1987])

Mechanism	Basis for Concern	Requirements	Conclusion
Creep rupture	Known creep behavior; long-term exposure of cladding to stress	Long-term exposure to stress	Primary degradation mechanism, set cladding temperature limits on basis of creep rupture
SCC	Observed in-reactor cladding breach due to SCC	K_{IC}[(a)]›3 I› $5x10^{-6}$	Not likely because of low stress and low free iodine concentrations
DHC	Hydride content of irradiated Zircaloy	Incipient defects; hydride; K_{IC}›12	Not likely because of low stress; probability of SCC cladding breach before DHC cladding breach
Hydride radial reorientation	Decreased fracture toughness	Hydride; σ›100	Not likely because of low stress
Hydrogen redistribution	Hydrogen content of irradiated Zircaloy	Hydrogen transport due to axial temperature gradient	Not likely because temperature and temperature gradients are too low
Irradiation embrittlement	Fracture toughness of Zircaloy reduced due to irradiation	K_{IC} › 40	Irradiated fracture toughness sufficiently high to preclude brittle fracture
Zircaloy/UO_2 oxidation	Reduced cladding thickness; UO_2 swelling increases cladding stress and strain	Free oxygen; temperature; time	Inert cover gas precludes oxidation
Strain rate embrittlement	Zircaloy ductility reduced during rapid strain	σ › 200	Not likely because of low stress

(a) K_{IC} is the critical stress intensity, MPa• $\sqrt{M}$; I is the iodine concentration, g/cm²; and σ is the stress, MPa.

Cunningham and his co-workers note the absence of experimental measurements of creep-rupture lifetimes of Zircaloy cladding but assume, without proof, that

> *"Intergranular fracture mechanisms dominate creep-rupture times at temperatures of interest for IDS. At stresses above ≈150 MPa fracture occurs by triple-point cracking. At stresses below ≈150 MPa, fracture occurs by grain boundary cavitation."*

They do report, however, some evidence of cavitation damage. Namely:

> *"Evidence for cavitation damage has been characterized by Keusseyan (1985) for Zircaloy-2 at temperatures from 350 to 400°C and at stresses near 100 MPa."*

and, therefore:

> *"Failure of the Zircaloy cladding by creep-rupture is caused by the formation of microscopic cracks/cavities within the material."*

Despite the obvious limitations associated with the above assumptions, the PNL investigators proceeded to generate models and a fracture map to predict time-to-fracture due to creep. Their predictions are reported in Figure 3.1. In this figure, the only relevant data obtained with actual Zircaloy cladding exposed to internal pressurization conditions are those of Peehs et al. [Peehs, 1983]. They show no fracture after a year of testing (total strain was less than 1%). Of the other data shown in Figure 3.1, those of Pahutová et al. [Pahutová, 1977] were obtained by uniaxial testing of thin strip specimens of Zr-Sn-Mo and Zr-Sn-Mo-Nb alloys. These data, perhaps not surprisingly, show little correlation with the predicted values. At the same time, while the data of Kreyns et al. [Kreyns, 1976], obtained by internal pressurization of Zircaloy-4 tubing, appear to show some correspondence between real and predicted values, they were actually iodine stress corrosion cracking experiments. This fact is not ignored by the authors of that report who qualify their findings thus:

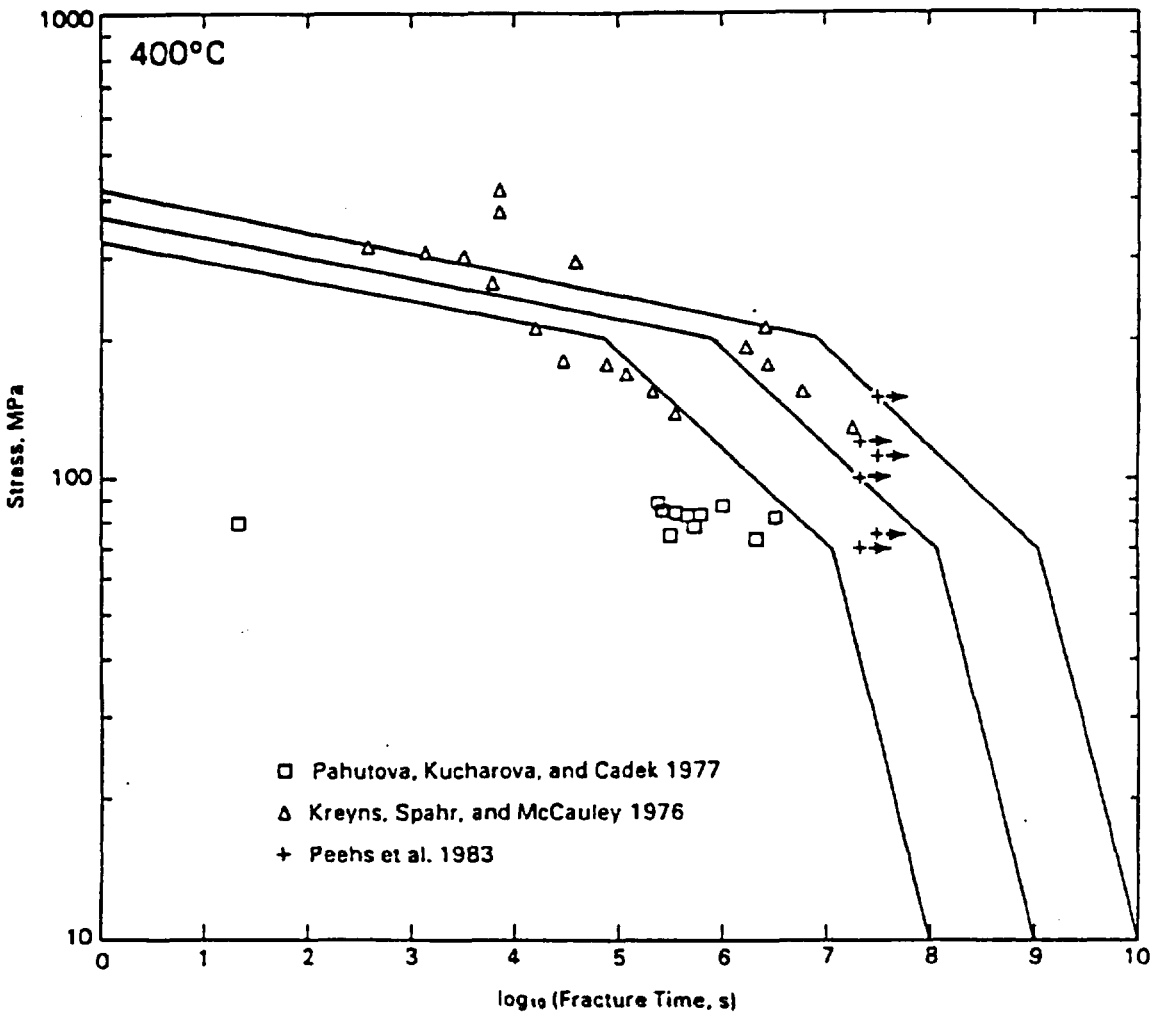

Figure 3.1 Comparison of predicted and measured creep time to fracture at 400°C. The middle curve is the prediction; the outer curves are order-of-magnitude shifts of the prediction. Arrows indicate that fracture did not occur. (From [Cunningham, 1987]).

"Additionally, much of the fracture data were obtained from programs investigating stress corrosion cracking (SCC) rather than creep rupture; experimental conditions (high stresses) were such that SCC occurred more rapidly than creep rupture occurred."

It could also have been added that all data points refer to stress levels of 70 MPa or higher (the [Kreyns, 1976] data were obtained with stresses in excess of 130 MPa). These are higher stresses than are considered likely to be encountered during the dry storage of both BWR and PWR fuel [Figure 2.2].

3.5 The German studies

3.5.1 General results

The German approach towards identifying the physical conditions under which spent fuel can be safely stored dry relies extensively on the utilization of experimental data. To that effect, a diversified experimental program has been carried out, including investigations of cladding integrity. [Peehs, 1986a] provides a general overview of the test programs that were performed and their results.

Initially, several potential degradation and failure modes of spent fuel cladding were identified [Peehs, 1986b]:

- creep from internal pressurization
- iodine-induced FSSCC
- external oxidation, and
- growth of a single, dominant crack.

These mechanisms were evaluated, both jointly and on a one-to-one basis, and empirical correlations of the experimental data were developed for extrapolation to longer dry storage times.

It was concluded that "*cladding creep is the mechanism which primarily limits the storage* *erature of the fuel in an inert atmosphere*" [Kaspar, 1985a]. Further, it has been stated that *the hoop strain* [resulting from the creep action] *limits the maximum insertion temperature, total strain is limited to 1% uniform elongation*" [Peehs, 1986b]. In the questions/answers on appended to [Peehs, 1986c], the authors indicate that the 1% strain limit "*was set* *rvatively as strain failure criteria*" and go on to point out that "*irradiated cladding can* *d hoop strains greater than 1% without failure.*" The German workers have concluded from the presently available data, "*the damage functions level very fast at non-problematic* *s, if the temperature decreases in accordance with the experience gained so far with the* *for dry storage and transportation. Different conditions, e.g., lower temperature decrease* *, need to be assessed in order to establish adequate storage strategies.*" [Peehs, 1986c]

Further details on the creep studies

The German researchers have utilized both unirradiated and irradiated internally-urized cladding tubes in their investigations. The initial creep studies with unirradiated ling provided an empirical correlation valid for Zircaloy-4 at temperatures between 300 and C and hoop stresses between 80 and 300 MPa [Romeiser, 1979]. This correlation was later ed to interpolate the hoop strain data of irradiated and unirradiated cladding creep-tested nperatures up to 450°C and hoop stresses of 50 to 70 MPa [Kaspar, 1985b; Porsch, 1986]. is found that the reference correlation compared well with the unirradiated creep data and istently predicted more conservative creep strain rates than were observed with the rimental data from the neutron-irradiated material (Figs. 3.2, 3.3 and 3.4). To some extent, atter result was to be expected because neutron radiation damage hardens the material, cing its ductility and impeding creep (i.e., slowing down the creep rate). Further, it was d that creep was more pronounced in the area of the fuel rod plenum compared with that her regions (Fig. 3.4). The plenum area is possibly the cladding section which undergoes east radiation damage, thus it is not surprising that it is apparently more ductile and eptible to creep than the other regions.

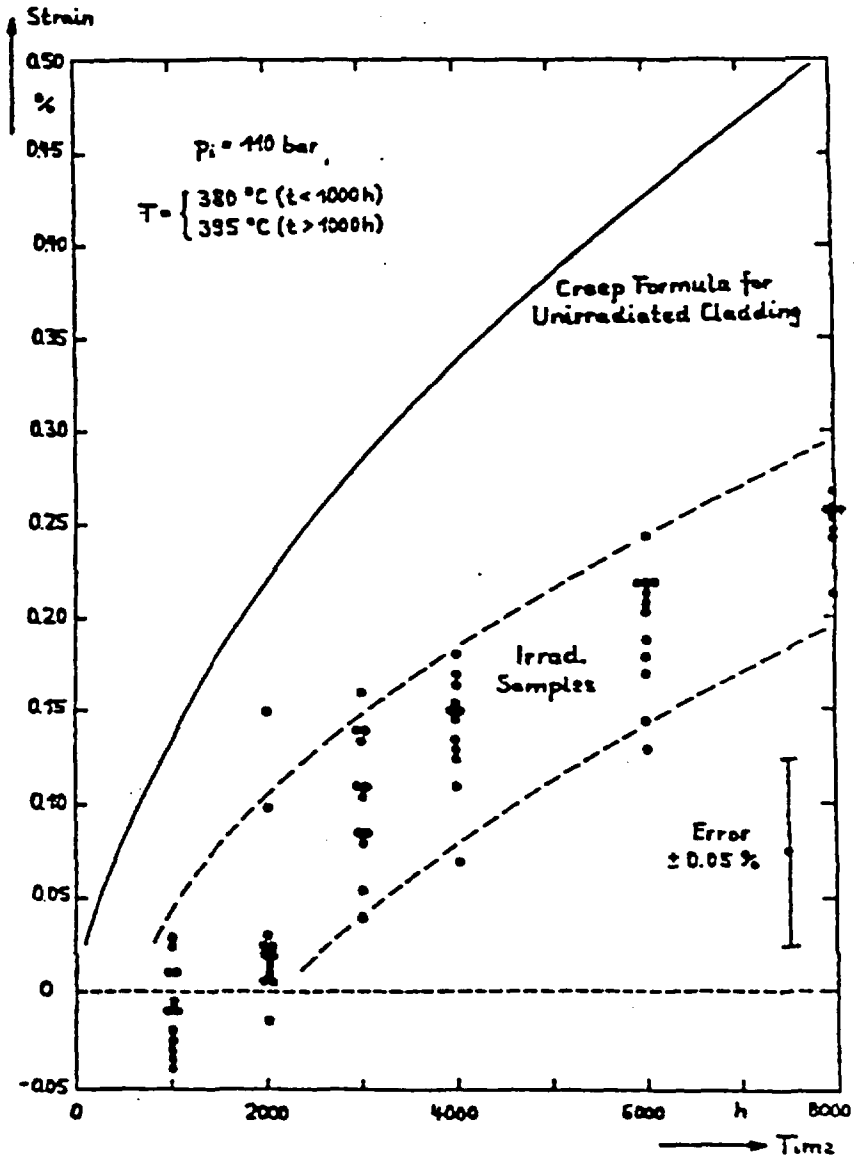

Figure 3.2 Creep strain as a function of time for unirradiated Zircaloy cladding. Dashed lines envelop the hoop strain data of Zircaloy cladding tested with a tensile hoop stress of 70 MPa. The solid line represents the predicted strain for unirradiated cladding (from [Kaspar, 1985b]). Note that some experimental samples exhibited negative initial strain. This effect is referred to in the text. Negative initial hoop strains appear with samples which possess a residual tensile hoop stress at reactor shutdown.

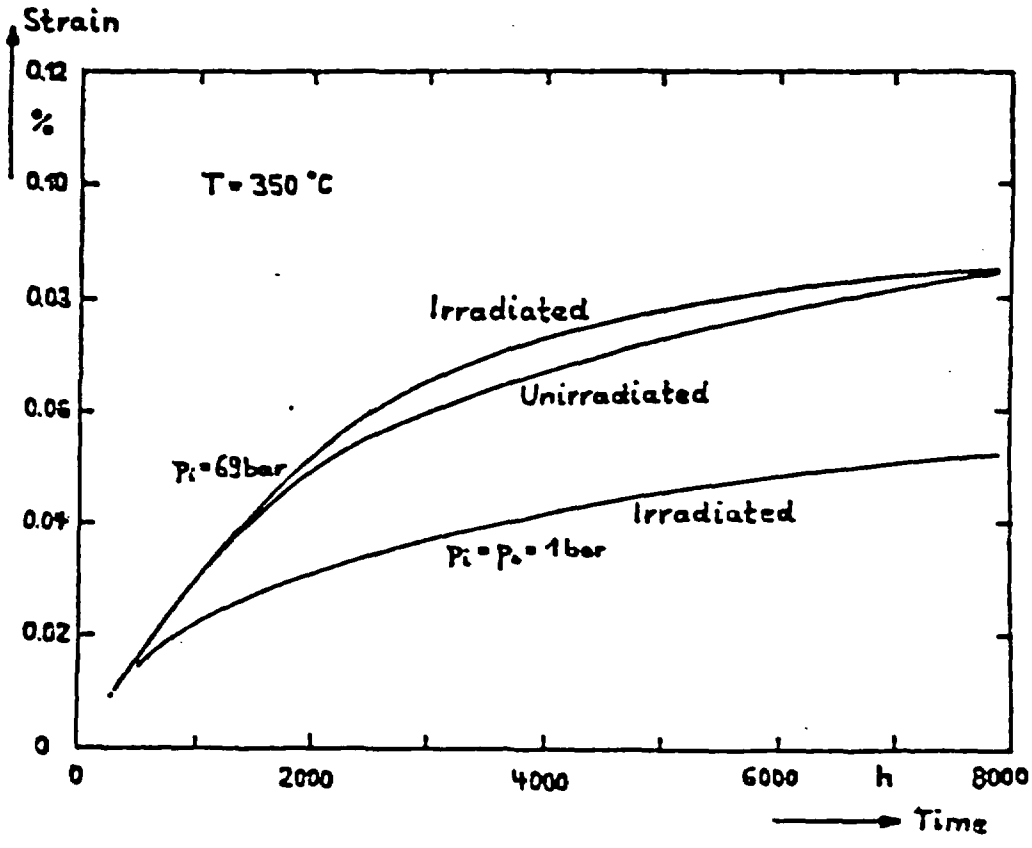

Figure 3.3 Creep strain as a function of time for irradiated and unirradiated Zircaloy cladding. The two upper curves represent the measured hoop strain of irradiated and unirradiated Zircaloy cladding for a hoop stress of 50 MPa. The absolute error of the data is $\pm 0.02\%$. The lowest curve represents the strain due to the release of the residual compressive stress present in the samples at reactor shutdown (from [Kaspar, 1985b]).

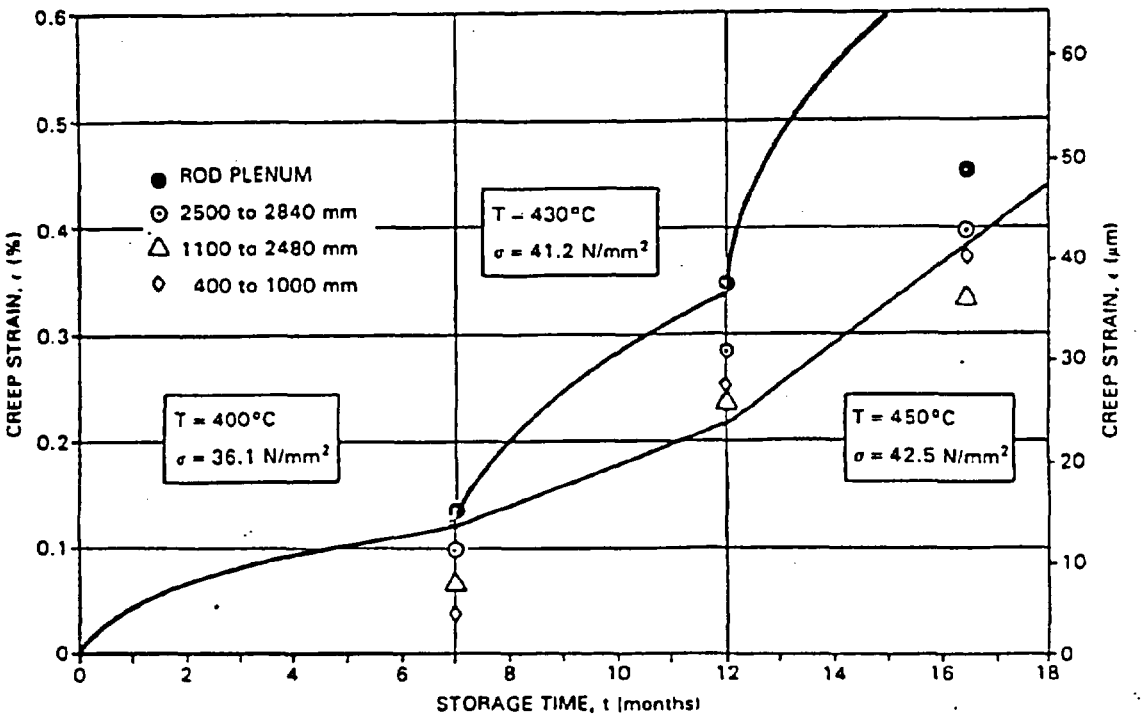

Figure 3.4 Variation of the hoop strain along a set of PWR fuel rods creep-tested within an increasing temperature regime. The solid lines represent hoop strain predictions based on different applications of the reference empirical correlation developed in Germany (from [Porsch, 1986]).

An unexpected finding of the German work is that the primary creep of irradiated Zircaloy is dependent on the residual stress which exists in the cladding at reactor shutdown. When the cladding is reheated and the temperature reaches a high enough value, this stress tends to be relieved, producing a tensile or compressive strain, depending on whether the residual stress was compressive or tensile, respectively. The phenomenon can be quite pronounced in the early stages of creep and may consume some of the conservatism in the empirical correlation. However, its overall effect is very small when compared with hoop strains of 1% or larger.

In general, the Germans appear to have adopted a practical and useful methodology for predicting fuel rod integrity during inert dry storage. The most important factor is that the predictions are based on actual creep data. In addition, the methodology has a built-in conservatism in that irradiated cladding creeps at a slower rate than the unirradiated cladding which forms the basis for the correlations. However, it must be emphasized that the reference empirical correlation is tuned to Zircaloy tubing for KWU PWR fuel and may not be directly applicable to clad tubing from other sources. The original study [Romeiser, 1979] employed tubing from two manufacturers and it was found that the model coefficients differed, although not substantially, with each manufacturer. Further analysis may be needed to determine the variability of those coefficients and their applicability to clad tubing from US manufacturers.

3.6 Conclusions

Several potential mechanisms for degradation and failure of spent fuel cladding while in IDS have been indentified. These mechanisms include SCC, DHC and creep. Of these, there exists a general consensus that the temperature limits which can be tolerated during IDS are determined primarily by the creep properties of the cladding.

SCC and DHC have been discounted by all researchers as requiring much higher activation stresses than are achievable during IDS. In the unlikely circumstance that these mechanisms form or help propagate a crack, the crack is thought to immediately relieve the internal pressure within the fuel rods and halt the failure mechanism at a stage where there

would not be a concern about gross ruptures. This would be true also of cracks whose propagation would be assisted by creep.

Creep, however, is viewed by the U.S. NRC as capable of producing sudden, non-ductile types of fracture with no external evidence of damage and without producing pressure relieving cracks. This type of damage would take place through the stress-assisted growth and linking of pre-existing microscopic cavities within the Zircaloy material.

The NRC view of creep as a mechanism which proceeds without external evidence of damage is in striking contrast with the common view of creep as a slow deformation phenomenon which manifests itself through the presence of measurable strain. Indeed, the engineering view of creep recognizes the successive deformation phases characterized, respectively, by a decreasing, an almost stable and an accelerating strain rate.

The engineering approach to Zircaloy creep study is commonly used in the design of fuel rods. It has also been applied extensively in Germany and, more recently, in Japan to study creep behavior during IDS. The results obtained in these countries support the view that strains of up to 1% are acceptable for total integrity of the spent fuel cladding during IDS.

4. EVALUATION OF CLADDING DEGRADATION AND FAILURE OBSERVATIONS

The preceding section summarized the most probable cladding degradation and failure mechanisms, and the approaches adopted by various groups in determining criteria for cladding performance in dry storage. There is a general consensus that the temperature limits which can be tolerated during dry storage are determined primarily by the creep properties of the cladding but the methods adopted to address degradation by creep differ from group to group. Discussion of some of the aspects of the problem follows.

4.1 The likelihood of gross rupture

It is a common thread among the various approaches that gross rupture must not occur. There are differences, however, in how determinations are made that gross rupture will not occur. The NRC methodology is based, in effect, on the assumption that failure of the spent fuel cladding will inevitably involve gross rupture. The DOE analysis, by contrast, has concluded that the operative failure mechanisms will result in pinhole or hairline cracks, not in gross ruptures. The Germans (and the Japanese) do not appear to address the failure characteristics directly but, rather, seek to minimize the possibility of the occurrence of any type of failure. Similarly, [Miller, 1989] does not differentiate between gross ruptures and small breaches, choosing instead to propose criteria involving permissible failure rates.

The most appropriate information for resolution of this problem would come from creep- or stress-rupture testing of internally-pressurized irradiated spent fuel cladding. However, there are few data available in this area, particularly of the most relevant type of test, stress-rupture at temperatures up to 450°C with stresses up to 100 MPa. Thus consideration has been taken also of observations made in other types of test:

- stress-rupture of internally-pressurized unirradiated cladding
- other tests involving internally-pressurized irradiated or unirradiated cladding (principally, iodine-induced stress corrosion cracking tests).

Review of the observations reported by the various researchers is complicated to some extent by their individual descriptions of the failure modes. [Shimada, 1983b] simplified the matter by providing photographic examples of the three types of failure they observed, so, for convenience, their descriptors were adopted for the present review. Briefly, the three modes are:

• ductile fracture	-	extensive damage, including both axial and circumferential tearing
	-	usually preceded by considerable deformation, probably of the ballooning type
• axial split	-	characterized by axial tearing only
	-	damage could be extensive
	-	may be accompanied by relatively little deformation.
• pinhole failure	-	damage restricted to very small area
	-	includes small narrow (hairline) cracks
	-	probably little deformation

Generally, the observations reported by other researchers could be assigned to one of these three categories, though occasionally some personal judgement had to be applied. For example, [Mattas, 1982], repeating observations originally presented in [Yagee, 1979 and 1980], described the failure mode of four tests as "rupture" and of three others as "crack." [Crescimanno, 1984] notes that the failure mode for all seven tests was by "axial split." From this, we have inferred that the four "ruptured" specimens had undergone axial tearing which had been preceded by some amount of deformation, whereas the other three specimens had developed axial cracks whose sizes were perhaps of only a small size, after a small amount of deformation. For the present review, we have generally adopted the [Crescimanno, 1984] interpretation but have provided additional comment when it was considered desirable.

In a similar vein, as indicated above, the term "pinhole failure" encompasses small hairline cracks. Photographs provided in [Yagee, 1980] indicate that the classification of

"pinhole failure mode" adopted by those authors included cracks of maximum width about 100 μm but whose length could be anywhere between 200-300 μm and several mm. Though such cracks represent breaching of the cladding, their geometric dimensions greatly restrict the migration of fuel particles to the surrounding environment. By contrast, both ductile fracture and axial splitting result in clad breaching which imposes few restrictions on the movement of fuel particles and thus these two modes should be considered as gross rupture phenomena.

4.1.1 Creep and stress-rupture testing of spent fuel cladding

With reference to spent fuel cladding, some creep and stress-rupture tests have been initiated but to date few ruptures have been recorded. The conditions surrounding those few are given in Table A-1 in Appendix A.

[Yagee, 1979 and 1980] investigated the susceptibility of spent fuel cladding to failure by stress corrosion cracking in the presence of iodine. In the process, two tests were conducted with pressurization using pure helium (no iodine added). An isothermal, isobaric (360°C, hoop stress 200 MPa) test on Zircaloy-4 cladding containing spent fuel from the H.B. Robinson PWR concluded with failure by what is described as "rupture" mode. The other test with pure helium (and also with fuel still in the specimen) involved a series of increasing pressure steps at 360°C, starting at 221 MPa and finally failing at 485 MPa, again by "rupture" (presumably axial splitting). The details of this particular test, which was not an isobaric stress-rupture test, are not included in Table A-1.

Other internally-pressurized stress-rupture tests on spent fuel cladding from H.B. Robinson plus some on Zircaloy-2 cladding from the Big Rock Point BWR are reported in [Chung, 1987]. Temperatures were 292 and 325°C, lower than those in [Yagee, 1979 and 1980], but the hoop stresses were much higher, ranging from 315 to 552 MPa. Such stresses are considerably in excess of those which will be experienced during dry storage but it must be emphasized that these tests were designed to study failure modes associated with PCI. However, the results are of some interest in defining the general characteristics of fracture resulting from creep of spent fuel cladding. The failure mode at the highest stresses, above 500 MPa, was

entirely ductile but some degrees of brittleness (defined by the existence of pseudocleavage on the fracture surfaces) were noted at the lower stresses. In a parallel series of expanding mandrel tests, the pseudocleavage morphology is associated with pinhole-type failure.

[Einziger, 1984] reported on five creep-rupture tests initiated on fuel rods from the Turkey Point Unit 3 PWR. The Zircaloy 4 rods were pressurized with helium to give a hoop stress of 145 MPa at 323°C but no cladding breaches were recorded for times up to 2101 h. The largest creep strain measured was 0.157%. Earlier, Einziger and coworkers had conducted tests at higher temperatures on fourteen rods from Turkey Point Unit 3 [Einziger, 1982]. Three temperatures were involved - 482, 510 and 571°C - and initial hoop stresses ranged from 25.2 to 75.7 MPa. Again, no cladding breaches were observed, although times were as long as 7680 h (at 510°C). At the same time, the rods accumulated significant amounts of creep strain, the smallest being 1.7% after 4652 h at 482°C and the highest about 7% after 740-1000 h at 571°C. As a consequence of the volume increase due to the creep strain, final hoop stresses were much lower than initial values and ranged from 19.5 to 35.6 MPa.

4.1.2 Stress-rupture testing of unirradiated fuel cladding

The database available on stress-rupture testing of unirradiated cladding is, of course, much more extensive than that on irradiated cladding. However, not every researcher has reported on the modes of failure observed. Figure 4.1 summarizes the reported observations in terms of failure modes at various stress-temperature combinations. In this figure, there is no differentiation between Zircaloy-2 and Zircaloy-4, nor is consideration given to the condition of the material (annealed, stress relieved, etc.). These details are listed together with the actual data and the sources in Table A-2 in Appendix A.

It is apparent from Fig. 4.1 that most of the unirradiated material underwent what we have defined as "gross rupture." This is not very surprising. The Zircaloys are known to be ductile materials, particularly in the annealed or fully recrystallized conditions, and gross rupture is normally associated with some significant deformation. The only instances of failure by pinhole leakage occurred at the lowest stress levels investigated, in the range 262-289 MPa, and

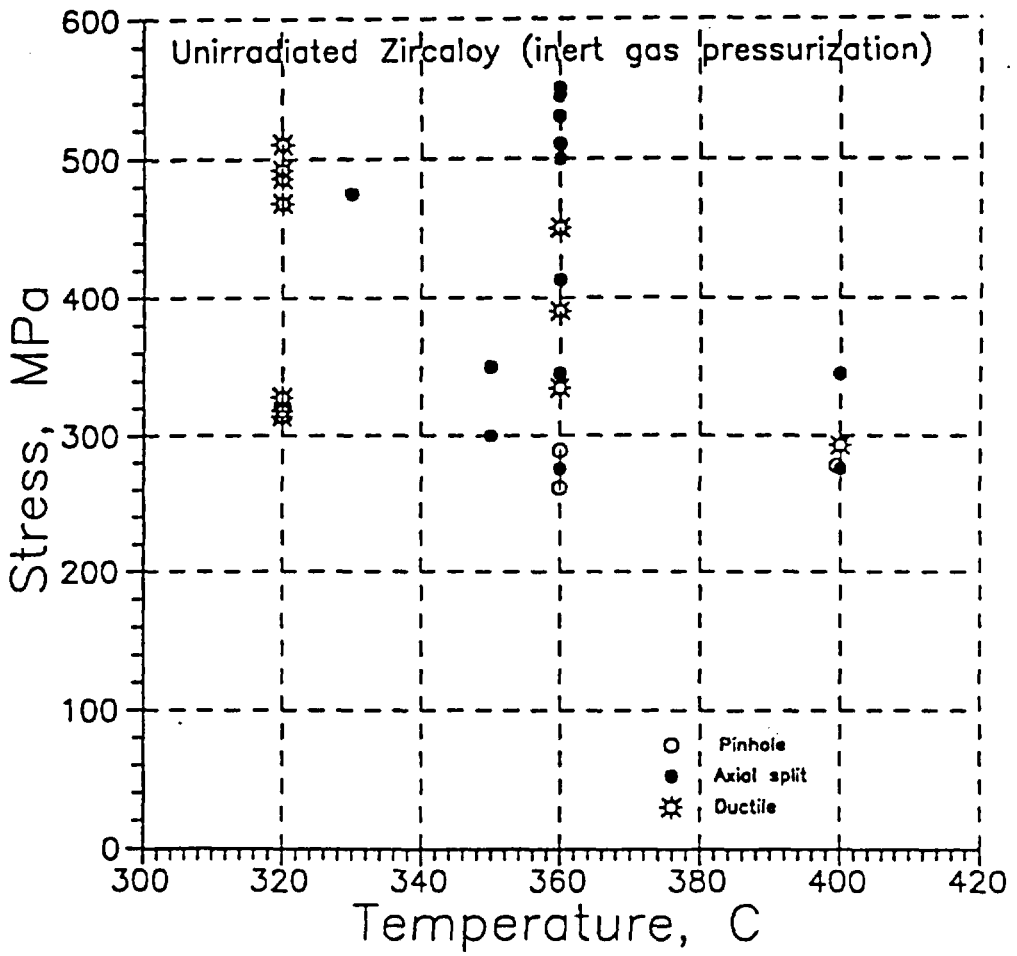

Figure 4.1 Failure mode observations resulting from inert gas internal pressurization tests on unirradiated Zircaloys

even in this range gross rupture was also recorded. However, these stresses are far in excess of those anticipated in fuel pins during dry storage, so the observations are really of only indirect relevance, merely inferring that, as the stresses are lowered, so the possibility of pinhole-type failure increases.

4.1.3 Stress corrosion cracking tests of fuel cladding

Interest in the susceptibility of fuel cladding to halogen-induced stress corrosion cracking promoted some extensive test programs in this area, with the result that a significant database has been created. This includes data obtained by internal pressurization of both irradiated and unirradiated cladding. Although one might hesitate to use the quantitative information generated (that is, rupture time at specific stress/temperature combinations) in evaluating the creep and stress-rupture properties of cladding material, the qualitative observations on failure modes are of some relevance.

The observations made during iodine-induced stress corrosion cracking (ISCC) tests on irradiated Zircaloys are assembled in Table A-3 and plotted in Figure 4.2. Some of the points shown have been displaced very slightly from their true coordinates in order to define more clearly the range of observations made at certain temperature/stress combinations. It is immediately obvious that none of these irradiated specimens underwent much deformation and no ductile ruptures were reported. In fact, pinhole leakage reports comprised more than 60% of the observations. Gross rupture, in the form of axial splitting, was noted in many instances when the stress was greater than about 270 MPa but at lower stresses pinhole leakage was by far the more common failure mode. Below a stress level of 200 MPa, only one instance of "axial splitting" was recorded (at 157 MPa). This particular specimen is a case where the [Crescimanno, 1984] classification of the failure has been used; the original report ([Yagee, 1979]) described the failure as a "crack." Reading a later paper ([Mattas, 1982]) by the same authors of [Yagee, 1979] indicates that this type of failure was viewed in much the same light as a pinhole failure and was of a relatively small size. Thus the damage incurred was probably much less than might be envisioned by the [Shimada, 1983b] example of "axial splitting." The same comment also applies to the observation of "axial splitting" at 360°C/205 MPa.

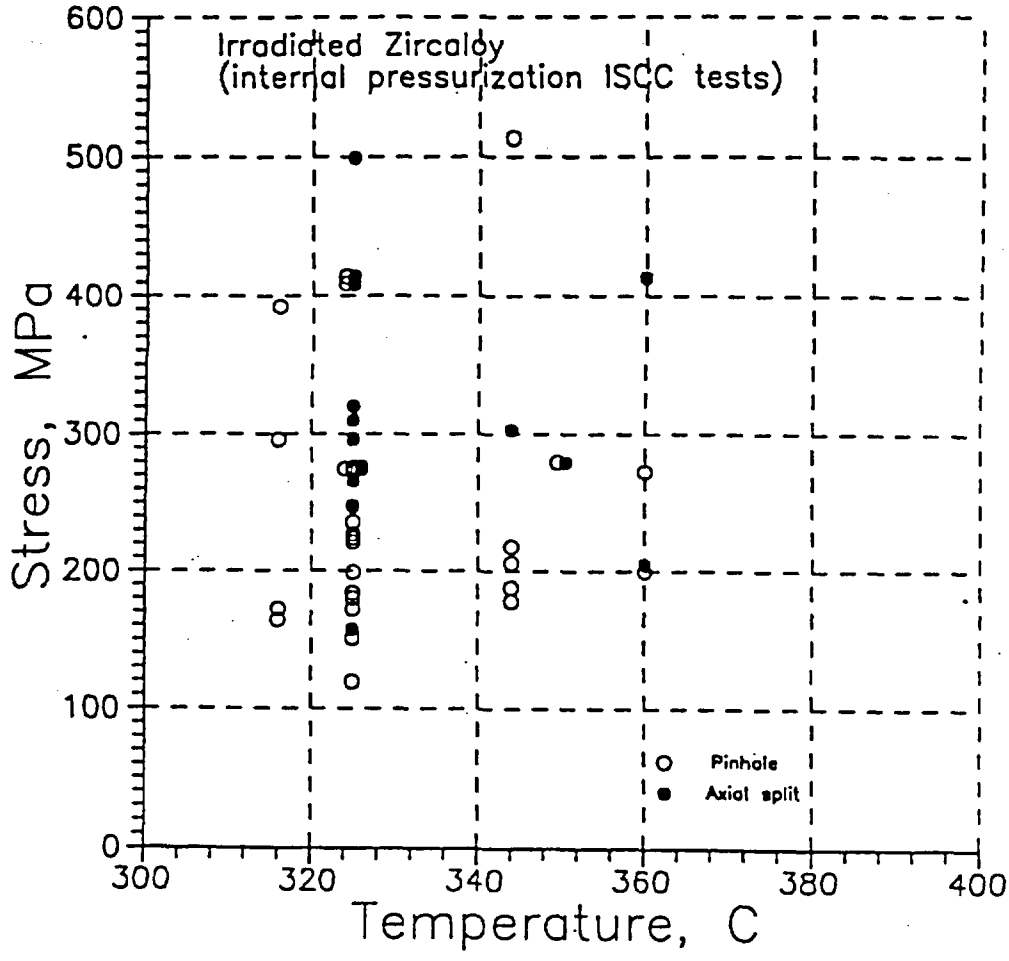

Figure 4.2 Failure mode observations resulting from internal pressurization ISCC tests on irradiated Zircaloys

The observations made during ISCC tests on unirradiated Zircaloys are listed in Table A-4 and plotted in Figure 4.3. As in Figure 4.2, some points have been displaced very slightly from their true coordinates in order to define more clearly the range of observations made at certain temperature/stress combinations. Pinhole leakage is again very prevalent and comprises more than 60% of the observations, similar to that noted for irradiated materials. When comparison is made with the latter materials, it would appear axial splitting was observed more frequently at stresses below 270 MPa and several instances of ductile rupture were noted. This is perhaps to be expected as the unirradiated materials are more ductile than the irradiated materials and "gross rupture" is more likely to be encountered (see Fig. 4.1)). Even so, it was not observed at stress levels less than 200 MPa.

4.1.4 Summary of failure mode observations

The observations described in the preceding subsections do not permit an unequivocal prediction of the failure mode most likely to be experienced by spent fuel cladding during dry storage. However, certain patterns are apparent. Unirradiated material will most probably undergo "gross rupture"-type failure in simple inert gas pressurization tests at the higher stress levels (above about 270 MPa). On the other hand, when a stress corrosion cracking agent such as iodine is introduced into the system, pinhole leakage becomes the most common failure mode, irrespective of whether the material is unirradiated or irradiated. Although "gross-rupture"-type failures are often observed under these conditions, they become much less frequent as the stress levels drop below about 270 MPa and are virtually absent at stresses below about 200 MPa. Such a stress level is at least twice that which will probably be the maximum encountered by the spent fuel cladding during dry storage.

The test conditions which produced the above observations are not prototypic of the spent fuel dry storage situation. However, it seems reasonable to conclude that spent fuel, if stored in an inert dry atmosphere at temperatures up to 400°C, will not fail (if it fails at all) in what would be described as a gross rupture mode. Alternatively, the implicit assumption by the NRC that the failure of the spent fuel cladding will inevitably involve gross rupture seems exceedingly conservative.

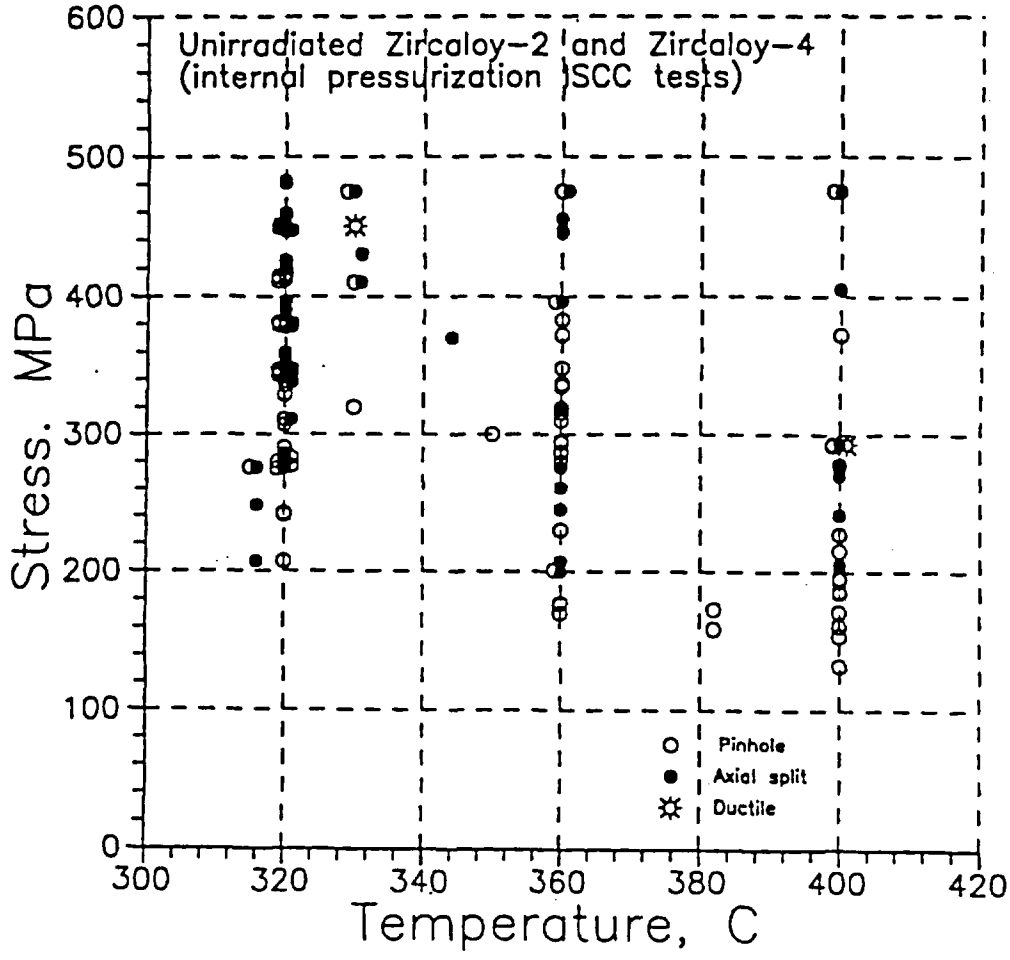

Figure 4.3 Failure mode observations resulting from internal pressurization ISCC tests on unirradiated Zircaloys

4.2 Creep of the Zircaloys and the contribution of cavities

4.2.1 Observations with unirradiated Zircaloys

Most of the creep data available on unirradiated Zircaloys have been derived from uniaxial tests. Generally, in these tests, creep may be characterized, at least in the intermediate temperature range of 200-500°C, by extended primary and tertiary stages coupled with a short secondary stage [Franklin, 1983]. There are few creep-to-rupture curves available from internally pressurized tests but those that are indicate a similar pattern (see, for example, [Aungst, 1965] and [Mayazumi, 1990b]). Typically, "*a large fraction of the strain and time in a creep rupture test in this temperature regime occurs during tertiary creep*" [Franklin, 1983]. Uniaxial creep tests on specimens cut from a cold-worked Zircaloy-2 pressure tube and tested in the temperature range 300-450°C spent more than 50% of the total test time and acquired more than 80% of the total strain while in the tertiary stage [Coleman, 1972]. Depending on the material and test conditions, fracture strains have been observed as low as a few percent and as high as over 100 percent. Eventual fracture is usually ductile in nature and microvoid coalescence is a contributory factor in the final stages. However, there is some dispute concerning the contribution of voids to the general effect of accelerating creep during the tertiary stage.

[Coleman, 1972] itemizes the four mechanisms which, in the absence of irradiation, lead to accelerating creep (i.e., tertiary creep) during constant load tests on Zircaloy-2:

(a) uniform reduction of load-carrying area
(b) specimen necking due to inhomogeneous deformation
(c) microstructural changes which reduce material strength
(d) reduction of load-carrying area due to the formation and growth of internal cracks.

Coleman found no evidence of the existence of grain boundary cavities in his specimens, even when they had been strained well into the tertiary stage, nor could he detect any other significant

microstructural changes. He concluded that the accelerating creep observed was caused by increases in stress due to uniform creep strain and that final failure was by necking and tensile fracture.

The observations of other researchers have generally supported Coleman's interpretation, in that microstructural examination of Zircaloy creep specimens have failed to detect any evidence of cavity formation (see, for example, [Povolo, 1981], [Fidleris, 1966]). The only exception has been in the work of Keusseyan et al. [Keusseyan, 1979 and 1985]. Keusseyan creep-tested specimens of Zircaloy-2 (in the temperature range 350-400°C for times from 120 to 960 hours) and Zircaloy-4 (at 375°C for 240 hours). These specimens acquired strains which ranged from less than 1% to over 10% for Zircaloy-2 and about 3% for Zircaloy-4. Cavities were reported in all specimens, even those with less than 1% strain, and the implication was that they nucleated in the very early stages, while the creep was still in the primary stage.

Among the differences between the Coleman and the Keusseyan tests, one of the more important may be the different methods used to reveal the presence (or otherwise) of cavities. Coleman, in his unsuccessful attempt to detect cavity formation during tertiary creep, used two approaches. In one, he took a specimen creep tested to 12% strain at 350°C, fractured it by impact at -196°C then examined the fracture surfaces by scanning electron microscopy (SEM); there was no evidence of micro-cavitation. The second, more indirect method, involved performing density measurements on samples taken from a specimen creep tested at 400°C to just prior to fracture (strain 20%). These showed a slight decrease in density but this was considered too small to be due to the presence of cavities. Keusseyan used neither of these methods. Instead, he took creep-strained specimens, fractured them by intergranular stress corrosion cracking in an iodine-containing solution and examined the fracture surfaces by SEM. The contribution of the prior creep deformation to the appearance of these fracture surfaces is not certain and the meaningfulness of the data are discussed in more detail in Appendix B. Suffice to say at this point that we have concluded that one should be hesitant in applying the observations of Keusseyan et al. to situations other than those pertaining to their specific tests.

4.2.2 Observations with irradiated Zircaloys

The above discussion concerned creep of unirradiated Zircaloys. Of more concern, however, is the performance of the alloys after irradiation, such as will be the case with spent fuel cladding. There is much information available of the in-reactor creep of the Zircaloys but there appear to be fewer data on out-of-reactor creep of irradiated material, which would be of more relevance in the present case. As a general rule, the creep rates measured in post-irradiation tests are lower than those obtained from unirradiated material, reflecting the effects of radiation hardening [Franklin, 1983] (in-reactor creep rates tend to be greater, sometimes exceeding those of unirradiated material). In addition, the secondary creep stage itself is much more easily defined than in the creep curves generated on unirradiated material. At the same time, the irradiation damage results in some loss of ductility at the lower temperatures. However, above about 350-400°C, damage recovery becomes increasingly important [Carpenter, 1974] and ductility is restored.

The microstructural condition of spent fuel cladding is significantly different from that of the original as-fabricated material and has been discussed previously, in Section 2.3. Briefly, the types and amount of damage inflicted by neutron irradiation are dependent on both the neutron fluence and the temperature [Northwood, 1977]. Among the most commonly observed forms of damage is the development of dislocation loops, both of interstitial and of vacancy in nature [Franklin, 1983; Griffiths, 1988]. The presence of these dislocation loops is a contributory factor in reducing the creep rate and the ductility, but their density (and hence effect) decreases as the defects are annealed out at temperature.

In contrast, another form of commonly observed radiation-induced defect, the void or cavity, is very infrequently seen in irradiated Zircaloys and it is generally accepted that these alloys are resistant to irradiation-induced void formation [Franklyn, 1983]. The only instances of the observation of cavities concern irradiated Zircaloy-2 [Gilbert, 1978; Holt, 1982; Griffiths, 1988] and in these cases, the numbers were few. As far as can be determined, no voids or cavities have been observed in irradiated Zircaloy-4. In the same context, examination of

fracture surfaces of post-irradiation tested spent fuel pins has also failed to reveal the presence of cavities [Chung, 1987].

One other type of microstructural feature is universally found in spent fuel cladding - the presence of hydride platelets formed as a consequence of hydrogen pick-up during reactor operation. While the platelets may lead to some loss of ductility at the lower temperatures, their presence is not thought to impact significantly on the creep properties.

4.2.3 Summary of cavity observations

Practically all the microstructural examinations of unirradiated Zircaloy creep specimens have failed to detect any evidence of cavity formation during creep. The only reports of such observations are in the work of Keusseyan et al. We have reached the conclusion that it is inappropriate to cite these observations because they were made on specimens fractured by intergranular stress corrosion cracking in an iodine-containing solution. With regard to materials in general, cavities are usually formed, if at all, during tertiary stage of creep. With this in mind, there would appear to be no need to use cavity growth models if engineering considerations are used whereby creep is never allowed to reach the tertiary stage.

Cavities are also often a byproduct of neutron irradiation but they have been seen very infrequently in irradiated Zircaloys. The only such observations have been in Zircaloy-2 and in these cases the numbers of cavities were very few. There have been no voids or cavities detected in irradiated Zircaloy-4. Thus cavity growth models based on the assumption that a large number of cavities exist even before creep begins are not justified in the case of the irradiated Zircaloys.

4.3 Conclusions

There is very little directly applicable information available on the failure mode most likely to be experienced by spent fuel cladding under IDS conditions. From a review of failure

modes observed under not-too-dissimilar conditions, it is concluded that failure by a gross rupture mode is extremely unlikely while in IDS.

In a related area, there is little evidence that cavities play a major role in the creep degradation of both irradiated and unirradiated Zircaloys. Thus the use of cavity growth models to describe the creep process is not justified in the case of spent fuel cladding.

5. DISCUSSION OF CREEP MODELING APPROACHES

5.1 Introduction

The term *creep* is used to describe the progressive deformation of a material under an applied stress. Curve A of Figure 5.1 represents a typical engineering creep curve of a metal under a constant load at a constant temperature. The curve is characterized by three stages: a primary stage of relatively rapid deformation during which the creep rate decreases with time; a secondary stage during which the creep rate stabilizes to a relatively constant value; and a tertiary stage where the creep rate increases rapidly with time until rupture occurs. The curve does not start with zero strain as it accounts for the instantaneous deformation, ϵ_o, which results upon the initial imposition of the load. When constant-stress tests are made, it is found that the onset of stage III is greatly delayed and a creep curve similar to curve B in Figure 5.1 is obtained [Dieter, 1986].

Primary creep spans a time interval during which the creep resistance of the material increases by virtue of its own deformation. Primary creep is the predominant creep regime at low stresses and temperature (less than one-half the melting point). The nearly constant creep rate of secondary creep results from the competing processes of strain hardening and recovery. Tertiary creep occurs at high stresses or temperature. During this stage an effective reduction in cross sectional area takes place either because of necking or because of internal structural changes in the metal. Four broad categories of creep-damage accumulation during this stage have been identified, each one containing one or more than one mechanism [Ashby, 1984]. In the case of Zircaloy, it has been reported that "*Creep damage is characterized by cavities which start at the grain boundary at the end of the second stage and which increase and multiply during the tertiary phase*" [Brun, 1987]. The latter observation was made relative to a uniaxial creep test on unirradiated, recrystallized Zircaloy-4 bar, at 350°C and relatively high stress (210 MPa). Recent creep fracture experiments at higher temperature (500°C) and lower stress (100 MPa) with internally-pressurized, unirradiated Zircaloy-4 fuel cladding led instead to the conclusion that " ... *the creep rupture at the test condition is induced by reducing the*

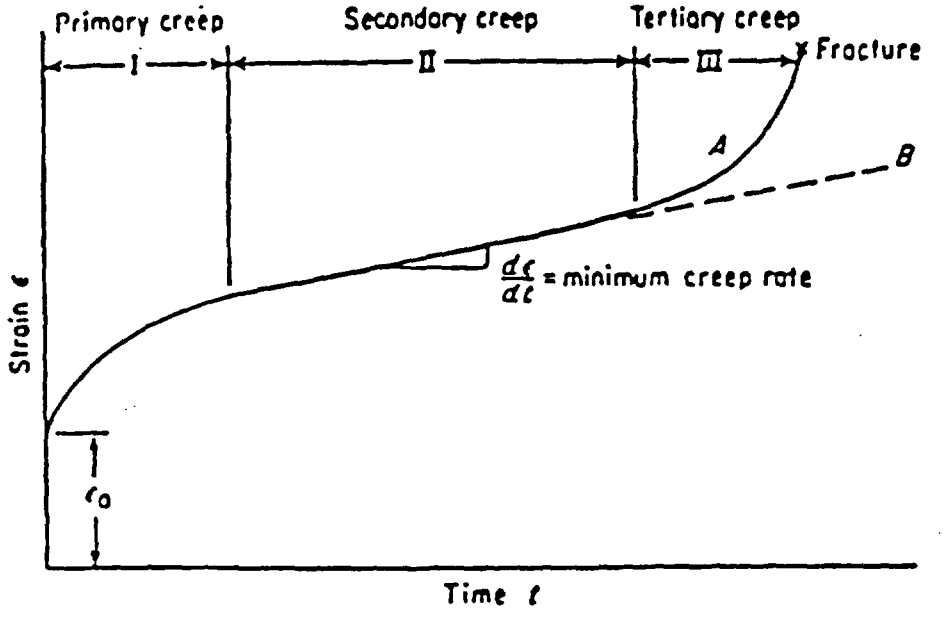

Figure 5.1 Typical creep curve showing the three steps of creep.
Curve A - constant load test
Curve B - constant stress test
(from [Dieter, 1986])

cross-sectional area in a manner similar to geometrical flow, neither by the grain boundary cavity [16] nor by the triple point cracking [17]" [Mayuzumi, 1990b].

A creep curve with three well defined stages is found generally only for a certain combinations of stresses and temperature. This is illustrated in Figure 5.2 which shows constant-stress creep curves at several stress levels and a single temperature. Internal pressurization tests under stress and temperature conditions comparable to those to be experienced during inert dry storage have never reached the tertiary stage and indicate two well defined creep stages for both irradiated and unirradiated Zircaloys. For internally pressurized unirradiated Zircaloy-4, the transition between primary and secondary creep appears to occur at a creep strain somewhat below 1% under the stress and temperature conditions of relevance to IDS. [Stehle, 1971] reports a value of ~0.8%, [Murty, 1977] 0.75% and [Matsuo, 1987] values from 0.47% to 0.85% for stresses between 74 MPa and 157 MPa.

In the past, in the absence of time-to-rupture data from internal pressurization tests, some investigators [Blackburn, 1978; Einziger, 1983; Miller, 1989] have attempted to estimate long-term time-to-rupture by extrapolation and have utilized the Larson-Miller parameter procedure. The NRC and the DOE researchers have been critical of this empirical approach [NRC, 1985; Cunningham, 1987; Chin, 1986 and 1989]. Indeed, the assessment made by Finnie in 1959 is still valid nowadays, namely:"*There is of course a limitation by which the testing time can be decreased. ... The loading conditions may strongly influence the rupture life in short-time tests, and even more important, the temperature required in short-term tests may be sufficient to cause grain growth, phase changes, or other effects in the material. Conversely, such effects as recrystallization, precipitation, and oxidation which may not be revealed by short-term tests can lead to faulty predictions. Extrapolation beyond the tested values of the parameters is also uncertain.*" [Finnie, 1959]

On the other hand, the uncertainty in the extrapolation may be reduced somewhat in the light of the recent accumulation of creep-rupture data by Mayuzumi [Mayuzumi, 1990b] and his findings that creep acceleration and rupture of internally-pressurized Zircaloy-4 cladding at high temperature is not associated with significant metallurgical changes in the material. Based on

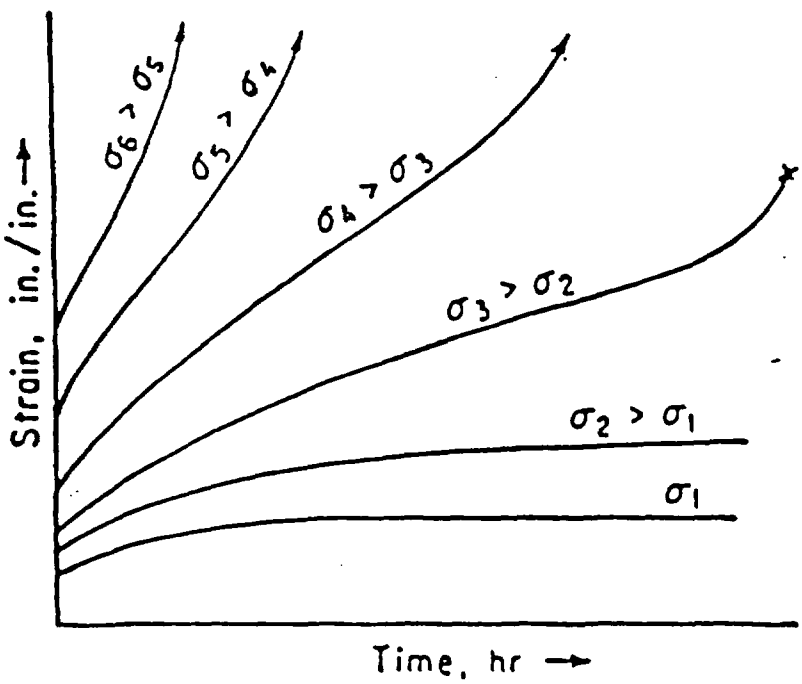

Figure 5.2 Schematic representation of the effect of stress on creep curves at constant temperature (from [Dieter, 1986])

Mayuzumi's fitting of his data to the Larson-Miller parameter equation, Figure 5.3, the time-to-rupture, t_f, under isothermal conditions can be expressed as follows in terms of the initial hoop stress, σ, and temperature, T:

$$t_f = 10^{\frac{\log(\sigma) - 5.024}{-0.000173T} - 20} \qquad (5.1)$$

where t_f is measured in hours; σ in MPa; and T in Kelvin.

Most investigators have focused their attention on a strain-to-failure criterion based on the shape of the creep curve. A strain-to-failure criterion is the approach implemented in dry storage programs in Germany (see Chapter 3) and in Japan [Mayuzumi, 1990a and 1991]. This approach is in keeping with standard creep engineering practices which implement operational conditions whereby the tertiary stage of creep is never reached. Indeed, whenever Zircaloy creep has been studied, all researchers have endeavored to identify the shape of the creep curve and a suitable correlation between the accumulated strain, time, the applied stress, and temperature.

The approach implemented by the DOE and the NRC is unique in terms of modeling in that it is based on creep-theoretical consideration applicable only to the tertiary stage of creep. This approach stems from an initial suggestion and consulting work by B. Chin on the use of deformation and fracture maps to predict creep rates and fracture mechanisms of unirradiated Zircaloy. The DOE and NRC basic reference model in the stress-temperature region of interest for dry storage views tertiary creep as dominated by the diffusion-assisted link-up of *pre-existing* cavities. The latter process generates grain-boundary decohesion and, eventually, failure. However, because grain-boundary decohesion cannot be directly linked to strain, the so-called DCCG-model (DCCG = Diffusion Controlled Cavity Growth) cannot be tested against actual engineering creep curves nor has the model been tested against actual cavitation data.

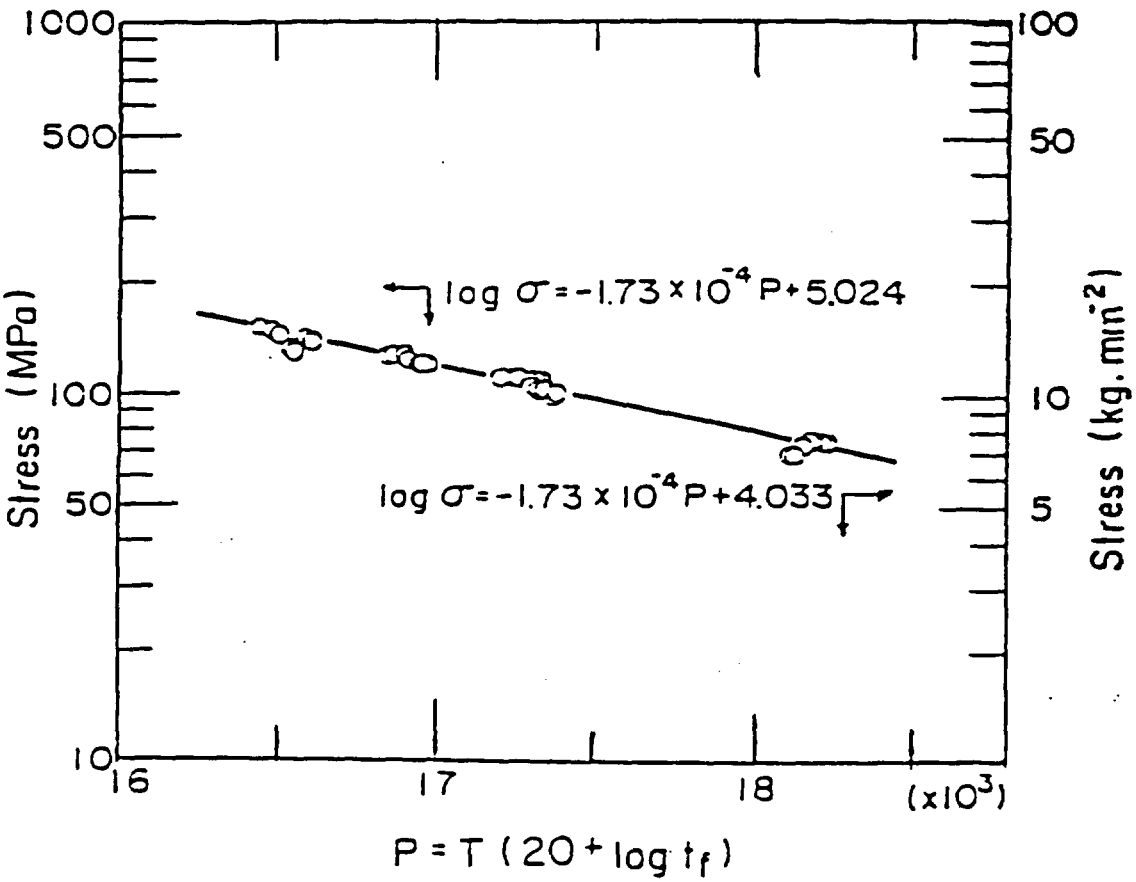

Figure 5.3 Relationship between the applied stress and the Larson-Miller parameter (from [Mayuzumi, 1990b]).

This chapter presents further details of the modeling approach of the DOE and NRC, and of the modeling approach implemented in Germany.

5.2 The NRC-sponsored work

The NRC modeling work [NRC, 1985; Schwartz, 1989] is based on the numerical implementation of a diffusion-controlled cavity growth model originally developed by R. Raj and M. F. Ashby (R&A, hereafter) to describe the process of intergranular cracking of metals at high temperatures [Raj, 1975]. Similar ideas were later proposed by Ashby for describing void growth during *tertiary* creep [Ashby, 1984].

5.2.1 The DCCG model

The nucleation process of intergranular cavities is not well understood, therefore cavitation models normally assume a fixed initial number of cavities of larger radius than the critical radius for void nucleation. These cavities are supposed to grow and link together upon the application of stress. The reference damage-accumulation variable of the R&A model is the fraction, A, of grain boundary which has undergone decohesion at a given time. The NRC allows only up to 15% decohesion during dry storage.

More in particular the model by R&A rests on the following assumptions:

1. A fixed initial number of critical-size voids are present in a periodic array and can grow as soon as stress is applied to the specimen;
2. Inclusion-free boundaries;
3. Only two-grain boundary junctions are present;
4. The stress is applied normally to the grain boundary;
5. Growth of the void volume occurs by diffusion of matter away from the void surface along the two-grain boundary.

A geometrical representation of the model is reported in Figure 5.4. Volume diffusion appears in the figure but it is not taken into account by the NRC although an addendum to the boundary diffusion model, also suggested by R&A, would make it possible.

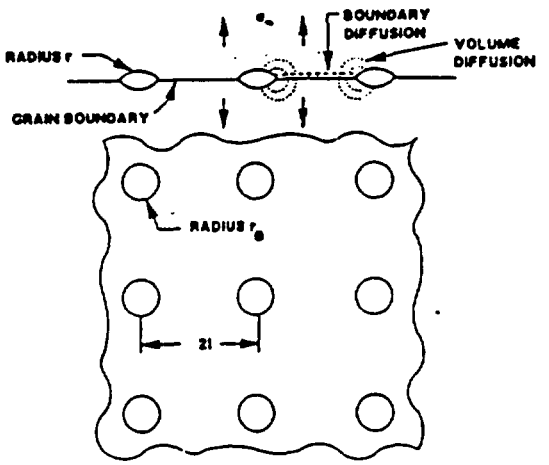

Figure 5.4 A periodic array of voids in a grain boundary. A tensile stress of σ_∞ is applied normal to the boundary [Raj, 1975].

In terms of A(t), the fractional amount of grain boundary area which has undergone decohesion by time t, the R&A model predicts the rate of decohesion to proceed as follows:

$$\frac{dA}{dt} = G(t) \cdot f(A) \qquad (5.2a)$$

where

$$G(t) = \frac{32}{3\sqrt{\pi}} \frac{[F_B(\alpha)]^{3/2}}{F_V(\alpha)} \frac{\Omega D_B(t)\,\delta}{kT(t)} \sigma(t)\,\rho^{3/2} \qquad (5.2b)$$

and

$$f(A) = \frac{1-A}{\sqrt{A}} \frac{[1-(r_c/r)(1-A)]}{-0.5\ln(A)-3/4+A(1-A/4)} \qquad (5.2c)$$

Equation (5.2a) is to be solved with the initial condition:

$$A(0) = A_{min} = \frac{r_c^2 F_B(\alpha)\rho}{\pi}$$

In the equations above, the indicated parameters are interpreted as follows:

- α - contact angle to the grain boundary; $\alpha=\cos^{-1}(\gamma_B/2\gamma)$, where γ_B is the energy per unit area of the grain boundary surface and γ is the energy per unit area of the free surface of the void,
- Ω - atomic volume of metal,
- ρ - number of critical-size voids per unit area in the grain boundary; $\rho=1/(2\ell)^2$, where 2ℓ is the average distance between cavities,
- δ - boundary thickness,
- σ - externally applied stress,
- D_B - grain boundary self-diffusion coefficient,
- k - Boltzmann constant,
- r - radius of curvature of the void surface,
- r_c - critical radius for void nucleation; $r_c=2\gamma/\sigma$, where γ is the surface free energy per unit area of the matrix material, and:

$$F_B(\alpha) = \pi \sin^2(\alpha),$$

$$F_V(\alpha) = \frac{2\pi}{3} [2 - 3\cos(\alpha) + \cos^3(\alpha)]$$

The functions F_V and F_B are related to the void volume, V, and to the boundary area, B, it replaces through the following relations:

$$V = r^3 F_V(\alpha)$$

and

$$B = r^2 F_B(\alpha).$$

The function f(A) represents the influence of the accumulated decohesion, A, on the instantaneous rate of decohesion, dA/dt. The shape of this function, Figure 5.5, is reminiscent of tertiary creep, in that it predicts an acceleration of the rate of damage as the level of damage increases. Figure 5.5 shows that at relatively high-damage levels, A>25%, say, the rate of decohesion is highly sensitive to the accumulated damage and varies non-linearly with it.

5.2.2 The NRC failure criterion

The NRC [NRC, 1985] re-expresses Equation (5.2a) as follows[3]:

$$\int_{A_i}^{A_f} \frac{dA}{f(A)} = \int_0^{t_f} G(t) \cdot dt \qquad (5.3a)$$

The integral in the LHS of Equation (5.3a) does <u>not</u> depend on adjustable parameters. Furthermore, as it was observed by R&A, that integral is not sensitive to the choice of A_i. Thus a master curve of the integral as function of A_f, a target degree of grain boundary decohesion,

[3] While Equation (5.3a) is formally correct, the NRC has obvious typos in the expression for G(t) and f(A). These appear correctly in the NRC-sponsored work of [Schwartz,1989].

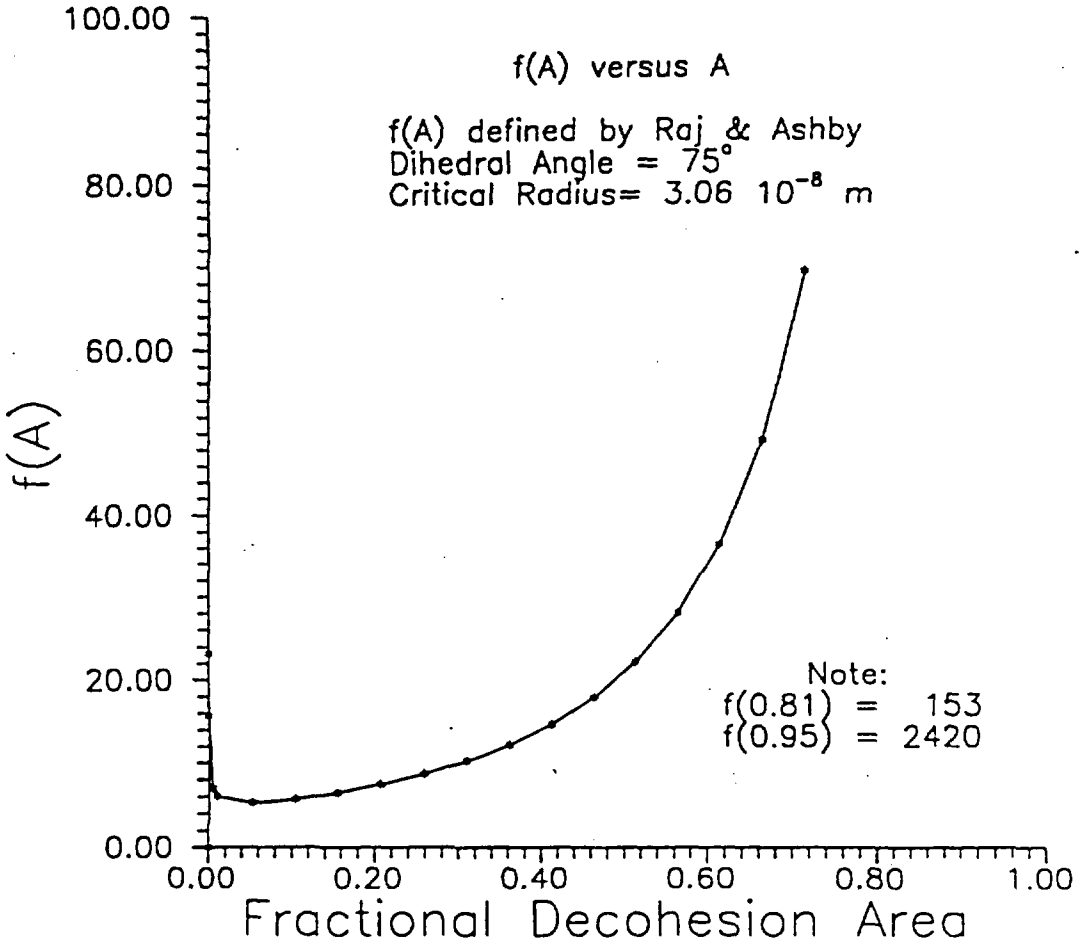

Figure 5.5 The variation of the area dependent term, f(A), of the R&A model.

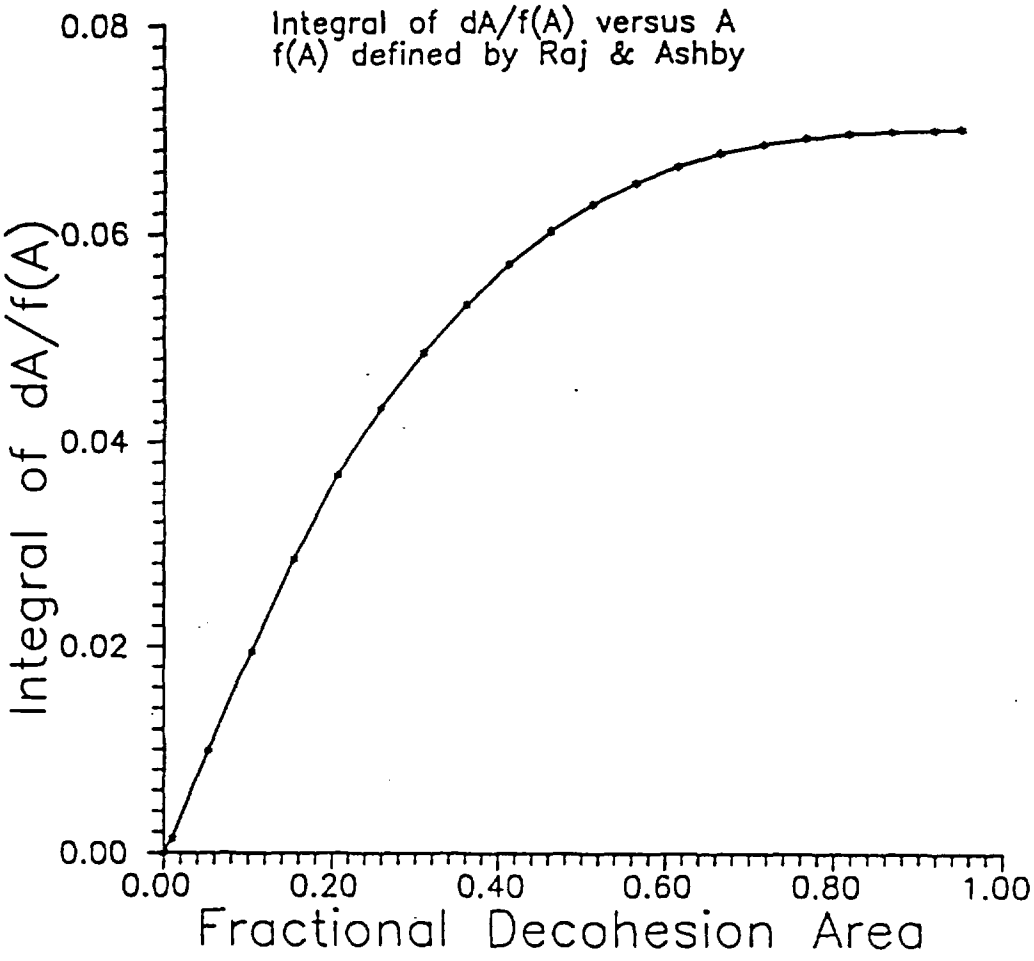

Figure 5.6 Variation of the LHS integral of Equation (5.3a) as a function of the fractional decohesion area.

can be easily generated. This curve is presented in Figure 5.6. The integral varies betweenzero and 0.067. In particular, when A_f=15%, its value is 0.026. Thus, in order to obtain the time-to-failure, t_f, according to the NRC decohesion criterion, it is sufficient to solve the following integral equality:

$$\int_0^{t_f} G(t)dt = 0.026 \qquad (5.3b)$$

The function G(t) in Equation (5.3b) depends on five physical parameters. The NRC reports that "*Much of the review effort focused on establishing the values of the parameters of the above expressions. Where there was wide divergence in reported values, the value that led to the most conservative result was selected.*" [NRC, 1985] The selected values and expressions were:

$\alpha = 50°$,
$\Omega = 3.37 \times 10^{-29}$ m^3/atom,
$\delta = 9.69 \times 10^{-10}$ m,
$2\ell = 10^{-5}$ m,

and:

$D_B = 5.9 \times 10^{-6} \exp(-131/RT)$ m^2/sec,

where R is the gas constant in units of kJ/mol-K.

5.2.3 Model validation

The NRC did not validate the model against actual grain-boundary decohesion-rate data during creep. Such data would not be available. In fact, voids or cavities are very infrequently

seen in irradiated Zircaloys and it is generally accepted that these alloys are resistant to irradiation-induced void formation (Section 4.2.2). Nor did the NRC attempt to test the model against a Zircaloy creep curve. Indeed, it would not be possible to relate grain-boundary decohesion to strain unless the full shape and scale of the engineering creep curve is known and additional modelling is made [Ashby, 1984]. Furthermore, the NRC did not attempt to verify the predictions of the DCCG model against those of other models.

5.2.4 Illustration of model predictions

Sensitivity analyses of the DCCG model were carried out at BNL (Appendix A in [Pescatore, 1989]) to test the effects of varying cavity spacing, temperature, initial pressure, and dihedral angle on grain-boundary decohesion. In these studies all parameters except one were held constant. These analyses show that the fractional decohesion area is sensitive to *all* parameters tested. It is most sensitive to the assumed temperature history and to cavity spacing.

In order to illustrate the high sensitivity of the DCCG model to the temperature history of the spent fuel rods during dry storage, we shall evaluate the NRC storage-time criterion, Equation (5.3b), against two realistic but slightly offset temperature histories. Namely:

$$T(t) = 350°C - 3.5\ t\ (\text{years}) \qquad (5.4a)$$

and

$$T(t) = 335°C - 3.5\ t\ (\text{years}) \qquad (5.4b)$$

We shall also assume, realistically, that the room-temperature gas pressure within the fuel rods is 32.5 atm and the associated cladding hoop stress 26 MPa. All other parameters are taken to coincide with the NRC suggested values (see Section 5.2.2). Our calculations show then that the maximum allowable storage time is 15 years at the lower temperature and 4 years at the higher temperature, i.e., a 4% increase in the storage temperature results in almost a 400% decrease in the allowable storage time. These results cast further doubts as to the applicability

of the DCCG model to predict Zircaloy cladding behavior under strain conditions far removed from tertiary creep.

5.3 The DOE-sponsored work

5.3.1 Main results

The creep modeling work sponsored by the DOE is summarized in [Levy, 1987] and [Chin, 1989].

The DOE-sponsored studies are especially important for, in the USA, they provide the temperature limit curves which are normally utilized for determining the maximum allowable temperature (MAT) during IDS.

The DOE-suggested MAT limit curves supporting a storage time of 40 years are reported in Figure 5.7. The temperature limit values depend on the initial hoop stress in the cladding and on the age of the fuel. The older the fuel, the lower the MAT limits. This is because, all other conditions being the same, older fuel decays at a slower rate than younger fuel and results in longer-lasting high temperature fields and stress conditions.

The calculational procedure developed on behalf of the DOE is claimed to be consistent with the grain-boundary decohesion criterion of the NRC (see Section 5.2.2 of this report), if the latter is increased from 15% to 20%. Indeed, the NRC has approved the use of the DOE-generated temperature limit curves for the preparation of topical safety analysis reports of dry storage casks [NRC, 1989]. In actuality, we shall show that the two approaches are not numerically consistent with each other and exhibit similar theoretical and experimental deficiencies.

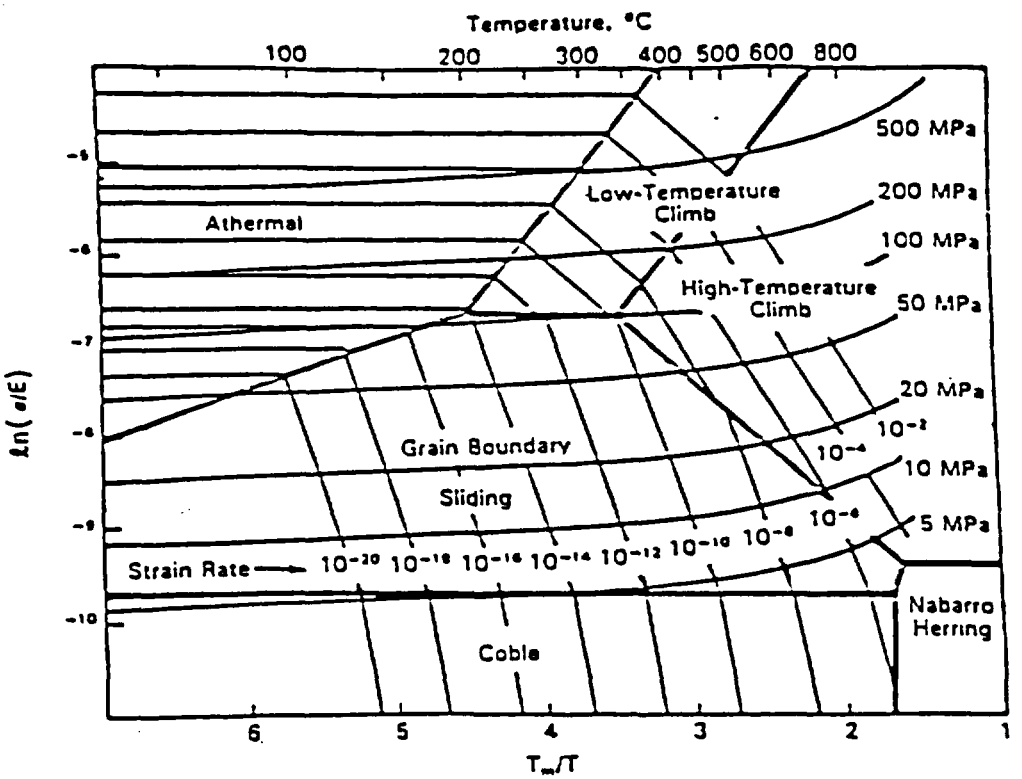

Figure 5.8 Deformation map for Zircaloy with constant stress and strain rate contours (strain rate is in s^{-1}) (from [Chin, 1989]).

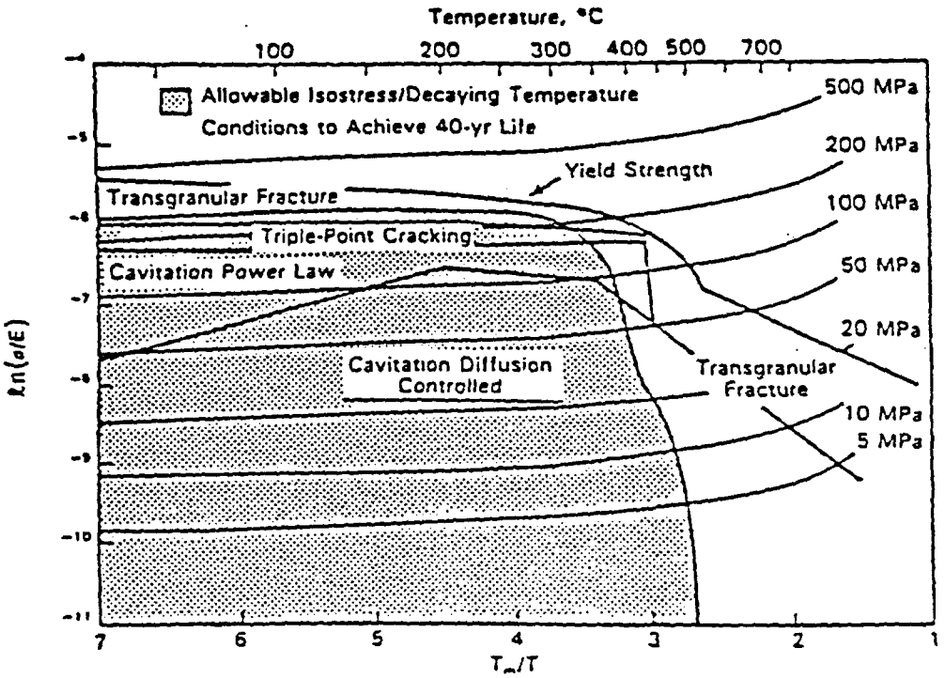

Figure 5.9 Fracture map for Zircaloy showing dominant fracture mechanisms (from [Chin, 1989]).

5.3.3 Model predictions

Eventually the DOE-researchers found themselves with the task to provide the appropriate values for their model parameters and to validate their predictions. It was then realized that no reference tertiary-creep data could be utilized in the stress-temperature region typical of IDS. Namely:

Table 5.1 Fracture Equations

Theoretical shear strength	$\sigma_{th} = \left(\frac{E\gamma_f}{a_o}\right)^{1/2} \approx \frac{E}{10}$
Transgranular fracture	$t_f^{TG} = \left[\epsilon_n + \left(\frac{1}{4.937}\right)\left(\frac{n}{n-1}\right)\ln\left(\frac{0.38}{f_v^{1/2}} - 1\right)\right]\epsilon^{-1}$
Triple-point cracking	$t_f^{TP} = \frac{\gamma_f}{Ed\xi}\left(\frac{\sigma}{E}\right)^{-1}\epsilon^{-1}$
Cavitation-diffusional growth	$t_f^{CD} = \frac{2.525 \times 10^{-3} l^3}{\delta D_{0gb} b^2 \exp(\frac{-Q_{gb}}{RT})}\left(\frac{kT}{Eb}\right)\left(\frac{\sigma}{E}\right)^{-1}$
Cavitation-power law growth	$t_f^{CP} = \left[\frac{(1 - 0.78 P_0 l_0)}{4.87}\right]\epsilon^{-1}$

Table 5.2 Symbols and Coefficient Values For Fracture Equations

t_f = time to fracture(s)

ϵ_n = hole nucleation strain = 0.08

f_v = volume fraction of intragranular inclusions = 0.025

P_o = average particle diameter = 10 nm (100 Å)

l_o = particle spacing along boundary = 2.0×10^{-6} m

ξ = ϵ_{GBS}/ϵ = contribution of grain boundary strain rate to total strain rate = 0.2

l = average cavity spacing = 2.6×10^{-6} m (6/grain segment)

σ = width of grain boundary = 1.6×10^{-8} m (50 Burger's vectors)

γ_f = free surface energy created by fracture = 35 J/m^2

α_o = lattice spacing (m)

σ_{th} = maximum theoretical stress

D_{0gb} = Grain boundary self-diffusion coefficient = 3.89×10^{-6} m^2/s

Q_{gb} = Activation energy for grain boundary diffusion = 175 kJ/mol

b = Burger's vector = 3.23×10^{-10} m

E = Young's modulus

"Measured creep-rate data and creep-rupture-time data are required in the CSFM model to calibrate the mechanism equations. Measured rupture times, however, are lacking at temperatures below 400°C and stresses below 100 MPa. ...the model predictions, therefore, are principally based on the selection of material parameters used in the mechanism equations. In this study, key parameters that can affect the predicted creep-rupture lifetime were evaluated. These predictions were then related to failure limits based on an assessment of reasonable creep strain limits." [Levy, 1987]

Therefore, in the process of selecting the "best" parameter values according to their subjective criteria, Chin, Levy, and their co-workers indirectly decided on which would be "reasonable" strain-to-failures. The lowest curve in Figure 5.10 indicates that the strain-to-failure built-in in the CSFM model is less than 0.5% below 50 MPa and reaches 1% above 100 MPa. Also, the strain-to-failure is larger at 20 MPa than between 30 and 90 MPa, say, whereas one would expect the strain-to-failure to increase monotonically with the applied stress (see Figure 5.2). These built-in values are in stark contrast with the available data base from internally pressurized cladding creep tests which suggests strains to failure much larger that 1%.

The poor representation of the physical reality afforded by the CSFM model is also demonstrated in Figure 5.11 which reports the model predictions against the creep strain data from the so-called Ispra experiment, an internal pressurization test with actual fuel rods which was run under a temperature field increasing with time. The CSFM model grossly overestimates the experimental creep strain data and the strain rate[5].

[5] The CSFM model predictions should be contrasted with the predictions of the same data which are afforded by the creep model developed in Germany. A preliminary glimpse at the latter can be obtained by examining Figure 16a,b which also refer to the Ispra experiment.

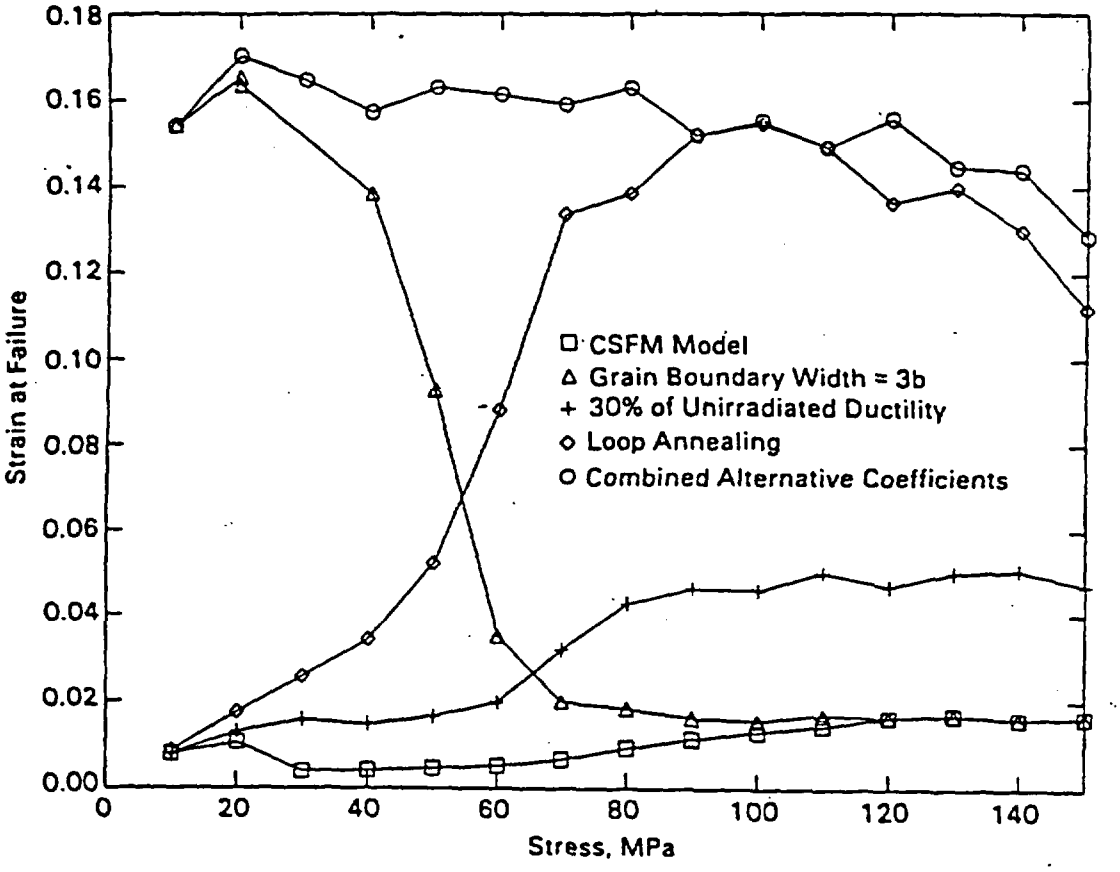

Figure 5.10 Effect of alternate values of theoretical and empirical coefficients on failure strain (from [Levy, 1987]).

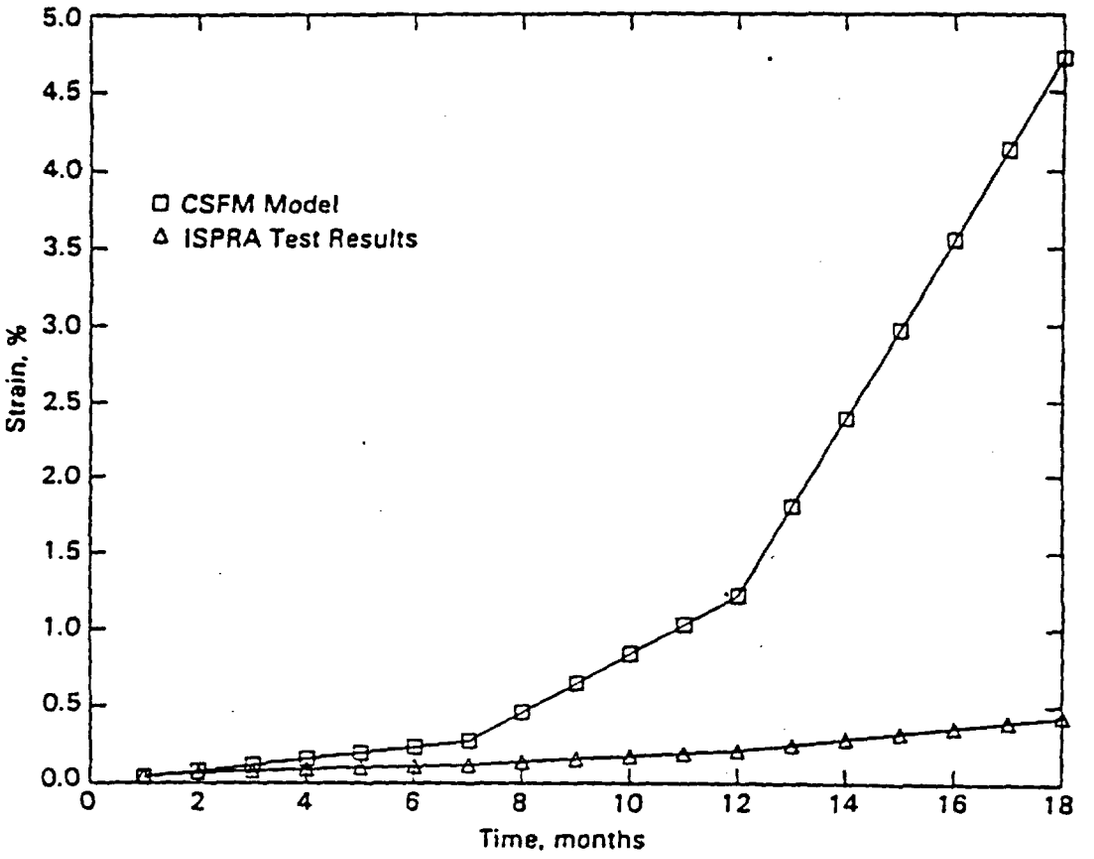

Figure 5.11 Comparison of CSFM-predicted creep-strain to measured creep-strain for the ISPRA spent fuel tests (from [Levy, 1987]).

5.3.4 Inconsistency with the NRC criterion

The reported congruency of the CSFM model temperature-limit predictions with those based on the NRC criterion for grain boundary decohesion reflects a mistake made by the developers of the CSFM model when they interpreted the NRC failure criterion and the original paper by Raj and Ashby. According to R&A, 100% decohesion implies that a certain monotonic positive integral function, which has been plotted before as Figure 5.6, has the value of 0.067. Thus, for decohesion to be less or equal to 100% it must be:

$$\int_0^{t_f} G(t)\,dt \leq 0.067 \qquad (5.4a)$$

where the function G(t) has been defined in Section 5.2. When decohesion is 15%, as in the NRC failure criterion, the integral equals 0.026 and about 0.036 for 20% decohesion. The DOE researchers reported instead a good agreement with the following would-be NRC criterion:

$$\int_0^{t_f} G(t)\,dt = 0.15 \qquad (5.4b)$$

The latter is not only inconsistent with the failure criterion of the NRC, Equation (5.3b), but also internally inconsistent with the DCCG model according to which, on physical grounds, grain boundary decohesion can never exceed 100%, Equation (5.4a).

Thus the CSFM model appears to have no defensible experimental and theoretical basis and its predictions are both internally inconsistent (because the DCCG model is part of the

CSFM model) and not consistent with the NRC failure criterion. On the other hand, because the CSFM model

(a) seemingly implements faster creep strain rates than are observed experimentally (see Figure 5.11), and

(b) it assumes artificially small strains to failure,

it likely provides very conservative predictions of cladding creep behavior.

5.3.5 Illustration of model predictions

For consistency with Section 5.2.3, we shall evalute the MAT limits for spent fuel cladding with a room temperature gas pressure of 32.5 atm and an associated cladding hoop stress of 26 MPa. Taking Equation (5.4a) as the reference temperature decay curve, the initial storage temperature decreases at a rate of 3.5 degrees per year. The latter is a decay rate typical of older fuel, i.e., 10- to 15-years old fuel. We have shown that if the initial temperature were 350°C, and therefore the initial hoop stress 54 MPa, the NRC criterion would allow only 4 years in storage. Following the 10-years-old-fuel curve of Figure 5.7, we realize that the DOE suggests that the same fuel could be stored safely for 40 years (less if the fuel were 15-years old).

Once again, the above predictions demonstrate the inconsitency between the NRC criterion and the DOE-suggested MAT limits. The DOE predictions may be conservative with respect to the actual creep data but not so with respect to the NRC criterion. From the point of view of the DCCG model and grain boundary decohesion, the DOE allows the cladding to fail several times over, while that can happen only once in the DCCG model as used by the NRC.

5.4 The experimental correlation developed in Germany

Realizing that creep-rupture data under temperature and stress conditions typical of IDS were not available and could not be obtained in a reasonable time frame, the German researchers concentrated on the engineering creep curve of Zircaloy-4 and on the primary and secondary stage of creep under internal pressurization conditions. An empirical correlation was initially obtained [Romeiser, 1979] for unirradiated Zircaloy-4 cladding creep-tested at temperatures between 300 and 400°C, hoop stresses between 80 and 300 MPa, and up to 1.5% hoop strains. An example data fit is provided in Figure 5.12.

The empirical correlation is meant to apply to primary creep and to the initial stages of secondary creep [Romeiser, 1979] under iso-thermal and iso-tonic conditions and reads as follows:

$$\epsilon = A\,[B/T - \ln(\sigma/C)/\ln(t+1) - 1]^m \qquad (5.5)$$

where ϵ is the percent hoop strain, σ is the hoop stress in MPa, T is the temperature in degrees Kelvin, t is the time in hours. The parameter values applicable to KWU's PWR Zircaloy-4 cladding are:

$A = 1.89 \times 10^{-3}$

$B = 610$ K

$C = 450$ MPa

$m = -2.58$

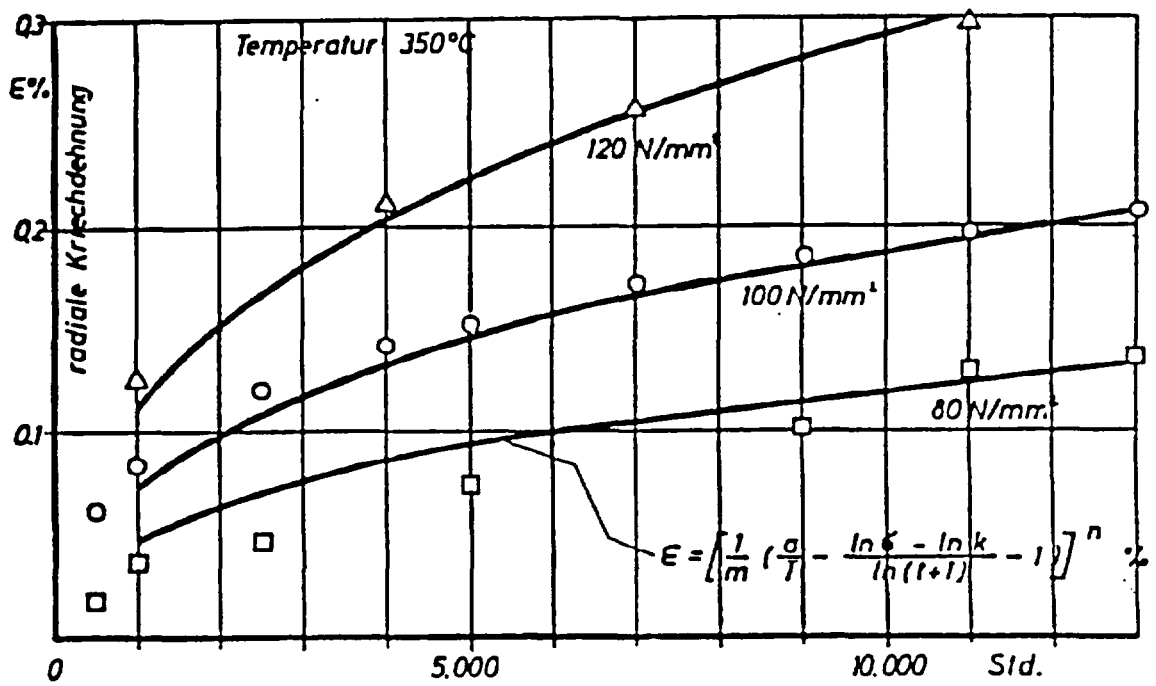

Figure 5.12 Creep of fuel rods under internal pressure (from [Romeiser, 1979]).

5.4.1 Model validation

The correlation has been tested against later creep strain data of both unirradiated cladding and irradiated cladding under internal pressurization conditions. These creep tests were carried out at temperatures up to 450°C, up to 10% hoop strains, and at more typical dry storage hoop stresses of 50 to 70 MPa [Kaspar, 1985b; Porsch, 1986]. It was found that the correlation compares favorably with the unirradiated creep data (Figures 5.13 and 5.14). For irradiated cladding, the correlation predicts more conservative creep-strain rates than are observed experimentally (Figures 5.15 and 5.16). To some extent the latter results are to be expected because neutron radiation damage hardens the material, reducing its ductility and slowing down the creep rate. Figure 5.16 is especially instructive to that effect in that it shows that creep is more pronounced in the area of the fuel rod plenum than in other regions. The plenum area is possibly the cladding section which undergoes the least radiation damage. Thus it is not surprising that it is apparently more ductile and susceptible to creep than the other regions.

5.4.1.1 Application of the strain-hardening rule

With reference to Figure 5.16, the reported fit of the data can be improved further. It must be observed first that the reported hoop stresses do not increase proportionately with the increase in the absolute temperature, as one would expect. This follows from the test procedure. Thus, the Ispra test can be considered as one where the temperature and the hoop stress were changed independently from each other. In generalizing the correlation to non-isothermal and non-isotonic conditions, the strain-hardening rule should be used [Lucas, 1981; Mayazumi, 1991b]. The lower curve of Fig. 5.16 represents the application of the strain-hardening rule for a condition where the hoop stress increases proportionately with temperature, starting with 31 MPa at 400°C. The middle curve represents instead the full non-isothermal and non-isotonic case. It provides a better fit of the data and a conservative, but still reasonable, strain rate. The upper curve is a brute force use of the correlation starting with the accumulated strain and resetting the time to zero at each change of experimental conditions.

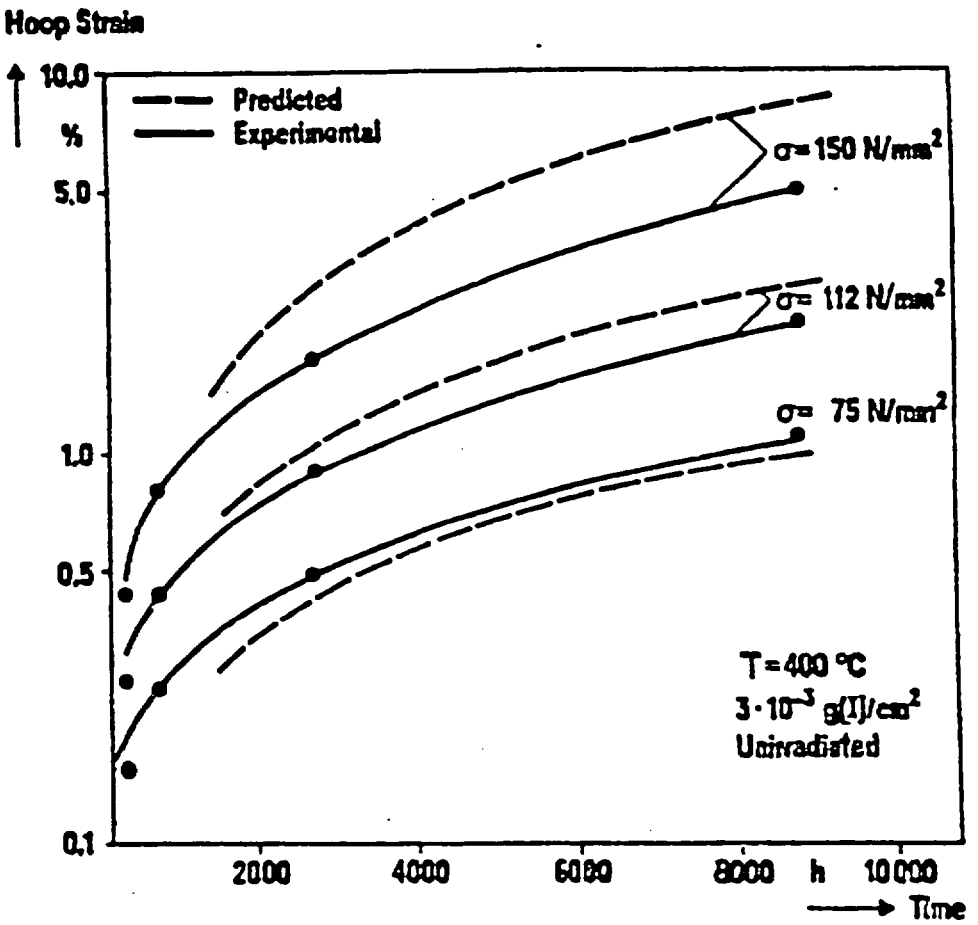

Figure 5.13 Creep of unirradiated fuel rod (from [Kaspar, 1985b]).

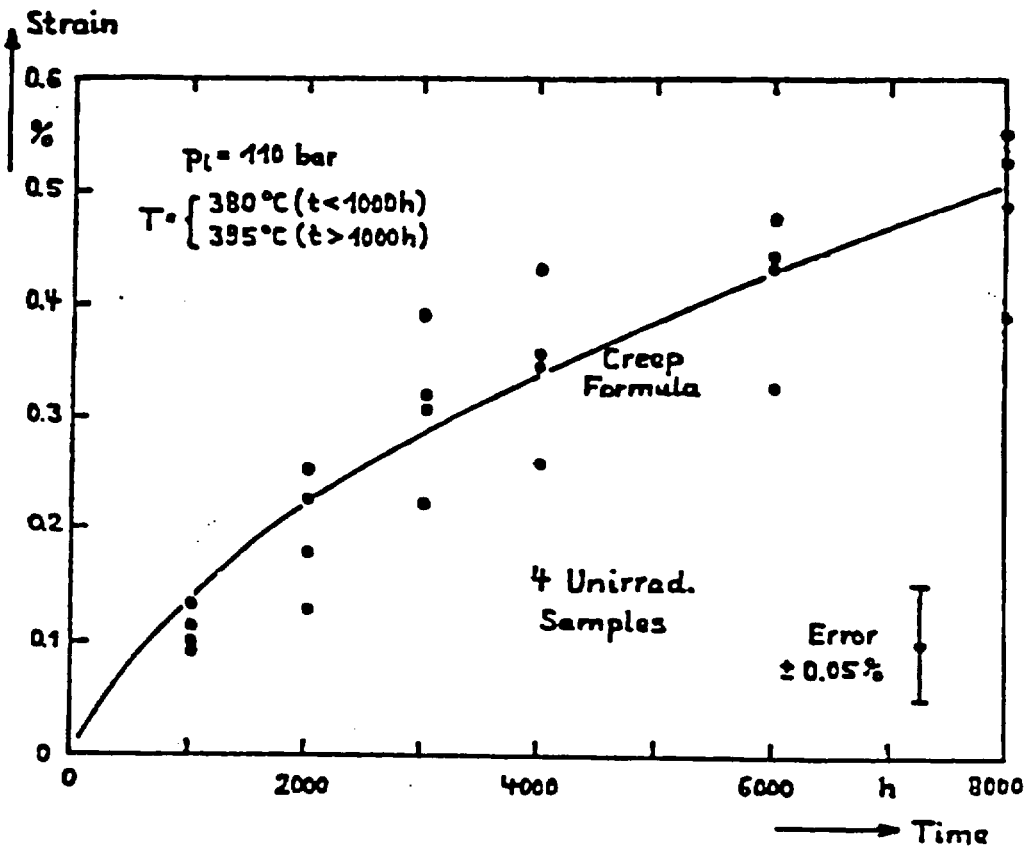

Figure 5.14 Creep of unirradiated FRG-2 reference fuel rod material (from [Kaspar, 1985b]).

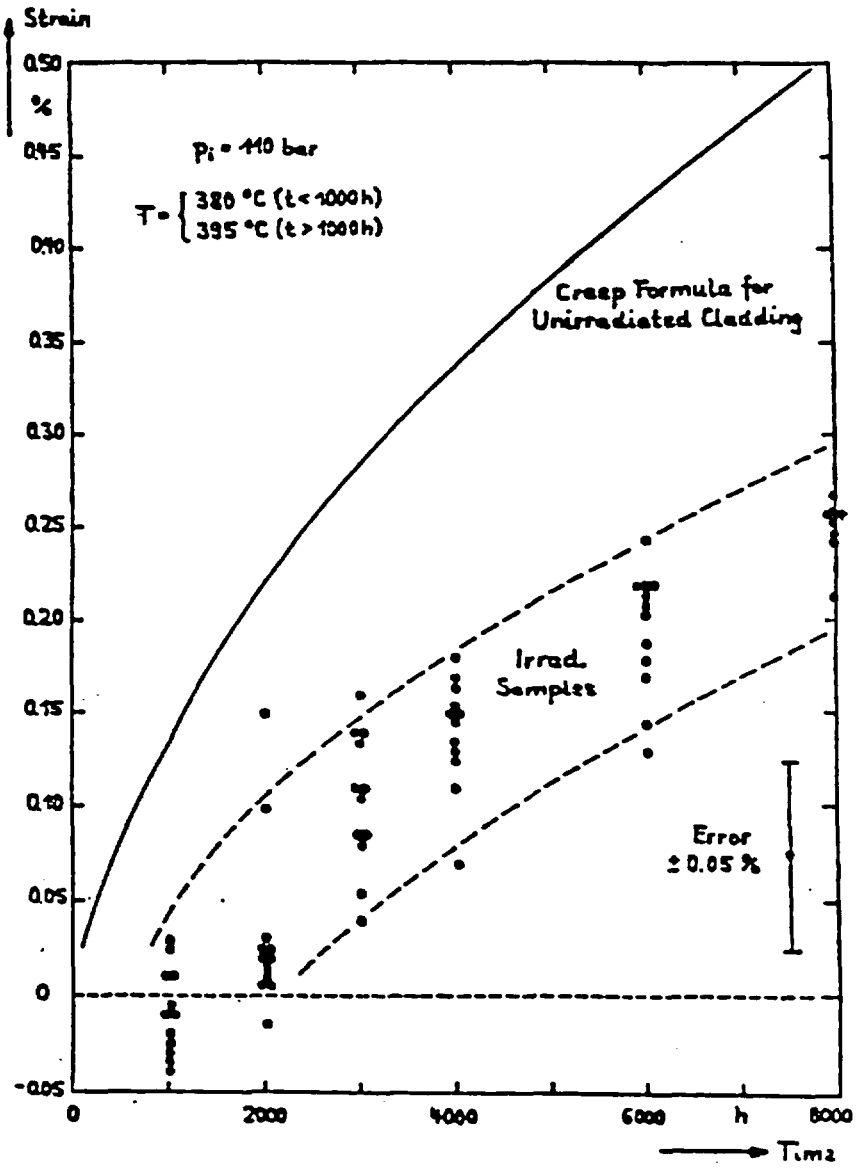

Figure 5.15 Creep strain data of Zircaloy cladding tested with tensile hoop stress of 70 MPa. The solid line represents the predicted strain for unirradiated cladding (from [Kaspar, 1985b]).

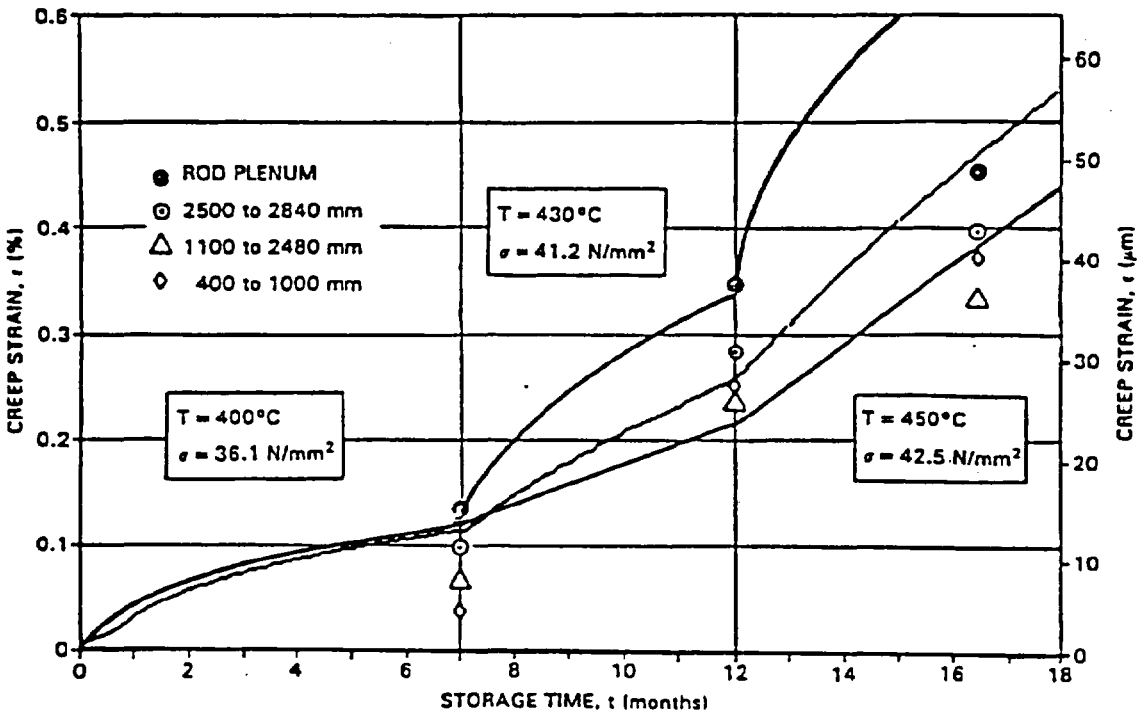

Figure 5.16 Variation of hoop strain along a set of PWR fuel rods tested within an increasing temperature regime. The solid lines represent hoop strain predictions based on different applications of the reference empirical correlation developed in Germany (from [Porsch, 1986]). The dashed line represents the predictions based on the full non-isothermal and non-isotropic case.

By comparing the predictions based on the German correlation with those by the CSFM model, one realizes that the former offers more robust predictions than the latter. The strength of the German correlation derives from its foundation in the experimental data. Furthermore the creep-prediction methodology based on the German correlation has a built-in conservatism in that irradiated cladding creeps at a slower rate than the unirradiated cladding which forms the basis of the correlation.

5.4.1.2 Domain of applicability of the reference correlation

The German correlation has been tested over a wide enough range of temperatures, hoop stresses, and strains to cover all expected operating conditions during IDS. On the other hand, because it is empirically based, it should not be extended significantly beyond those conditions under which it has been validated. Namely, $300°C < T < 450°C$, $50 \text{ MPa} < \sigma < 300 \text{ MPa}$, and $\epsilon < 10\%$.

5.4.2 Illustration of model predictions

A detailed analysis was performed in [Pescatore, 1989] to show how sensitive the predicted strain is to changes in temperature, pressure, and in all the empirical constants of Equation (5.5). The analysis shows that the correlation is fairly insensitive to changes in all parameters.

For consistency with the example calculations made in sections 5.2.3 and 5.3.3, we shall apply the correlation to predict the hoop strain of spent fuel cladding with a room-temperature gas pressure of 26 atm and a corresponding hoop stress of 32.5 MPa. The reference temperature-decay curve is as follows (Case 1):

$$T(t) = 350°C - 3.5\ t \text{ (years)}$$

We shall impose a further restriction, that the temperature never decays below 300°C. With the latter stipulation, we shall consider also an alternative temperature-decay curve (Case 2) starting at 400°C. Namely:

$$T(t) = 400°C - 3.5\ t\ (\text{years})$$

Applying the strain-hardening rule, in Case 1 the hoop strain is predicted to increase as shown by the lower curve of Figure 5.17, i.e., after a few years, the hoop strain stabilizes at a value of about 0.15% and does not grow significantly over the next decades. The upper curve of Figure 5.17 refers to Case 2. In this case the hoop strain stabilizes at a value of 0.75%. Both temperature histories result in low and, most likely, safe strain values over several decades.

Comparing the above predictions with the analogous ones based on the NRC and the DOE models and acceptance criteria, it is readily realized that the use of the German correlation, along with their 1%-strain acceptance criterion, would make possible substantially higher storage temperatures than are presently achievable in the US program.

5.4.3 Potential application in the U.S. program

It is not clear to what extent the German correlation would apply with unchanged parameter values to spent PWR fuel generated in the U.S. program. The correlation should be tested against data applicable to those rods. A preliminary check with data obtained with Turkey Point spent fuel tested at 482°C and 49.5 MPa (both values are not significantly different from the applicability limits of 450°C and 50 MPa for the German correlation) over 4652 hours is promising. The calculated value for the hoop strain is 1.85% while the observed value was 1.65% [Einzinger, 1982]. In another whole-rod test with irradiated fuel at 323°C and with a hoop stress of 150 MPa, the measured hoop strain [Einziger, 1983] was 0.16% over a test duration of 2101 hours. The German correlation gives an estimated strain of 0.18%.

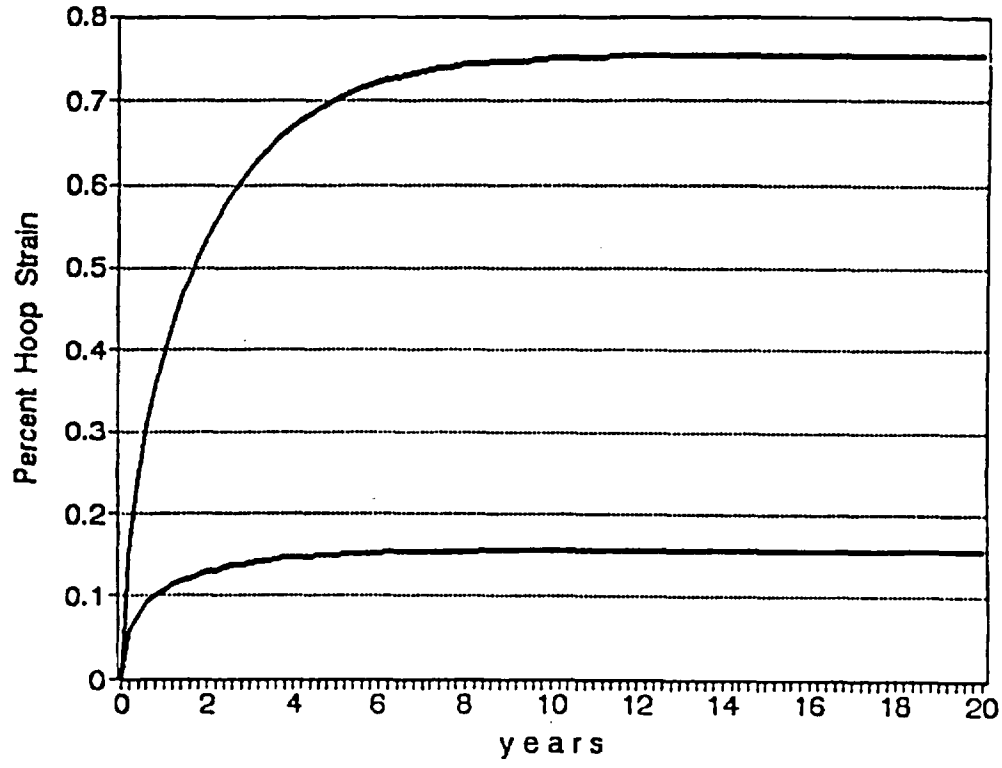

Figure 5.17 Hoop strain predictions as a function of storage time for two different temperature-decay relationships.

Lower curve: Case 1, T(t) = 350°C - 3.5 t (years)

Upper curve: Case 2, T(t) = 400°C - 3.5 t (years)

5.5 Conclusions

The creep modeling approaches of the NRC and the DOE are similar in nature and are based on creep-theoretical considerations applicable, at most, during the tertiary stage of creep. On the other hand, tertiary creep has never been observed with internally-pressurized Zircaloy specimens within the IDS stress-temperature region. It appears that tertiary creep would take place at creep strain levels well beyond 1%. Thus both the NRC and DOE approaches are, in principle, very conservative, as they treat creep as accelerating from its onset.

The NRC model is based on stress-assisted growth of pre-existing cavities. The model has never been validated against cavitation data. Indeed, voids or cavities are very infrequently seen in irradiated Zircaloys.

The DOE core model is also based on the stress-assisted growth of pre-existing cavities. Although the model parameters were chosen somewhat subjectively, its predictions do not compare well with the experimental data. Furthermore, the model is internally inconsistent and, despite claims to the contrary, highly incongruent with the predictions of the NRC model. The predictions of storage time based on the DOE model are less conservative than with the NRC model, in that the former allows full decohesion of the cladding to be reached several times over.

The German correlation is based on empirical data from unirradiated Zircaloy and has been validated against internally-pressurized creep test data with both unirradiated and irradiated Zircaloy specimens. The empirical correlation is meant to apply to primary creep and to the initial stages of secondary creep. The domain of applicability is typical of IDS conditions but the parametric values are applicable with certainty only to KWU's PWR Zircaloy-4 cladding. The application of the correlation to U.S. data obtained with internally-pressurized spent fuel is encouraging and would show its applicability also to PWR fuel of U.S. design.

The German correlation appears to be the most defensible of the three creep models that were analyzed. Its use, along with a 1%-strain acceptance criterion, would allow substantially higher temperature limits than are presently achievable using the NRC and DOE model predictions.

6. CONCLUSIONS AND RECOMMENDATIONS

Cladding creep from fill gas overpressure is the rate-determining degradation and failure mechanism for setting maximum allowable temperature limits during inerted dry storage of spent fuel. In this respect the BWR and PWR spent fuel rods constitute two very distinct population groups.

Because of their much lower internal pressure, the BWR fuel rods are much less susceptible to cladding creep and a case could be made more readily for their safe storage at MATs of 400°C and higher over long periods of time.

Cladding creep is a more important concern for PWR fuel rods. However, gross rupture leading to potential release of spent fuel particles can be excluded under IDS conditions. If creep were allowed to proceed to rupture, the fracture mode would be most likely of the pinhole type. Nevertheless, it is desirable to restrict the possiblity of all potential failures. This can be accomplished by confining the creep degradation mechanism to its primary and early secondary stages.

Internally pressurized creep tests of both irradiated and unirradiated Zircaloy cladding in the stress-temperature region of relevance to IDS show a two-stage behavior involving primary and secondary creep. These tests could be analyzed further in order to identify the critical strain region at which Zircaloy creep enters the secondary stage. If it can be shown that the creep strain never exceeds significantly that critical strain domain during IDS, the break-away creep regime (tertiary creep, leading to fracture) could be excluded from consideration and, with it, all potential failures. This approach is in keeping with standard creep engineering practices and, in a fundamental way, is the same approach which has been implemented in Germany and is presently under study in Japan.

The recommended methodology relies on the analysis and availability of:

(a) a data base of Zircaloy creep test under internal pressurization conditions, and

(b) a suitable model which is able to predict the evolution of creep through its primary and secondary stages.

A few creep-engineering models and supporting data are available in the literature and need to be investigated to identify a preferred model. This review has analyzed the empirical correlation which was developed in Germany and found it to be sound, well-validated, and with built-in conservatism in its predictions. When the same correlation is applied to predict independent data generated in the U.S., it shows excellent agreement with the data. Application of the German correlation would allow substantially higher MATs than are presently allowed in the U.S. program.

Indeed, there exists a need to improve the current U.S. methodology for determining MATs during IDS. Although two independent methodologies are available in principle, one developed at PNL on behalf of the DOE and one by the NRC, they are not totally independent and show important similarities. In particular, they suffer from the same shortcoming in that they are not based on experimental data and facts, but rather rely on creep-theoretical considerations which have never been tested with Zircaloy cladding and which may be applicable only to the tertiary stage of creep. The model developed at PNL is also internally inconsistent and not congruent with the NRC model and their acceptance criterion for IDS of spent fuel. Both the NRC and the PNL models appear to provide extremely conservative predictions, therefore they do not pose a safety concern.

7. REFERENCES

[Ashby, 1984]

M.F. Ashby and B.F. Dyson, *Creep Damage Mechanics and Micromechanisms*, DMA(A)77, National Physics Laboratory, Teddington, England, March 1984.

[Aungst, 1965]

R.C. Aungst, *Stress Rupture Tests of Zircaloy-2 Pressure Tubes*, BNWL-8, Battelle-Northwest, Richland, WA, January 1965.

[Blackburn, 1978]

L.D. Blackburn, D.G. Farwick, S.R. Fields, L.A. James, and R.A. Moen, *Maximum Allowable Temperature for Storage of Spent Nuclear Reactor Fuel*, HEDL-TME 78-37, Hanford Engineering Development Laboratory, Richland, Washington, May 1978.

[Brun, 1987]

G. Brun, J. Pelchat, J.C. Floze and M. Galimberti, *"Cumulative Fatigue and Creep-Fatigue Damage at 350°C in Recrystallized Zircaloy-4,"* in Zirconium in the Nuclear Industry: Seventh International Symposium, ASTM STP 939 (R.B. Adamson and L.F.P. Van Swam, Eds.), American Society for Testing and Materials, Philadelphia (1987), pp. 597-616.

[Brunisholz, 1987]

L. Brunisholz and C. Lemaignan, *"Iodine-Induced Stress Corrosion of Zircaloy Fuel Cladding: Initiation and Growth,"* in Zirconium in the Nuclear Industry: Seventh International Symposium, ASTM STP 939 (R.B. Adamson and L.F.P. Van Swam, Eds.), American Society for Testing and Materials, Philadelphia (1987), pp. 700-716.

[Busby, 1975]

C.C. Busby, R.P. Tucker and J.E. McCauley, *"Halogen Stress Corrosion Cracking of Zircaloy-4 Tubing,"* J. Nucl. Mat. 55:64-82 (1975).

[Carpenter, 1974]
G.J.C. Carpenter and J.F. Watters, "*Irradiation Damage Recovery in Some Zirconium Alloys,*" in Zirconium in Nuclear Applications, ASTM STP 551, American Society for Testing and Materials, Philadelphia (1974), pp. 400-415.

[Charquet, 1988]
D. Charquet, R. Hahn, E. Ortlieb, J.-P. Gros and J.-F. Wadier, "*Solubility Limits and Formation of Intermetallic Precipitates in ZrSnFeCr Alloys,*" in Zirconium in the Nuclear Industry (Eighth Symposium), ASTM STP 1023, American Society for Testing and Materials, Philadelphia (1988), pp. 405-422.

[Cheadle, 1977]
B.A. Cheadle, "*Fabrication of Zirconium Alloys into Components for Nuclear Reactors,*" in Zirconium in the Nuclear Industry (Third Conference), ASTM STP 633, American Society for Testing and Materials, Philadelphia (1977), pp. 457-485.

[Chin, 1986]
B.A. Chin, M.A. Khan, J.C.L. Tarn, *Deformation and Fracture Map Methodology for Predicting Cladding Behavior During Dry Storage*, PNL-5998, Pacific Northwest Laboratory, Richland, Washington, September 1986.

[Chin, 1989]
B.A. Chin, E.R. Gilbert, "*Prediction of Maximum Allowable Temperatures for Dry Storage of Zircaloy-clad Spent Fuel in Inert Atmosphere,*" Nucl. Technol. 85:57-65 (1989).

[Chung, 1987]
H.M. Chung, F.L. Yaggee and T.F. Kassner, "*Fracture Behavior and Microstructural Characteristics of Irradiated Zircaloy Cladding,*" in Zirconium in the Nuclear Industry: Seventh International Symposium, ASTM STP 939 (R.B. Adamson and L.F.P. Van Swam, Eds.), American Society for Testing and Materials, Philadelphia, pp. 775-801 (1987).

[Cocks, 1982]
A.C.F. Cocks and M.F. Ashby, "*Creep Fracture by Coupled Power-Law and Diffusion under Multi-Axial Stress*," Metal Science, 16, 465-474, (1982).

[Coleman, 1972]
C.E. Coleman, "*Tertiary Creep in Cold-Worked Zircaloy-2*," J. Nucl. Mat. 42:180-190 (1972).

[Crescimanno, 1984]
P.J. Crescimanno, W.R. Campbell and I. Goldberg, "*A Fracture Mechanics Model for Iodine Stress Corrosion Crack Propagation in Zircaloy Tubing*," in Environment-Sensitive Fracture: Evaluation and Comparison of Test Methods, ASTM STP 821 (S.W. Dean, E.N. Pugh and G.M. Ugiansky, Eds.), American Society for Testing and Materials, Philadelphia (1984), pp. 150-169.

[Cubicciotti, 1978]
D. Cubicciotti and R.L. Jones, *EPRI-NASA Cooperative Project on Stress Corrosion Cracking of Zircaloys*, U. S. Report EPRI-NP-717, March 1978.

[Cunningham, 1987]
M.E. Cunningham, *Control of Degradation of Spent LWR Fuel During Dry Storage in an Inert Atmosphere*, PNL-6364, Pacific Northwest Laboratory, Richland, Washington, October 1987.

[Dieter, 1986]
G. E. Dieter, Mechanical Metallurgy, Third Edition, McGraw-Hill Book Company, New York, 1986

[Einziger, 1982]
R.E. Einziger, S.D. Atkin, D.E. Stellrecht and V.S. Pasupathi, "*High Temperature Postirradiation Materials Performance of Spent Pressurized Water Reactor Fuel Rods under Dry Storage Conditions*," Nucl. Technol. 57:65-80 (1982).

[Einziger, 1983]

R. E. Einziger and R. Kohli, *Low Temperature Rupture Behavior of Zircaloy Clad Pressurized Water Reactor Spent Fuel Under Dry Storage Conditions*, HEDL-7400, Westinghouse Hanford Report, Richland Washington, February 1983.

[Einziger, 1984]

R.E. Einziger and R. Kohli, *"Low-Temperature Rupture Behavior of Zircaloy-Clad Pressurized Water Reactor Spent Fuel Rods Under Dry Storage Conditions,"* Nucl. Technol. 67:107-123 (1984).

[Fidleris, 1966]

V. Fidleris and C.D. Williams, *"Influence of Neutron-Irradiation on the Creep of Zircaloy-2 at 300°C,"* Electrochem. Tech. 4:258-267 (1966).

[Finnie, 1959]

I. Finnie and W. R. Heller, Creep of Engineering Materials, McGraw-Hill, 1959.

[FR, 1988]

Federal Register, Vol. 53, No. 161, Friday, August 19, 1988, pp. 31651 - 31682.

[Franklin, 1983]

D.G. Franklin, G.E. Lucas and A.L. Bement, Creep of Zirconium Alloys in Nuclear Reactors, ASTM STP 821, American Society for Testing and Materials, Philadelphia (1983).

[Garde, 1986]

A.M. Garde, Hot Cell Examination of Extended Burnup Fuel from Fort Calhoun, DOE/ET/34030-11, September 1986.

[Garlick, 1973]

A. Garlick, *"Fracture of Zircaloy Cladding under Simulated Power Ramp Conditions,"* J. Nucl. Mat. 49:209-224 (1973/74).

[Garzarolli, 1979]
F. Garzarolli, R. von Jan, and H. Stehle, *"The Main Causes of Fuel Element Failure in Water-Cooled Power Reactors,"* Atomic Energy Review, 17, 1, p. 31, 1979.

[Gilbert, 1978]
R.W. Gilbert and K. Farrell, *Damage structure in zirconium alloys irradiated at 573 to 923°K*, CONF-780818-6 (1978).

[Gilbert, 1988]
E. R. Gilbert, W.J. Bailey and A.B. Johnson, Jr., "*Results of Studies on the Behavior of Spent Fuel in Storage*," J. Inst. Nucl. Mat. Man., XVI:32-35 (1988).

[Gilbert, 1989a]
E.R. Gilbert, "*LWR Spent Storage Technology: Advances and Experience*," in Waste Management '89, University of Arizona, Tucson, Arizona, 1989.

[Griffiths, 1987]
M. Griffiths, R.W. Gilbert and G.J.C. Carpenter, *"Phase Instability, Decomposition and Redistribution of Intermetallic Precipitates in Zircaloy-2 and -4 during Neutron Irradiation"*, J. Nucl. Mat. 150:53-66 (1987).

[Griffiths, 1988a]
M. Griffiths, *"A Review of Microstructure Evolution in Zirconium Alloys during Irradiation"*, J. Nucl. Mat. 159:190-218 (1988).

[Griffiths, 1988b]
M. Griffiths, R.W. Gilbert and C.E. Coleman, *"Grain Boundary Sinks in Neutron-Irradiated Zr and Zr Alloys"*, J. Nucl. Mat. 159:405-416 (1988).

[Holt, 1982]
R.A. Holt, R.W. Gilbert and V. Fidleris, *"Dislocation Substructure in Zirconium Alloys Irradiated in EBR-II"*, in Effects of Radiation on Materials (Eleventh Symposium), ASTM STP 782, American Society for Testing and Materials, Philadelphia (1982), pp. 234-250.

[IAEA, 1982]
International Atomic Energy Agency, *"Storage of Water Reactor Spent Fuel in Water Pools - Survey of World Experience"*, Technical Report Series No. 218, International Atomic Energy Agency, Vienna, Austria, 1982.

[Jones, 1980]
R.L. Jones, D. Cubiciotti and B.C. Syrett, *"Effects of Test Temperature, Alloy Composition and Heat Treatment on Iodine-Induced Stress Corrosion Cracking of Unirradiated Zircaloy Tubing,"* J. Nucl. Mat. 91:277-292 (1980).

[Jones, 1979]
R.L. Jones, F.L. Yagee, R.A. Stoehr and D. Cubiciotti, *"Threshold Conditions for Iodine-Induced Stress Corrosion Cracking of Unirradiated Zircaloy-4 Tubing under Internal Pressurization,"* J. Nucl. Mat. 82:26-38 (1979).

[Kaspar, 1985a]
G. Kaspar, M. Peehs, E. Steinberg and H. Schönfeld, *"Experimental Investigations of Post-Pile Creep on Zircaloy Cladding Tubes,"* in Transactions of the 8th International Conference on Structural Mechanics in Reactor Technology, North Holland, Amsterdam, 1985, Vol. C-D, pp. 51-57.

[Kaspar, 1985b]
G. Kaspar, M. Peehs, R. Bokelmann, D. Jorde, H. Schönfeld, W. Haas, A. Bleier and F. Rutsch, *Spaltproduktfreisetzung und Post-pile-Kriechverhalten trocken gelagerter, abgebrannter Brennstäbe*, BMFT-KWA 2100 BO, Erlangen, Germany, June 1985 (also as INIS-MF-10394).

[Keusseyan, 1979]
R.L. Keusseyan, C.P. Hu and C.Y. Li, *"Creep Damage in Zircaloy-4 at LWR Temperatures"*, J. Nucl. Mat. 80:390-392 (1979).

[Keusseyan, 1985]
R.L. Keusseyan, Grain Boundary Sliding and Related Phenomena, Ph.D. Dissertation, Cornell University, University Microfilms International, Ann Arbor, MI (1985).

[Kreyns, 1976]
P.H. Kreyns, G.L. Spahr and J.E. McCauley, *"An Analysis of Iodine Stress Corrosion Cracking of Zircaloy-4 Tubing,"* J. Nucl. Mat. 61:203-212 (1976).

[Levy, 1987]
I.S. Levy, B.A. Chin, E.P. Simonen, C.E. Beyer, E.R. Gilbert and A.B. Johnson, Jr., *Recommended Temperature Limits for Dry Storage of Spent Light Water Reactor Zircaloy-clad Fuel Rods in Inert Gas*, PNL-6189, Pacific Northwest Laboratory, Richland, Washington, May 1987.

[Lucas, 1981]
G.E. Lucas and R.M.N. Pelloux, *"Some Observation on Time-Hardening and Strain-Hardening Rules for Creep in Zircaloy-2"*, J. Nucl. Tech. 53:46-57 (1981).

[MacDonald, 1984]
E. MacDonald, Certificate of Compliance for Radioactive Materials Packages, U.S. Nuclear Regulatory Commission, No. 9016, Rev.6, Washington, D.C., 1984.

[Matsuo, 1987]
Y.K. Matsuo, *"Thermal Creep of Zircaloy-4 Cladding under Internal Pressure,"*, J. Nuclear Science and Technology, 24:111-119, 1987.

[Mattas, 1982]
R.F. Mattas, F.L. Yagee and L.A. Neimark, *"Effect of Zirconium Oxide on the Stress-Corrosion Susceptibility of Irradiated Zircaloy Cladding,"* in Zirconium in the Nuclear Industry: Fifth International Symposium, ASTM STP 754 (D.G Franklin, Ed.), American Society for Testing and Materials, Philadelphia (1982), pp. 158-170.

[Mayuzumi, 1990a]
M. Mayuzumi and T. Onchi, "*Creep Deformation of an Unirradiated Zircaloy-4 Nuclear Fuel Cladding Tube under Dry Storage Conditions*", J. Nucl. Mat. 171:381-388 (1990).

[Mayuzumi, 1990b]
M. Mayuzumi and T. Onchi, "*Creep Deformation and Rupture Properties of Unirradiated Zircaloy-4 Nuclear Fuel Cladding Tube at Temperatures of 727 to 857 K*", J. Nucl. Mat. 175:135-142 (1990).

[Mayuzumi, 1991a]
M. Mayuzumi and T. Onchi, "*A Method to Evaluate Maximum Allowable Temperature of Spent Fuel in Dry Storage during a Postulated Accident*", Nucl. Tech. 93:382-388 (1991).

[Mayuzumi, 1991b]
M. Mayuzumi and T. Onchi, "*The Applicability of the Strain-Hardening Rule to the Creep Deformation of Zircaloy Fuel Cladding Tube under Dry Storage Conditions,*" J. Nucl. Mat. 178:73-79.

[Miller, 1989]
A.K. Miller, M. Brooks, T.Y. Cheung, A. Tasooji, J.C. Wood and J.R. Kelm, *Estimates of Zircaloy Integrity During Dry Storage of Spent Nuclear Fuels*, EPRI NP-6387, Electric Power Research Institute, Palo Alto, CA, May 1989.

[Murty, 1977]
K.L. Murty, G.S. Clevinger, T.P. Papazoglou, "*Thermal Creep of Zircaloy-4 Cladding,*" in Transactions of the 4th International Conference on Structural Mechanics in Reactor Technology, San Francisco, CA, Aug. 15-19, 1977.

[Northwood, 1977]
D.O. Northwood," *Irradiation Damage in Zirconium and Its Alloys*", Atomic Energy Review 15:547-610 (1977).

[NRC, 1989]
U.S. Nuclear Regulatory Commission, *Safety Evaluation Report related to the Topical Report for the NUTECH Horizontal Modular Storage System for Irradiated Nuclear Fuel NUHOMS-24P submitted by NUTECH Engineers, Inc.*, NRC-89-4, Washington, D.C., 1989.

[NRC, 1985]
U.S. Nuclear Regulatory Commission, *Safety Evaluation Report Related to the Topical Safety Analysis Report for Castor V/21 Dry Spent Fuel Storage Cask Submitted by General Nuclear Systems, INC.*, NRC-SER-85-9, Washington, D.C., 1985.

[Pahutová, 1977]
M. Pahutová, K. Kuchařová and J. Čadek, "*Some Basic Creep Characteristics of Zr-Sn-Mo and Zr-Sn-Mo-Nb Alloys. Part II. Fracture in Creep,*" Matls. Sci. and Eng. 27:249-255 (1977).

[Peehs, 1983]
M. Peehs et al., *"Zircaloy Post-Pile Creep Experimental Procedure, Test Samples and First Results."* Paper presented at IAEA Seminar of Technical and Environmental Aspects of Spent Fuel Management, September 27-30, 1983, Madrid, Spain.

[Peehs, 1986a]

M. Peehs, R. Bokelmann and J. Fleisch, "*Spent Fuel Dry Storage Performance in Inert Atmosphere,*" in Proc. 3rd International Spent Fuel Storage Technology Symposium/Workshop, Vol. 1, pp. S-215 to S-230, CONF-860417, 1986.

[Peehs, 1986b]

M. Peehs and J. Fleisch, *"LWR Spent Fuel Storage Behaviour,"* J. Nucl. Matls. 137:190-202 (1986).

[Peehs, 1986c]

M. Peehs, G. Kaspar, and E. Steinberg, "*Experimentally Based Spent Fuel Dry Storage Performance Criteria,*" in Proc. 3rd International Spent Fuel Storage Technology Symposium/Workshop, Vol. 1, pp. S-316 to S-331, CONF-860417/UC-85, 1986.

[Pescatore, 1989]

C. Pescatore, M.G. Cowgill and T.M. Sullivan, Zircaloy Cladding Performance Under Spent Fuel Conditions. Progress Report May 1 - October 31 1989, BNL 52235, Brookhaven National Laboratory, Upton, NY (1989).

[Polan, 1977]

N.W. Polan and R.F. Tucker, *The Susceptibility of Unirradiated Recrystallized Zircaloy-4 Tubing to Stress Corrosion Cracking*, WAPD-TM-1313, Bettis Atomic Power Laboratory, West Mifflin, PA (1977).

[Porsch, 1986]

G. Porsch, J. Fleisch and B. Heits, *"Accelerated High-Temperature Tests with Spent PWR and BWR Fuel Rods under Dry Storage Conditions,"* Nucl. Technol. 74:287-298 (1986).

[Povolo, 1981]

F. Povolo and A.J. Marzocca, *"Creep of Cold-worked Zry-4 at 673K,"* J. Nucl. Matls. 97:323-332 (1981).

[Raj, 1975]
R. Raj and M.F. Ashby, "*Intergranular Fracture at Elevated Temperature*," Acta Met. 23:653-667 (1975).

[Roark, 1975]
R.J. Roark and W.C. Young, Formulas for Stress and Strain, Fifth Edition, McGraw-Hill Book Company, New York, 1975.

[Romeiser, 1979]
H.-J. Romeiser and E. Steinberg, Anwendungsorientierte Hüllrohrstudie, BMFT-FB K 79-08, Bundesministerium für Forschung und Technologie, Bonn, Germany, June 1985.

[Rothman, 1984]
A. J. Rothman, *Potential Corrosion and Degradation Mechanisms of Zircaloy Cladding on Spent Nuclear Fuel in a Tuff Repository*, UCID-20172, Lawrence Livermore National Laboratory, September 1984.

[Ryu, 1988]
W.S. Ryu, Y.H. Kang and J.-Y. Lee, "*Effects of Iodine Concentration on Iodine-Induced Stress Corrosion Cracking of Zircaloy-4 Tube*," J. Nucl. Mat. 152:194-203 (1988).

[Santanam, 1989]
L. Santanam, S. Raghavan, H. Shaw, B.A. Chin, "*Modeling of Zircaloy Cladding Degradation under Repository Conditions*," Presented at FOCUS '89 Conference on Nuclear Waste Isolation in the Unsaturated Zone, Las Vegas, NV, Sept. 18-21, 1989.

[Schwartz, 1989]
M.W. Schwartz and M.C. Witte, "*Zircaloy Fuel Cladding Integrity During Dry Storage*," in Proc. of The 9th International Symposium on the Packaging and Transportation of Radioactive Materials, PATRAM '89, Washington DC, June 11-16, 1989.

[Shimada, 1983a]
S. Shimada and M. Nagai, *"A Fractographic Study of Iodine-Induced Stress Corrosion Cracking in Irradiated Zircaloy-2 Cladding,"* J. Nucl. Mat. 114:222-230 (1983).

[Shimada, 1983b]
S. Shimada, T. Matsuura and M. Nagai, *"Stress Corrosion Cracking of Zircaloy-2 by Metal Iodides,"* J. Nucl. Sci. & Tech. 20:593-602 (1983).

[Stehle, 1972]
H. Stehle, *Progress in Zircaloy-4 Canning Technology*, AED-CONF-71-100-26, Zentralstelle für Atomkernenergie-Dokumentation (ZAED), 7501 Leopoldshafen, Kernforschungezentrum, Germany (1971).

[Strasser, 1987]
A.A. Strasser, K.D. Sheppard, L. Goldstein and S. Rajan, *Extended Burnup Potential and Plant Capacity Factor Savings of Improved LWR Fuel Designs*, in Improvements in Water Reactor Fuel Technology and Utilization (Proc. Int. Symp. Stockholm 1986), International Atomic Energy Agency, Vienna, Austria, 1987.

[Syrett, 1980]
B.C. Syrett, D. Cubiciotti and R.L. Jones, *"The Origin of Variations in the Iodine Stress Corrosion Cracking Susceptibility of Commercial Zircaloy-2 Tubings,"* J. Nucl. Mat. 92:89-102 (1980).

[Syrett, 1981]
B.C. Syrett, D. Cubiciotti and R.L. Jones, *"The Effect of Texture and Surface Condition on the Iodine Stress Corrosion Cracking Susceptibility of Unirradiated Zircaloy-2,"* Nucl. Tech. 55:628-641 (1980).

[Tucker, 1976]
R.F. Tucker, P.H. Kreyns and J.J. Kearns, *The Effects of Internal Surface Flaws, Iodine Concentration and Temperature on the Stress Corrosion Cracking Behavior of Zircaloy-4 Tubing*, WAPD-TM-1248, Bettis Atomic Power Laboratory, West Mifflin, PA (1976).

[Wolfenden, 1972]
A. Wolfenden and K. Farrell, *"On the Question of Void Formation in Neutron Irradiated Zirconium,"* Scripta Met. 6:127-130 (1972).

[Yagee, 1979]
F.L. Yagee, R.F. Mattas and L.A. Neimark, *Characterization of Irradiated Zircaloys: Susceptibility to Stress Corrosion Cracking. Interim Report*, EPRI NP-1155, Electric Power Research Institute, Palo Alto, CA, September 1979.

[Yagee, 1980]
F.L. Yagee, R.F. Mattas and L.A. Neimark, *Characterization of Irradiated Zircaloys: Susceptibility to Stress Corrosion Cracking. Final Report*, EPRI NP-1557, Electric Power Research Institute, Palo Alto, CA, October 1980.

[Yang, 1986]
W.J.S. Yang, R.P. Tucker, B. Cheng and R.B. Adamson, *"Precipitates in Zircaloy: Phase Identification and the Effects of Irradiation and Thermal Treatment"*, J. Nucl. Mat. 138:185-195 (1986).

[Yang, 1988a]
W.J.S. Yang, *Precipitate stability in Zircaloy-4*, EPRI NP-5591, Electric Power Research Institute, Palo Alto, California, January 1988.

[Yang, 1988b]
W.J.S. Yang, *"Precipitate Stability in Neutron-Irradiated Zircaloy-4"*, J. Nucl. Mat. 158:71-80 (1988).

[Yoo, 1974]
M.H. Yoo, "*Suppression of Void Formation in Zirconium*," in Zirconium in Nuclear Applications, ASTM STP 551, American Society for Testing and Materials, Philadelphia, pp. 292-307 (1974).

Appendix A

Tabulation of Failure Mode Observations in Unirradiated and Irradiated Zircaloy Fuel Cladding under Internal Pressurization Conditions

Table A-1

Stress-rupture Observations On Irradiated Zircaloys

Material	Temp. (°C)	Stress (MPa)	Strain (%)	Failure Mode	Spec. ID	Reference
Zr-2 (SR)	325	337	0.4	S?	165AE4B	Chung, 1987
Zr-2 (SR)	325	344	0.8	D	165AE4A	Chung, 1987
Zr-2 (SR)	325	384	1	P?	165AG10	Chung, 1987
Zr-2 (SR)	325	514	1	D	165W21	Chung, 1987
Zr-4 (SR)	292	498	1	S?	217B4B	Chung, 1987
Zr-4 (SR)	292	545	2	D	217B2B	Chung, 1987
Zr-4 (SR)	292	552	11	D	217A2G	Chung, 1987
Zr-4 (SR)	325	275	0.01	P	155BC9	Yagee, 1980
Zr-4 (SR)	325	315		S?	217C4B	Chung, 1987
Zr-4 (SR)	325	315		S?	217A4B	Chung, 1987
Zr-4 (SR)	325	469	2	S?	217C2B	Chung, 1987
Zr-4 (SR)	360	200	0.4	S	155BD4	Yagee, 1979

Notes

(SR) - stress-relieved.
D - ductile rupture; S - axial split; P - pinhole leakage.
All strains of 1% or greater approximated to whole numbers.

Table A-2

Stress-rupture Observations On Unirradiated Zircaloys

Material	Temp. (°C)	Stress (MPa)	Strain (%)	Failure Mode	Spec. ID	Reference
Zr-2 (Ann)	320	314	50	D	2S23	Jones, 1980
Zr-2 (Ann)	320	318	51	D	2S22	Jones, 1980
Zr-2 (Ann)	320	328	52	D	2S21	Jones, 1980
Zr-2 (SR)	320	468		D	2H19	Jones, 1980
Zr-2 (SR)	320	486		D	2H20	Jones, 1980
Zr-2 (SR)	320	492	10	D	2H18	Jones, 1980
Zr-2 (SR)	320	510	23	D	2H16	Jones, 1980
Zr-2 (SR)	400	293	26	D	R1	Shimada, 1983b
Zr-2 (SR)	400	293	27	D	R2	Shimada, 1983b
Zr-4 (RX)	350	300	50	S		Brunisholz, 1987
Zr-4 (RX)	350	350	15	S		Brunisholz, 1987
Zr-4 (RX)	360	262	11	P	61	Busby, 1975
Zr-4 (RX)	360	276		S	B16	Polan, 1977 [c]
Zr-4 (RX)	360	289	45	P	126	Busby, 1975
Zr-4 (RX)	400	276		S	D10	Polan, 1977 [c]
Zr-4 (RX)	400	276	43	S	128	Busby, 1975
Zr-4 (RX)	400	278	3	P	67	Busby, 1975
Zr-4 (SR)	330	475	12	S		Ryu, 1988
Zr-4 (SR)	360	335	3	D	413	Cubiciotti, 1978
Zr-4 (SR)	360	345	11	S	73S	Busby, 1975
Zr-4 (SR)	360	390	2	D	412	Cubiciotti, 1978
Zr-4 (SR)	360	413	11	S	72S	Busby; 1975
Zr-4 (SR)	360	450	3	D	411	Cubiciotti, 1978
Zr-4 (SR)	360	500	15	S	1	Yagee, 1979
Zr-4 (SR)	360	500	4	S	SRI16	Yagee, 1979
Zr-4 (SR)	360	510	16	S	2	Yagee, 1979
Zr-4 (SR)	360	530	5	S	SRI22	Yagee, 1979
Zr-4 (SR)	360	545	5	S	ANL8	Yagee, 1979
Zr-4 (SR)	360	550	3	S	ANL9	Yagee, 1979
Zr-4 (SR)	400	276	23	S	82S	Busby, 1975
Zr-4 (SR)	400	345	7	S	79S	Busby, 1975

Table A-2 (continued)

Notes

(Ann) - annealed; (SR) - stress-relieved; (RX) - recrystallized.
D - ductile rupture; S - axial split.
All strains approximated to whole numbers.
[c] - failure mode information from [Crescimanno, 1984].

Table A-3

Observations On Stress Corrosion Cracking of Irradiated Zircaloys

Material	Temp. (°C)	Stress (MPa)	Strain (%)	Failure Mode	Spec. ID	Reference
Zr-2 (RX)	344	178	0.1	P	24L2	Yagee, 1979 [c]
Zr-2 (RX)	344	188	0.1	P	24L1	Yagee, 1979 [c]
Zr-2 (RX)	344	206	0.1	P	13L	Yagee, 1979 [c]
Zr-2 (RX)	344	218	0.1	P	12L	Yagee, 1979 [c]
Zr-2 (RX)	344	303	1	S	18L	Yagee, 1979 [c]
Zr-2 (RX)	344	513	1	P	22L	Yagee, 1979
Zr-2 (SR)	325	119	0.05	P	165T18B	Yagee, 1980
Zr-2 (SR)	325	151	0.05	P	165T18A	Yagee, 1980
Zr-2 (SR)	325	157	0.05	S	165W12	Yagee, 1979 [c]
Zr-2 (SR)	325	172	0.05	P	165W10	Yagee, 1979 [c]
Zr-2 (SR)	325	180	0.05	P	165W8	Yagee, 1979 [c]
Zr-2 (SR)	325	184	0.01	P	190D25	Yagee, 1979 [c]
Zr-2 (SR)	325	199	0.01	P	190D16	Yagee, 1979 [c]
Zr-2 (SR)	325	221	0.04	P	165AG19	Yagee, 1980
Zr-2 (SR)	325	221	0.04	P	165AG20	Yagee, 1980
Zr-2 (SR)	325	224	0.04	P	165AA8	Yagee, 1980
Zr-2 (SR)	325	227	0.04	P	165AB12	Yagee, 1980
Zr-2 (SR)	325	236	0.02	P	165AA7	Yagee, 1980
Zr-2 (SR)	325	247	0.03	S	165F9	Yagee, 1980
Zr-2 (SR)	325	248	0.01	S	165F11	Yagee, 1980
Zr-2 (SR)	325	266	0.08	S	165F7	Yagee, 1980
Zr-2 (SR)	325	273	0.05	P	165V5	Yagee, 1980
Zr-2 (SR)	325	274		S	165W20	Yagee, 1980
Zr-2 (SR)	325	274	0.01	P	190D13	Yagee, 1979 [c]
Zr-2 (SR)	325	274	0.01	P	190D14	Yagee, 1979 [c]
Zr-2 (SR)	325	275		S	165W18	Yagee, 1980
Zr-2 (SR)	325	275	0.07	P	165AA10	Yagee, 1980
Zr-2 (SR)	325	277		S	165E11	Mattas, 1982 [c]
Zr-2 (SR)	325	296	2	S	165E9	Yagee, 1979 [c]
Zr-2 (SR)	325	310	1	S	165E7	Yagee, 1979 [c]
Zr-2 (SR)	325	320		S	165E10	Mattas, 1982 [c]
Zr-2 (SR)	325	408		S	165W19	Yagee, 1980
Zr-2 (SR)	325	409	0.18	P	165AB9	Yagee, 1980
Zr-2 (SR)	325	411	0.03	S	190D15	Yagee, 1979 [c]
Zr-2 (SR)	325	411	0.16	S	190D17	Yagee, 1979 [c]

Table A-3 (continued)

Material	Temp. (°C)	Stress (MPa)	Strain (%)	Failure Mode	Spec. ID	Reference
Zr-2 (SR)	325	414	0.14	S	165V10	Yagee, 1980
Zr-2 (SR)	325	499	0.01	S	165U4	Yagee, 1980
Zr-2 (SR)	350	280+		S		Shimada, 1983a
Zr-2 (SR)	350	280+		P		Shimada, 1983a
Zr-4 (RX)	316	164		P	2835	Kreyns, 1984 [c]
Zr-4 (RX)	316	172		P	2836	Kreyns, 1984 [c]
Zr-4 (RX)	316	296		P	2841	Kreyns, 1984 [c]
Zr-4 (RX)	316	392		P	2853	Kreyns, 1984 [c]
Zr-4 (SR)	325	276	0.1	P	155BC6	Yagee, 1980
Zr-4 (SR)	325	414	0.19	P	155BC5	Yagee, 1980
Zr-4 (SR)	360	200	1	P	155BD5	Yagee, 1979
Zr-4 (SR)	360	205	0.26	S	155CA3	Yagee, 1979
Zr-4 (SR)	360	273	0.1	P	155BC7	Yagee, 1980
Zr-4 (SR)	360	413		S	155BC8	Yagee, 1980

Notes

RX - fully recrystallized; (SR) - stress-relieved.
D - ductile rupture; S - axial split; P - pinhole leakage.
All strains of 1% or greater approximated to whole numbers.
[c] - failure mode information from [Crescimanno, 1984].

Table A-4

Observations On Stress Corrosion Cracking of Unirradiated Zircaloys

Material	Temp. (°C)	Stress (MPa)	Strain (%)	Failure Mode	Spec. ID	Reference
Zr-2 (Ann)	320	282	5	S	2S16	Jones, 1980
Zr-2 (Ann)	320	286	5	S	2S17	Jones, 1980
Zr-2 (Ann)	320	290	4	P	2S15	Jones, 1980
Zr-2 (Ann)	330	320	11	P		Garlick, 1973
Zr-2 (RX)	344	370	7	S	183Y4	Yagee, 1979
Zr-2 (SR)	320	207		P	24C5	Syrett, 1981
Zr-2 (SR)	320	241		P	B4	Syrett, 1980
Zr-2 (SR)	320	241		P	24A6	Syrett, 1981
Zr-2 (SR)	320	242		P	24B2	Syrett, 1981
Zr-2 (SR)	320	242		P	24C2	Syrett, 1981
Zr-2 (SR)	320	275		P	23C3	Syrett, 1981
Zr-2 (SR)	320	276		P	24C1	Syrett, 1981
Zr-2 (SR)	320	277		P	24B1	Syrett, 1981
Zr-2 (SR)	320	278		P	23B2	Syrett, 1981
Zr-2 (SR)	320	280	0.4	P	B3	Syrett, 1980
Zr-2 (SR)	320	281		P	24A4	Syrett, 1981
Zr-2 (SR)	320	283		P	24A5	Syrett, 1981
Zr-2 (SR)	320	307		P	24B3	Syrett, 1981
Zr-2 (SR)	320	311		S	24C3	Syrett, 1981
Zr-2 (SR)	320	311		P	24A9	Syrett, 1981
Zr-2 (SR)	320	311		P	22C3	Syrett, 1981
Zr-2 (SR)	320	329	1	P	2H12	Jones, 1980
Zr-2 (SR)	320	336	0.7	P	2H11	Jones, 1980
Zr-2 (SR)	320	336	0.7	P	2H14	Jones, 1980
Zr-2 (SR)	320	338	1.2	S	2H15	Jones, 1980
Zr-2 (SR)	320	339	0.7	P	2H10	Jones, 1980
Zr-2 (SR)	320	342	0.1	P	B6	Syrett, 1980
Zr-2 (SR)	320	343	0.4	P	2H9	Jones, 1980
Zr-2 (SR)	320	343		P	23A6	Syrett, 1981
Zr-2 (SR)	320	343		P	24A3	Syrett, 1981
Zr-2 (SR)	320	344		P	B9	Syrett, 1980
Zr-2 (SR)	320	344		P	B10	Syrett, 1980
Zr-2 (SR)	320	344		P	24A12	Syrett, 1981
Zr-2 (SR)	320	344		P	24A14	Syrett, 1981

Table A-4 (continued)

Material	Temp. (°C)	Stress (MPa)	Strain (%)	Failure Mode	Spec. ID	Reference
Zr-2 (SR)	320	344		P	22C1	Syrett, 1981
Zr-2 (SR)	320	345		S	24C4	Syrett, 1981
Zr-2 (SR)	320	345		P	A14	Syrett, 1980
Zr-2 (SR)	320	345		P	24A16	Syrett, 1981
Zr-2 (SR)	320	345		P	24B4	Syrett, 1981
Zr-2 (SR)	320	346		S	A12	Syrett, 1980
Zr-2 (SR)	320	346		S	B11	Syrett, 1980
Zr-2 (SR)	320	346		S	23C1	Syrett, 1981
Zr-2 (SR)	320	346		P	22A3	Syrett, 1981
Zr-2 (SR)	320	346		P	23A3	Syrett, 1981
Zr-2 (SR)	320	346		P	23B1	Syrett, 1981
Zr-2 (SR)	320	347		P	B8	Syrett, 1980
Zr-2 (SR)	320	348	0.4	S	2H8	Jones, 1980
Zr-2 (SR)	320	348		P	A10	Syrett, 1980
Zr-2 (SR)	320	356	0.3	S	2H7	Jones, 1980
Zr-2 (SR)	320	359	0.4	S	2H6	Jones, 1980
Zr-2 (SR)	320	378		S	23A5	Syrett, 1981
Zr-2 (SR)	320	378		P	21A4	Syrett, 1981
Zr-2 (SR)	320	378		P	24A11	Syrett, 1981
Zr-2 (SR)	320	378		P	21C2	Syrett, 1981
Zr-2 (SR)	320	379		P	A9	Syrett, 1980
Zr-2 (SR)	320	380		P	21A12	Syrett, 1981
Zr-2 (SR)	320	381		S	24A13	Syrett, 1981
Zr-2 (SR)	320	381		P	24A15	Syrett, 1981
Zr-2 (SR)	320	382		P	A6	Syrett, 1980
Zr-2 (SR)	320	390	0.7	S	2H5	Jones, 1980
Zr-2 (SR)	320	396		S	A11	Syrett, 1980
Zr-2 (SR)	320	411		P	22A6	Syrett, 1981
Zr-2 (SR)	320	412		P	22A5	Syrett, 1981
Zr-2 (SR)	320	413		P	23A7	Syrett, 1981
Zr-2 (SR)	320	414		P	21C1	Syrett, 1981
Zr-2 (SR)	320	416		P	21A5	Syrett, 1981
Zr-2 (SR)	320	420		S	B2	Syrett, 1980
Zr-2 (SR)	320	425	4	S	A3	Syrett, 1980
Zr-2 (SR)	320	447		S	21A14	Syrett, 1981
Zr-2 (SR)	320	447		P	21B7	Syrett, 1981
Zr-2 (SR)	320	448		P	21A13	Syrett, 1981
Zr-2 (SR)	320	448		P	21B8	Syrett, 1981

Table A-4 (continued)

Material	Temp. (°C)	Stress (MPa)	Strain (%)	Failure Mode	Spec. ID	Reference
Zr-2 (SR)	320	448		P	21C8	Syrett, 1981
Zr-2 (SR)	320	449		P	21C5	Syrett, 1981
Zr-2 (SR)	320	449		P	21C3	Syrett, 1981
Zr-2 (SR)	320	449		P	21C7	Syrett, 1981
Zr-2 (SR)	320	449		P/S	21A8	Syrett, 1981
Zr-2 (SR)	320	451	3	S	2H4	Jones, 1980
Zr-2 (SR)	320	457		S	A8	Syrett, 1980
Zr-2 (SR)	320	459		S	B5	Syrett, 1980
Zr-2 (SR)	320	481		S	21A15	Syrett, 1981
Zr-2 (SR)	320	482		S	21A7	Syrett, 1981
Zr-2 (SR)	320	482		S	21B6	Syrett, 1981
Zr-2 (SR)	330	410	25	S		Garlick, 1973
Zr-2 (SR)	330	410	25	P		Garlick, 1973
Zr-2 (SR)	330	430	23	S		Garlick, 1973
Zr-2 (SR)	330	450		D		Garlick, 1973
Zr-2 (SR)	360	287	1	P	2H24	Jones, 1980
Zr-2 (SR)	360	319	0.9	P	2H26	Jones, 1980
Zr-2 (SR)	360	383	1	P	2H23	Jones, 1980
Zr-2 (SR)	360	447	4	S	2H22	Jones, 1980
Zr-2 (SR)	400	293	24	D	C3	Shimada, 1983b
Zr-2 (SR)	400	293	25	D	F2	Shimada, 1983b
Zr-2 (SR)	400	293	25	D	Q1	Shimada, 1983b
Zr-2 (SR)	400	293	25	D	L1	Shimada, 1983b
Zr-2 (SR)	400	293		D	F1	Shimada, 1983b
Zr-2 (SR)	400	293	2	S	A6	Shimada, 1983b
Zr-2 (SR)	400	293	15	S	M1	Shimada, 1983b
Zr-2 (SR)	400	293	2	S	K1	Shimada, 1983b
Zr-2 (SR)	400	293	4	S	P1	Shimada, 1983b
Zr-2 (SR)	400	293	3	S	P3	Shimada, 1983b
Zr-2 (SR)	400	293		S	M2	Shimada, 1983b
Zr-2 (SR)	400	293	2	P	A7	Shimada, 1983b
Zr-2 (SR)	400	293	3	P	E3	Shimada, 1983b
Zr-2 (SR)	400	293	2	P	N4	Shimada, 1983b
Zr-2 (SR)	400	293	2	P	S1	Shimada, 1983b
Zr-2 (SR)	400	293	1	P	S2	Shimada, 1983b
Zr-2 (SR)	400	293	4	P	D3	Shimada, 1983b
Zr-2 (SR)	400	293	1	P	P2	Shimada, 1983b
Zr-2 (SR)	400	293	6	P	C1	Shimada, 1983b

Table A-4 (continued)

Material	Temp. (°C)	Stress (MPa)	Strain (%)	Failure Mode	Spec. ID	Reference
Zr-2 (SR)	400	293	2	P	J1	Shimada, 1983b
Zr-2 (SR)	400	293	5	P	J2	Shimada, 1983b
Zr-2 (SR)	400	293	2	P	G1	Shimada, 1983b
Zr-2 (SR)	400	293	2	P	G2	Shimada, 1983b
Zr-2 (SR)	400	293	3	P	K2	Shimada, 1983b
Zr-2 (SR)	400	293	2	P	O1	Shimada, 1983b
Zr-2 (SR)	400	293	2	P	O2	Shimada, 1983b
Zr-2 (SR)	400	293	3	P	H1	Shimada, 1983b
Zr-2 (SR)	400	293	4	P	H2	Shimada, 1983b
Zr-2 (SR)	400	293	1	P	E1	Shimada, 1983b
Zr-2 (SR)	400	293	1	P	E2	Shimada, 1983b
Zr-2 (SR)	400	293	6	P	N1	Shimada, 1983b
Zr-2 (SR)	400	293	2	P	N2	Shimada, 1983b
Zr-2 (SR)	400	293	10	P	N3	Shimada, 1983b
Zr-2 (SR)	400	293	2	P	D1	Shimada, 1983b
Zr-2 (SR)	400	293	2	P	D2	Shimada, 1983b
Zr-2 (SR)	400	293		P	C2	Shimada, 1983b
Zr-4 (RX)	316	207		S	8K6	Kreyns, 1984 [c]
Zr-4 (RX)	316	248		S	8K3	Kreyns, 1984 [c]
Zr-4 (RX)	316	276		S	8K4	Kreyns, 1984 [c]
Zr-4 (RX)	316	276		S	8K5	Kreyns, 1984 [c]
Zr-4 (RX)	350	300		P		Brunisholz, 1987
Zr-4 (RX)	350	300		P		Brunisholz, 1987
Zr-4 (RX)	360	177	0.4	P	10	Busby, 1975 [c]
Zr-4 (RX)	360	177	0.3	P	25	Busby, 1975 [c]
Zr-4 (RX)	360	200		S	B20	Polan, 1977 [c]
Zr-4 (RX)	360	201	0.6	P	22	Busby, 1975 [c]
Zr-4 (RX)	360	201	0.6	P	54	Busby, 1975 [c]
Zr-4 (RX)	360	207		S	B2	Polan, 1977 [c]
Zr-4 (RX)	360	261	1	S	82	Busby, 1975 [c]
Zr-4 (RX)	360	276		S	B6	Polan, 1977 [c]
Zr-4 (RX)	360	276		S	B9	Polan, 1977 [c]
Zr-4 (RX)	360	276		S	B21	Polan, 1977 [c]
Zr-4 (RX)	360	295	1	P	63	Busby, 1975
Zr-4 (RX)	360	295	1	P	64	Busby, 1975
Zr-4 (RX)	400	154	1	P	130	Busby, 1975 [c]
Zr-4 (RX)	400	171	0.8	P	53	Busby, 1975 [c]

Table A-4 (continued)

Material	Temp. (°C)	Stress (MPa)	Strain (%)	Failure Mode	Spec. ID	Reference
Zr-4 (RX)	400	186		P	83	Busby, 1975 [c]
Zr-4 (RX)	400	194	1	P	66	Busby, 1975 [c]
Zr-4 (RX)	400	204		S	D20	Polan, 1977 [c]
Zr-4 (RX)	400	205		S	D17	Polan, 1977 [c]
Zr-4 (RX)	400	227	0.78	P	79	Busby, 1975 [c]
Zr-4 (RX)	400	241		S	D21	Polan, 1977 [c]
Zr-4 (RX)	400	241		S	D18	Polan, 1977 [c]
Zr-4 (RX)	400	241		S	D13	Polan, 1977 [c]
Zr-4 (RX)	400	270		S	D7	Polan, 1977 [c]
Zr-4 (RX)	400	276		S	D12	Polan, 1977 [c]
Zr-4 (RX)	400	276		S	D16	Polan, 1977 [c]
Zr-4 (RX)	400	278	1	P	81	Busby, 1975
Zr-4 (SR)	316	276		P		Kreyns, 1984 [c]
Zr-4 (SR)	330	475	17	S		Ryu, 1988
Zr-4 (SR)	330	475	8	S		Ryu, 1988
Zr-4 (SR)	330	475	5	P		Ryu, 1988
Zr-4 (SR)	330	475	4	P		Ryu, 1988
Zr-4 (SR)	360	170	1	P	47S	Busby, 1975 [c]
Zr-4 (SR)	360	230	0.5	P	81S	Busby, 1975
Zr-4 (SR)	360	230	0.8	P	38S	Busby, 1975 [c]
Zr-4 (SR)	360	245	0.35	S	419	Jones, 1979
Zr-4 (SR)	360	280	0.45	P	420	Jones, 1979
Zr-4 (SR)	360	294		P	1739	Tucker, 1976 [c]
Zr-4 (SR)	360	294		P	2455	Tucker, 1976 [c]
Zr-4 (SR)	360	294		P	2512	Tucker, 1976 [c]
Zr-4 (SR)	360	294		P	258A1	Tucker, 1976 [c]
Zr-4 (SR)	360	294		P	2625	Tucker, 1976 [c]
Zr-4 (SR)	360	310	1	P	428	Jones, 1980
Zr-4 (SR)	360	316	0.68	P	ANL10	Yagee, 1979
Zr-4 (SR)	360	320	1	S	427	Jones, 1980
Zr-4 (SR)	360	335	0.26	P	SRI17	Yagee, 1979 [c]
Zr-4 (SR)	360	335	0.75	P	418	Jones, 1979
Zr-4 (SR)	360	337	0.7	P	63S	Busby, 1975
Zr-4 (SR)	360	348	1	P	433	Jones, 1980
Zr-4 (SR)	360	348	1	P	434	Jones, 1980
Zr-4 (SR)	360	348	1	P	435	Jones, 1980
Zr-4 (SR)	360	372	0.6	P	68S	Busby, 1975

Table A-4 (continued)

Material	Temp. (°C)	Stress (MPa)	Strain (%)	Failure Mode	Spec. ID	Reference
Zr-4 (SR)	360	396	2	S	431	Jones, 1980
Zr-4 (SR)	360	396	2	P	432	Jones, 1980
Zr-4 (SR)	360	445	4	S	429	Jones, 1980
Zr-4 (SR)	360	445	4	S	430	Jones, 1980
Zr-4 (SR)	360	455	5	S	65S	Busby, 1975
Zr-4 (SR)	360	475	16	S		Ryu, 1988
Zr-4 (SR)	360	475	5	P		Ryu, 1988
Zr-4 (SR)	360	475	6	P		Ryu, 1988
Zr-4 (SR)	360	475	14	P		Ryu, 1988
Zr-4 (SR)	382	159	0.7	P	37S	Busby, 1975 [c]
Zr-4 (SR)	382	173	0.4	P	32S	Busby, 1975 [c]
Zr-4 (SR)	400	132	6	P	43S	Busby, 1975 [c]
Zr-4 (SR)	400	161	7	P	9S	Busby, 1975 [c]
Zr-4 (SR)	400	185	4	P	31S	Busby, 1975 [c]
Zr-4 (SR)	400	196	9	P	48S	Busby, 1975 [c]
Zr-4 (SR)	400	215	6	P	67S	Busby, 1975
Zr-4 (SR)	400	292	0.9	P	56S	Busby, 1975
Zr-4 (SR)	400	372	2	P	64S	Busby, 1975
Zr-4 (SR)	400	405	16	S	8S	Busby, 1975 [c]
Zr-4 (SR)	400	475	16	S		Ryu, 1988
Zr-4 (SR)	400	475	16	S		Ryu, 1988
Zr-4 (SR)	400	475	14	P		Ryu, 1988
Zr-4 (SR)	400	475	7	P		Ryu, 1988

Notes

(ANN) - annealed; (RX) - fully recrystallized; (SR) - stress-relieved.
D - ductile rupture; S - axial split; P - pinhole leakage.
All strains of 1% or greater approximated to whole numbers.
[c] - failure mode information from [Crescimanno, 1984].

Appendix B

Discussion of the Observations of Cavities by Keusseyan and his Coworkers

THE OBSERVATIONS OF CAVITIES BY KEUSSEYAN AND HIS COWORKERS

The results of Keusseyan and co-workers [Keusseyan, 1979 and 1985] are of particular importance as they have been cited as supporting evidence for the development of cavities in the Zircaloys in the transient (primary) and secondary stages of creep. As they represent the only extensive report of the existence of cavities in creep-tested Zircaloys, their results need to be examined in some detail.

The first reference reports on the observation of cavities in Zircaloy-4 creep-tested at 375°C while the second one, in addition to repeating the earlier results, records the details of a more extensive study carried out on Zircaloy-2 creep-tested in the temperature range 350-400°C. A close reading of both references indicates that the applicability of the observations to the storage of spent fuel is questionable and the evidence is far from conclusive.

Zircaloy-4

[Keusseyan, 1979] describes the results of tests performed on Zircaloy-4 sheet which had been annealed at 700°C (i.e., much higher than the normal stress-relieving temperatures) and consequently had a fully recrystallized structure. The tests involved subjecting a couple of specimens to an initial stress of 132 MPa at 375°C for 240 hours, during which each accumulated a strain of about 3%.

One of the creep-strained specimens was notched along the width of the specimen (presumably on the gauge section) and tensile tested at 350°C. Failure occurred "at the notch in the transgranular mode with a significant reduction in ductility" when compared with an equivalent specimen which had received the same thermal treatment but had not been subjected to creep deformation. The latter failed by necking away from the notch. The authors attribute the lower ductility observed with the creep-strained specimen to the presence of grain boundary cavities which, they believe, led to a reduced internal cross-section. A more logical explanation, perhaps, would have been to recognize that the material had, in fact, been strain-hardened and that this would have contributed to a reduction in ductility. This is borne out by studying the

shapes of the stress-strain curves: the yield point of the creep-strained specimen is much higher (by about 30%) than that of the thermally-treated specimen. Strain hardening is generally thought to arise from dislocation-solute interactions.

The second creep-strained specimen "was notched and fractured intergranularly," and the fracture surface examined by scanning electron microscope (SEM). The precise method by which the fracture was accomplished is not described but, based on the later work on Zircaloy-2 [Keusseyan, 1985], it seems legitimate to infer that the intergranular fracture was induced by immersing a stressed specimen in an iodine solution. It was on the fracture surfaces thus obtained that grain boundary cavities were observed. The reference paper presents one SEM micrograph of a grain boundary which contains cavities (the copy of the micrograph available to the present reviewers was of less than optimal quality and it was difficult to identify the cavities). No cavities were detected on the fracture surfaces of a specimen subjected only to the equivalent thermal treatment (nor, for that matter, were any second phase particles detected). No quantitative information is provided on the size, number and distribution of the cavities. The salient point, though, is that the cavities were observed on surfaces **formed as a consequence of (probably) ISCC**, not from creep-rupture testing. It is interesting to note that, by contrast, the creep-strained specimen which was tensile tested failed in a transgranular mode and (presumably) gave no evidence of grain boundary cavitation.

There remains one final comment on the data presented in [Keusseyan, 1979] and this concerns the observation that, whereas the creep-strained specimen fractured at the notch in the tensile test, the thermally-treated sample did not do so. The orientation of the notch with respect to the texture of the material is important in dictating how deformation will proceed at the base of the notch. Although no texture information is provided, it can be assumed that the imposition of creep strain resulted in a texture which was different from that present initially and from the one developed in the thermally-treated material. It is conceivable that the orientation of the notch relative to the texture of the creep-strained specimen was such that deformation proceeded preferentially at the base of that notch. However, a similarly defined texture did not exist in the thermally-treated specimen, although remnants of the original fabrication texture were probably

present. Consequently, the grains in the thermally-treated specimen were much more randomly oriented, which led to inhomogeneous deformation and permitted fracture to occur away from the notch.

Zircaloy-2

The Zircaloy-2 used in the tests described in [Keusseyan, 1985] was supplied by EPRI and was in the annealed ("soft") condition [Cubiciotti, 1978]. Details provided in [Jones, 1980] indicate that the annealing had been carried out at 570°C and that the microstructure was that of recrystallized material. Of most relevance, however, the creep tests were not performed by internal pressurization of clad tubing but by uniaxial tension testing of longitudinal sections taken from the tubing. The immediate consequence of this approach was that, in cutting the test specimen out of the tube, the residual stresses present in the tube would have been released (these stresses are of the order of 100 MPa, according to [Cubiciotti, 1978]). In addition, alignment of the specimen in the test machine would be extremely critical with such specimens. However, even when this is achieved, the resulting stress distribution will be radically different from that present in an internally pressurized tube, particularly when considering the textured hcp structure of the Zircaloy-2.

The creep tests were carried out at two stress levels (118 and 132 MPa) at 350 and 375°C, and at four stress levels (72.4, 92.4, 116 and 132 MPa) at 400°C. As in the earlier work on Zircaloy-4, the tests were not continued to rupture. Rather, they involved:

(a) subjecting the specimen to creep for a specific length of time (120, 240, 480 or 960 hours) then discontinuing the test;

(b) cutting a piece out of the gauge section of the specimen and making a small notch in it;

(c) fixing the notched piece in a vise and applying a small (unquantified) stress to it;

(d) immersing the stressed piece (together with the vise setup) in a solution of iodine in methyl alcohol for several minutes;

(e) removing the whole setup and washing it clean;

(f) and, finally, if the piece had not already fractured completely, applying more stress until it did so.

Thus the fracture surfaces that were examined had been produced by ISCC and the contribution of prior creep deformation to the appearance of these surfaces is somewhat uncertain. Nonetheless, grain boundary cavities were apparently observed on the fracture surfaces of all the specimens examined, including those containing the smaller creep strains (less than one percent at 350°C). As with the earlier reference, the only copy available of the one supporting micrograph was of poor quality.

[Keusseyan, 1985] presents cavity count data (in graphical form) which indicate that, generally, the cavities were fairly evenly distributed between what he terms "surface cavities" (located on the face of a grain) and "corner cavities" (located at the intersection of two or more grain boundaries). Although cavity counts were performed at four strain levels for each combination of stress and tempererature, no information is provided of the sizes of the cavities. Thus there is no way of determining whether the variations in cavity counts at different strain levels reflect simply the nucleation of more cavities or, possibly, more complex changes involving both the nucleation and growth of cavities. It would have aided the evaluation immensely if quantifications could have been provided of cavity sizes and size distributions.

It would also been of interest if [Keusseyan, 1985] had provided some indication of what might be considered the critical conditions which would lead to cavity formation. In the absence of this, we have plotted the cavity count data as a function of creep strain (both quantities estimated from the graphs in [Keusseyan, 1985]) at each of the three temperatures in an attempt to determine at what strains the cavities began to nucleate. The results of this cursory examination are shown in Figure B-1. The data at each of the three temperatures were fitted to a logarithmic relationship, each of which was then extrapolated back to zero cavities to determine the critical creep strains for cavity nucleation. From this, it might be inferred that the critical strains are:

at 350°C - 0.37%;
at 375°C - 0.66%;
at 400°C - 1.34%.

The Origin of the Cavities

Keusseyan et al. have observed grain boundary cavities on the fracture surfaces specimens of both Zircaloy-2 and Zircaloy-4 which had been subjected to creep. However, that they were formed during the prior creep tests, as suggested by Keusseyan et al., might be open to question. The actual fractures were accomplished through ISCC and with this context in mind, the observations of ISCC fracture surfaces recorded by Shimada and Nagai (S&N) [Shimada, 1983a] may be of relevance.

S&N conducted a fractographic study of ISCC in irradiated Zircaloy-2 tubing at 350°C and concluded that the most common morphology in the initiation regions of SCC cracks was a mixture of both intergranular and transgranular fracture. They also noted that "*W-type voids were often observed in intergranular fracture*" and postulated that "*the mechanism of intergranular fracture might be similar to that of intergranular fracture in creep failure, that is, the intergranular fracture might be caused by slip on the grain boundaries.*" These W-type voids appear to be equivalent to the "corner cavities" observed by Keusseyan et al. Further, S&N comment that "*a considerable amount of small pits were observed on the surface of the transgranular fracture, or cleavage facet, adjacent to the inner surface of the specimen.*" "*The cleavage facet with many pits suggests that it was attacked by iodine after the cracking took place.*" This raises the possibility that the "surface cavities" seen by Keusseyan et al. were, in fact, the consequence of iodine attack and were not formed during the prior creep action.

representative of the more complex loading extant in the internally pressurized spent fuel pins. Finally, some doubt exists that the cavities observed were indeed the product of the creep process and not some artefact introduced during the iodine-assisted fracture. In any event, even the Keusseyan observations do not support the view that creep will accelerate from its onset. We thus reach the conclusion that it is inappropriate to use the observations made on these materials, and the associated calculations, in evaluating the performance of spent fuel cladding during dry storage.

References

[Cubicciotti, 1978]
D. Cubicciotti and R.L. Jones, *EPRI-NASA Cooperative Project on Stress Corrosion Cracking of Zircaloys*, U. S. Report EPRI-NP-717, March 1978.

[Keusseyan, 1979]
R.L. Keusseyan, C.P. Hu and C.Y. Li, *"Creep Damage in Zircaloy-4 at LWR Temperatures"*, J. Nucl. Mat. 80:390-392 (1979).

[Keusseyan, 1985]
R.L. Keusseyan, Grain Boundary Sliding and Related Phenomena, Ph.D. Dissertation, Cornell University, University Microfilms International, Ann Arbor, MI (1985).

[Shimada, 1983a]
S. Shimada and M. Nagai, *"A Fractographic Study of Iodine-Induced Stress Corrosion Cracking in Irradiated Zircaloy-2 Cladding,"* J. Nucl. Mat. 114:222-230 (1983).